
[All ETDs from UAB](#)

[UAB Theses & Dissertations](#)

2023

Regulatory Elements of Polyphosphate Biosynthesis

Marvin Qortez Bowlin
University of Alabama at Birmingham

Follow this and additional works at: <https://digitalcommons.library.uab.edu/etd-collection>

 Part of the [Medical Sciences Commons](#)

Recommended Citation

Bowlin, Marvin Qortez, "Regulatory Elements of Polyphosphate Biosynthesis" (2023). *All ETDs from UAB*. 3481.

<https://digitalcommons.library.uab.edu/etd-collection/3481>

This content has been accepted for inclusion by an authorized administrator of the UAB Digital Commons, and is provided as a free open access item. All inquiries regarding this item or the UAB Digital Commons should be directed to the [UAB Libraries Office of Scholarly Communication](#).

REGULATORY ELEMENTS OF POLYPHOSPHATE BIOSYNTHESIS

by

MARVIN Q. BOWLIN

PETER PREVELIGE, COMMITTEE CHAIR

MICHAEL GRAY, MENTOR

TODD GREEN

NATALIA KEDISHVILI

JANET YOTHER

A DISSERTATION

Submitted to the graduate faculty of The University of Alabama at Birmingham,
in partial fulfillment of the requirements for the degree of
Doctor of Philosophy

BIRMINGHAM, ALABAMA

2023

Copyright by
Marvin Q. Bowlin
2023

REGULATORY ELEMENTS OF POLYPHOSPHATE BIOSYNTHESIS

MARVIN Q. BOWLIN

GRADUATE BIOMEDICAL SCIENCES

ABSTRACT

Polyphosphate (polyP) is an ancient, conserved, inorganic biomolecule. Biological systems have adapted many functions for this high-energy molecule, ranging from immune regulation in mammals to gene regulation in prokaryotes. Of particular interest is its use in bacterial stress responses. Bacteria use polyP to resist hazardous environmental elements like toxic molecules or nutrient starvation. In many bacterial species, polyP is synthesized by polyphosphate kinases (PPKs). PPK – discovered in *Escherichia coli* (*E. coli*) – hydrolyzes adenosine-5'-triphosphate (ATP) to synthesize polyP. Species that use PPK develop multiple pathogenic defects when PPK activity is impaired, including, among others, antibiotic susceptibility. There is no mammalian homolog of PPK, making it a prime therapeutic target. Unfortunately, there are many unanswered questions regarding PPK and polyP synthesis regulation.

In this work we report several novel PPK regulatory elements. We begin with a review of the state of polyP research and an exploration of the complicated interaction of bacterial and host polyP utilization. Next, we identify new regulatory elements of polyP synthesis using genetic techniques. Nitrogen-regulation elements such as the nitrogen phosphotransferase regulator PtsN and nitrogen metabolism factors GlnG and GlnR were discovered to have regulatory effects on polyP production. Cellular nitrogen levels were implicated in RpoN-dependent polyP synthesis, though multiple factors in nitrogen regulation were eliminated as potential as PPK regulators.

We next characterize purified PPK enzymes. Our results indicate that the widely used polyhistidine tag significantly alters PPK activity, oligomeric stability, and sensitivity to substrate inhibition. We describe an alternative purification method using the C-tag system and confirm its similarity to untagged enzyme. The therapeutic PPK inhibitor mesalamine (5-aminosalicylic acid, 5-ASA), a poor inhibitor of polyH-tagged PPK, was found to be more effective when tested on the C-tagged enzyme. Finally, subtle differences in the previously described PPK* mutant enzymes were identified that suggest that each mutation leads to increased polyP accumulation through different mechanisms.

We conclude with data regarding the development of PPK purification and detection methods and propose several questions to inform future polyP studies. Collectively, this project has identified multiple novel regulatory elements in polyP biosynthesis which will inform future studies of polyP biology.

Keywords: Bacterial Stress Response, Polyphosphate, Enzymology, Oligomerization

DEDICATION

To my Mom, who has always pushed me to learn more. Your support and encouragement built the passion for learning that drives me to this day. This work is just a small part of the education I have had the extreme joy to obtain thanks to you. Anything in this work that is good has its roots in your nurturing.

ACKNOWLEDGEMENTS

First, I want to acknowledge and thank my mentor, Michael Gray, who saw something of value in a broken, lost graduate student and took a risk on mentoring him when others would not. This work is the result of that risk. It is my earnest hope that it was worth the risk. His guidance and support were essential not only in the research herein presented, but in my personal development as a researcher, scientist, and professional. Some of the lessons he has taught be go beyond the laboratory, like how to utilize the backburner, to be satisfied with good instead of perfect, and to take time to breathe. I would also like to acknowledge members of the Gray lab past and present. Dr. Rhea Derke was a great help to me in getting acclimated to the new environment of a microbiology lab. Amanda Rudat developed the PPK* mutants that are the foundation of this work. Abigail Long, a fellow Team Polyphosphate student, suffered with me over the study of our “favorite” enzyme. Avery Liber was a clever student to teach and learned fast, as evident from his jumping ship from Team Polyphosphate as soon as he joined the lab proper. Finally, the laboratory culture and attitude of positive energy and support could not have existed or thrived without Julia Williams and Sierra Hansen kept the lab stocked with good vibes and better feedback on crazy ideas.

I would be remise if I did not thank my dissertation committee members, Drs. Peter Prevelige, Todd Green, Natalia Kedishvili, and Janet Yother. Your guidance, wisdom, and patience were essential in my progress, and I thank you deeply for the time you’ve invested in me.

I also want to acknowledge Dr. Stephanie Carmicle, my first research mentor, who lured a pre-med student away from the bedside and into the lab. Her guidance, along with that of Drs. Elizabeth Brandon, Angelia Reiken, and Robert Sample, awakened a passion in me for the discovery of new knowledge and, more importantly, the sharing of that knowledge with others.

Finally, to all my family and friends who have supported me and cheered me on through these long years. There are too many to name and to forget one would be an unforgivable failing. So, to all those who have supported me, listened to me ramble on about my work, and asked when I would be done, how much more I had left, is there a date yet... Here, at last, is my answer. This work is done, fueled by your encouragement and pestering. Thank you all, from the bottom of my heart.

TABLE OF CONTENTS

	<i>Page</i>
ABSTRACT.....	iii
DEDICATION.....	v
ACKNOWLEDGEMENTS.....	vi
LIST OF TABLES.....	x
LIST OF FIGURES.....	xi
INTRODUCTION.....	1
Polyphosphate.....	1
Universal, Valuable, Simple, and Complex.....	1
Functions of Bacterial Inorganic Polyphosphate.....	3
Understanding Stress and Polyphosphate.....	5
The Importance of Studying Polyphosphate.....	6
Bacterial Polyphosphate Metabolism.....	7
Enzymes of Bacterial Polyphosphate Metabolism.....	7
The Biological Value of Polyphosphate Metabolism.....	10
<i>E. coli</i> Polyphosphate Kinase: A Model.....	11
INORGANIC POLYPHOSPHATE IN HOST AND MICROBE BIOLOGY.....	15
THE ROLE OF NITROGEN-RESPONSIVE REGULATORS IN CONTROLLING INORGANIC POLYPHOSPHATE SYNTHESIS IN <i>ESCHERICHIA COLI</i>	45
A C-TERMINAL POLY-HISTIDINE TAG ALTERS POLYPHOSPHATE KINASE ACTIVITY AND MASKS POTENTIAL REGULATORY EFFECTS.....	93
OBSERVATIONS ON PPK PURIFICATION, ACTIVITY, AND DETECTION.....	133
DISCUSSION AND CONCLUSIONS.....	145
GENERAL METHODS.....	155

GENERAL REFERENCES.....159

APPENDICES

A. DEVELOPED AND OPTIMIZED PROTOCOLS.....173

B. A PSEUDO-UNCOMPETITIVE INIBITION MODEL OF
POLY-HISTIDINE TAGGED PPK187

LIST OF TABLES

<i>Table</i>	<i>Page</i>
1. Structures and Activities of PPK1 Inhibitors.....	42
2. Strains and Plasmids Used To Identify the Role of Nitrogen-Responsive Regulators in Controlling Inorganic Polyphosphate Synthesis in <i>E. coli</i>	85
3. Summary of PPK* Differences.....	114
4. PPK27 and PPK28 Vector Construction Primers	134

LIST OF FIGURES

<i>Figure</i>	<i>Page</i>
1. Enzymes of Polyphosphate Biology	8
2. The Structure and Regulation of PolyP in Bacteria.	18
3. The PolyP Wars: The Struggle Between Host and Pathogen PolyP.....	29
4. The RpoN bEBPs GlnG and GlnR Influence PolyP Production.	48
5. RpoN-Dependent Regulation of PolyP Synthesis Is Dependent on Cellular Nitrogen Status, but Not on GlnB or GlnK.....	64
6. GlnS Regulation Has Minimal Impact on PolyP Production.	67
7. PtsN Positively Regulates PolyP Production.....	69
8. PtsN Regulation of PolyP Synthesis Is Not Dependent on PtsN Phosphorylation State, Changes in PtsN Abundance or Direct Interaction with PPK.	72
9. Current Model for PolyP Regulation in <i>E. coli</i>	73
10. Nutrient Limitation Induces <i>glnK</i> Expression in <i>E. coli</i>	88
11. Simple Nitrogen Starvation Does Not Induce Robust PolyP Accumulation in <i>E. coli</i>	88
12. Overexpressing GlnG or GlnR Does Not Significantly Impact PolyP Production in Wild-Type <i>E. coli</i>	89
13. Glutamine Limitation Explains the Growth Defect of an <i>rpoN</i> Mutant in LB Medium.....	89
14. RecA Protein Concentration Does Not Change in Response to PolyP-Inducing Nutrient Limitation Stress.....	90

15. PolyP-Inducing Nutrient Limitation Does Not Affect PtsN Protein Levels <i>In Vivo</i>	91
16. Nitrogen Metabolites Do Not Allosterically Regulate PPK Activity	92
17. PolyP, PPK, and Protein Purification Methods	96
18. A Poly-histidine Tag Increases the Specific Activity of PPK	102
19. Kinetics of Tagged PPK Enzymes.....	103
20. Oligomeric Distributions of Purified PPK.....	105
21. Activity and Kinetics of PPK* Enzymes	107
22. Oligomeric Distribution of PPK* Variants.....	109
23. Sensitivity to ADP Inhibition	110
24. 5-ASA Inhibition Sensitivity of PPK-CT and PPK*-CT Enzymes	112
25. Purification Of Untagged PPK from Overexpression Culture.....	130
26. Mass Photometry of PPK-HT Enzyme.....	130
27. Location of PPK* Mutation Sites in Dimeric Structure	131
28. Expression and Isolation of Profinity-tagged PPK.....	135
29. PPK Purification Using the Profinity System Results in Protein Degradation and Loss in Activity	137
30. Quantification of Low Copy Number PPK Plasmids <i>In Vivo</i>	140
31. Development of PPK Western Blotting Techniques	143
32. Localization of <i>ppk*</i> Mutations and Predicted Protease Target Sites.....	151

INTRODUCTION

Polyphosphate

Universal, Valuable, Simple, and Complex

“Polyphosphate” generally refers to a multiplicity of phosphate units in a molecule, typically linked together by a phosphorus-oxygen bond. The heterogeneous nature of this class of chemicals is unsurprising, as polyphosphates are widely varied in form, synthesis, and function. Compounding this complexity is the lack of nomenclature homogeneity. There are instances where labs have studied polyphosphate under a different name (such as metaphosphate), only to change to the term polyphosphate without any consistent reference to a new nomenclature (1, 2). Many molecules of biological significance have been classified as a polyphosphate, such as adenosine-5'-triphosphate (ATP), pyrophosphate (PPi), and inositol phosphates like inositol hexaphosphate (phytic acid, IP6). While calling molecules lacking a direct phosphate-phosphate bond like IP6 polyphosphates is not without some controversy, the study of such non-polymeric polyphosphates has yielded some fascinating observations (3-6). Generally, multiple phosphates are all that are required to be called a polyphosphate.

The simplest, truest form of polyphosphate is inorganic polyphosphate (polyP), which is a polymer of phosphate monomers linked together by phosphate-oxygen bonds. Organic additions, such as nucleosides, produce more complicated molecules such as ATP and guanosine pentaphosphate ((p)ppGpp). PolyP is universally conserved in all domains of life and has biological and abiological sources. Many organisms, from

bacteria and archaea to humans, synthesize polyP. Abiologically, it can easily be synthesized by heating phosphate compounds, due largely to the simplicity of its structure. Yet, for all its simplicity, polyP is incredibly versatile. The accumulation of multiple phosphate bonds within a polyP chain results in a high-energy storage molecule that can also sequester cations like Fe^{2+} and Mg^{2+} (7, 8). PolyP also acts as a primordial chaperone, stabilizing damaged proteins and keeping them soluble until they can be degraded (9). The abundant availability of polyP in the environment, combined with the high energy stored in the phosphate bonds, makes it a valuable resource. The ability to scavenge polyP is highly conserved, with multiple mechanisms being developed to process and digest polyP from multiple angles of attack: endopolyphosphatases that hydrolyze polyP chains into smaller oligophosphates; exopolyphosphatases that progressively hydrolyze a polyP chain from the ends to release the phosphates; pyrophosphatases that specifically break apart the small pyrophosphate molecules that are often left after digestion by endo- and exo-polyphosphatases; and even dual polyP synthesizing and degrading enzymes like the polyphosphate kinases (PPKs).

The length of a chain of polyP varies based on many factors, from phosphate availability to species-specific traits (10-13). This gives rise to another level of disparity in the field: the definition of chain length. The use of terms such as long-chain polyphosphate (lcPolyP) and short-chain polyphosphate (scPolyP) are complicated by the difference in chain length between kingdoms, species, and even cellular environments. *E. coli* chain length is highly dependent on growth conditions, stressors, and available resources (12). Under anaerobic conditions the production of polyP chains in excess of 1000 units is common, while under aerobic growth conditions with stress the length can

fall to roughly 42 units (12). Conversely, eukaryotic *Saccharomyces cerevisiae* produces chains of around 60 units (14). The length of an inorganic polyphosphate chain is highly variable between species, with mammalian species having chain lengths averaging around 10-20 monomers, while bacterial species chain lengths range upwards of 800-1000 (15, 16).

Functions of Bacterial Inorganic Polyphosphate

These larger chains of polyP in bacteria represent a sizable energy pool, allowing polyP to act as a storage system for energy. The repetitive phosphoanhydride bonds between each phosphate monomer are the same bonds utilized in the universal energy currency of ATP, but in a significantly higher concentration per molecule. In terms of biochemically available energy, no other molecule in the cell comes close to the energy storage of polyP (17).

There are many different functions for polyP in bacteria. Large magnetotactic bacteria in suboxic zones of the Black Sea utilize heavily charged polyP for movement, collecting phosphate from the upper section of this oxygen-deplete region, forming it into polyP, and moving it to the lower parts to be degraded and released (18). Several bacterial species accumulate polyP in high-phosphate environments for later use, which make them a useful tool in wastewater treatment plants (19, 20). *Rhodopseudomonas palustris*, a polyP accumulating bacteria isolated from wastewater sludge, captures energy from light and stores it in the polyP phosphoanhydride bonds (21).

PolyP serves many functions besides an energy store. *Burkholderia pseudomallei* (*B. pseudomallei*) relies on polyP synthesis for quorum sensing, in addition to adhesion

and invasion into human lung epithelial cells (22). Defects in motility and biofilm formation were observed in *Bacillus cereus* in response to polyP accumulation impairment, while polyP degradation impairment decreased spore formation (23). *Acetonebma longum* (*A. longum*) utilizes polyP in the formation of spore outer membranes – which it retains – and stores polyP in granules in the membrane, possibly as an energy store for subsequent germination (24). In *Campylobacter jejuni* (*C. jejuni*), production of polyP is required for resistance to osmotic shock and nutrient starvation, in addition to being required for virulent traits like the ability to survive intracellularly or to colonize chicks (25, 26). PolyP production is linked to motility in pathogenic species like *E. coli*, *Pseudomonas aeruginosa* (*P. aeruginosa*), *Klebsiella pneumoniae* (*K. pneumoniae*), *Vibrio cholerae* (*V. cholerae*), and *Salmonella Enterica* (*S. enterica*) serovars Dublin and Typhimurium (27). *Helicobacter pylori* (*H. pylori*) displayed multiple phenotypes when the ability to synthesize polyP was eliminated: impaired murine colonization, poor growth on rich media, increased sensitivity to the antibiotic metronidazole, and decreased motility (28). For *Mycobacterium tuberculosis* (*M. tuberculosis*), the accumulation and degradation of polyP plays an essential part in the survival of the bacteria intracellularly and its ability to infect hosts (29). *M. tuberculosis*, along with *E. coli*, *P. aeruginosa*, *V. cholerae*, and *C. jejuni* also require polyP to maintain antibiotic resistance (30-34). PolyP protects *E. coli* DNA from damage caused by cisplatin treatment, primarily by acting as iron chelator to prevent the reaction of iron ions and peroxide to form hydroxyl radicals (7). In all there are many examples where regulated expression and use of polyP has been linked to a myriad of bacterial functions, including energy storage, metabolic regulation,

stress responses, viability, colonization, pathogenicity, virulence, mobility, and antibiotic resistance (16, 25, 27, 33-43).

Understanding Stress and Polyphosphate

In *E. coli*, the stress responses are triggered by multiple stressors that results in the arrest of cell cycle progression and shift into stationary phase. This shift to stationary phase allows the bacteria to “bunker down” and become resistant to a multitude of stresses – not just the initial stress (44). The key to this shift is the rapid expression and accumulation of the alternative sigma factors like RpoS (44, 45). Under supportive conditions RpoS expression is tightly regulated and any RpoS synthesized is rapidly degraded (45). Following exposure to stresses like nutrient starvation, reactive oxygen or nitrogen species, osmotic imbalances, changes in environmental pH, or toxic compounds, the expression of RpoS rapidly increases (45). RpoS interacts with the RNA polymerase complex (RNAP) and alters the transcriptional profile of the cell, either directly or indirectly regulating the expression of ~10% of *E. coli*'s genome (46). The specific genes regulated depend on the cause of stress (45). The stress response triggers a wide variety of signaling molecules, including (p)ppGpp and polyP. This is just one example of stress leading to polyP synthesis. The relationship between the occurrence of stress and the initiation of polyP synthesis has been a major source of interest in the field of polyP biology (2, 16, 27, 37, 39, 40, 47-52). Most recently, the expression of polyP (though not its degradation) has been shown to be independent of the stringent response alarmone (p)ppGpp, overturning decades of conventional assumption (53). Interestingly, polyP accumulation was linked to the expression of DksA, a secondary channel-binding

transcription factor. Our subsequent investigations into the DksA pathway have revealed yet another positive regulator of polyP synthesis, the nitrogen phosphotransferase regulator PtsN (54). Slowly, but surely, the web of polyP regulation is being unraveled.

The Importance of Studying Polyphosphate

The value of studying polyphosphate biology cannot be overstated. In the first chapter of this work, originally published in Trends of Microbiology, the complex dance of polyphosphate is explored in detail, with emphasis added to both the importance of the molecule to bacterial survival and in host health and disease. Both host and microbe utilize polyP in complex and intricate ways. It can easily be envisioned as a sort of “PolyP-nesian war”: a complex series of battles between two armies with a common heritage, each using similar weapons in different ways to outwit the other.

The PPK enzymes discussed so far are unique to the bacteria. Only one eukaryotic species, the social slime mold *Dictyostelium discoideum*, has been found to have an enzyme with some level of sequence homology to PPK1, which is likely the result of a horizontal gene transfer event (55, 56). Importantly, in higher level mammalian systems, including humans, the enzymes responsible for polyP synthesis are non-homologous to bacteria PPK enzymes (57). This represents a prime opportunity for therapeutic targeting, as the impairment of polyP synthesis is known to impair bacterial survival, pathogenesis, and colonization in many species (22, 25, 28, 29, 32, 33, 36, 38, 41, 43, 58-74). For some species, including pathogenic agents like *E. coli*, *C. jejuni*, *M. tuberculosis*, *P. aeruginosa*, and *V. cholerae*, impairing polyP synthesis resensitized the bacteria to the antibiotics they were previously resistant to (30, 31, 33, 34). The use of polyP synthesis

and PPK activity as a target for therapeutics is not idle speculation: the gold-standard treatment for irritable bowel syndrome and ulcerative colitis, mesalamine (5-aminosalicylic acid, 5-ASA), is a known PPK1 inhibitor that has a significant effect on the bacterial burden in the gut of patients and on bacterial polyP production (75-77).

Bacterial Polyphosphate Metabolism

Enzymes of Bacterial Polyphosphate Metabolism

There are three families of enzymes in bacterial polyP biology: polyphosphate kinase 1 enzymes (PPK or PPK1), polyphosphate kinase 2 enzymes (PPK2), and exopolyphosphatases (PPX). Many bacteria utilize polyphosphate kinase enzymes to regulate polyP metabolism. PPX enzymes are used to degrade polyP either synthesized internally or scavenged from the environment.

Figure 1 presents representative structures of each of these enzymes. Figure 1A is the monomeric structure of *E. coli* PPK1 (in *E. coli*, it is the only enzyme of this system and so is referred to as PPK). PPK was first identified, isolated, and characterized in the early 1990s by Arthur Kornberg's lab (78, 79). This family preferentially synthesizes polyP from ATP (78). There are two histidine residues (H435 and H454) essential for polyP synthesis activity, which are indicated by the residues in red (generated from structure data of PDB 1XDP) (78-80). The ATP binding pocket is indicated by the presence of an ATP molecule (yellow), while the two magnesium cofactors are indicated in white. Functionally, PPK acts as a dimer or tetramer depending on reaction conditions. The dimeric form is the form predominately responsible for polyP synthesis while the tetramer is an inactive form ready to activate when triggered (15, 80, 81).

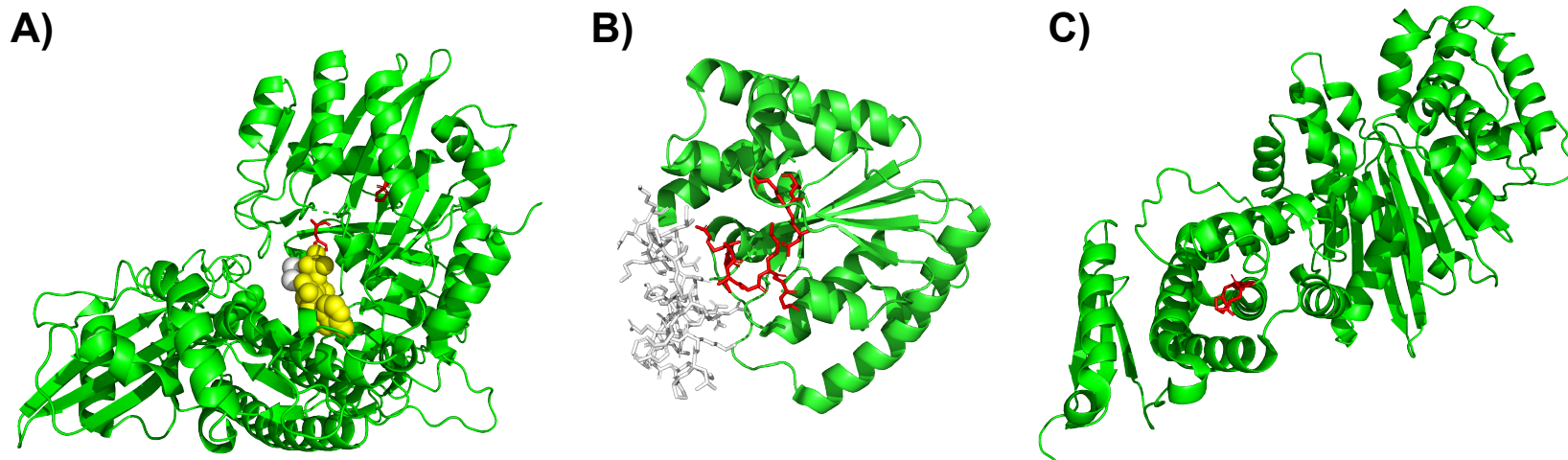


Figure 1 Enzymes of Polyphosphate Biology. A) An *E. coli* PPK1 monomer contains two essential histidines in the active site (red), with H434 directly binding to the substrate ATP (yellow) in the presence of two magnesium molecules (white spheres) to facilitate polyP production. B) Unlike PPK1, PPK2 enzymes preferentially degrade polyP to produce NTPs. They have a conserved motif of two sets of helices responsible for holding and guiding the polyP chain (red). A lid domain (white) serves to modulate activity. C) PPX monomers possess many charged residues on the outsides that allow for polyP binding. The active site catalytic residue is indicated in red. Monomeric structures of *E. coli* PPK1 (A), *F. tularensis* PPK2 (B), and *E. coli* PPX (C) were generated in PyMol with modifications using PDB files 1XDP for PPK1, 4YEG for PPK2, and 1U6Z for PPX.

Figure 1B is the monomeric structure of the Class I PPK2 enzyme from *Francisella tularensis* generated from the structural data from Batten et al. (PDB 4YEG) (59). This family of enzymes preferentially synthesizes nucleotide-triphosphates (NTPs) production through polyP hydrolysis (39, 82-85). There are two or three distinct classes of PPK2 enzymes, all with related structural elements (84). PPK2 enzymes appear to share a common P-loop kinase ancestor with that of thymidylate kinases (85). Thymidylate kinases utilize ATP hydrolysis to phosphorylate thymidine 5'-monophosphate (TMP), producing the essential DNA precursor thymidine 5'-diphosphate (TDP) (86, 87). The PPK2 family of enzymes hydrolyze polyP to produce NTPs from nucleotide diphosphates, with the ATP and GTP synthesis activity being over 70-fold higher than polyP synthesis activity (82). P-loop kinases have two signature motifs called Walker loop A and Walker loop B (red, Figure 1B), which are conserved in the PPK2 family enzymes (85, 87). A lid-like domain (white) allows for regulation of polyP access to the active site (59). A third class of PPK2, sometimes separated out as a third family of PPKs called PPK3, has many of the same structural features but preferentially catalyzes CTP and UTP production at a two-fold increased rate compared to ATP or GTP production (88).

The final enzyme family involved in bacterial polyP metabolism is comprised of exopolyphosphatases, or PPXs. These enzymes degrade polyP chains in a highly processive manner from the ends (89). In *E. coli*, the *ppx* gene forms an operon with *ppk*, indicating a strong association with polyP synthesis (PPK) a polyP degradation (PPX) (89). Figure 1C shows the structure of a monomer of *E. coli* PPX with the catalytic site indicated by red residues (structure generated from PDB 1U6Z) (90). Degradation

efficacy is determined by multiple polyP binding sites on the structure of the enzyme, with shorter polyP chains being degraded less efficiently (10). These sites have sulfate-holding charge regions that allow PPK2 to hold and guide longer polyP chains, with the channel leading to the active site capable of holding up to nine phosphate residues of a polyP chain (90).

The Biological Value of Polyphosphate Metabolism

PolyP is abundant in the environment from both biotic and abiotic sources. Synthesis of polyP can abiotically occur by means of the dehydration of orthophosphates at elevated temperatures like those around volcanic vents (48, 91). PolyP has long been considered an evolutionary fossil and has even been thought to be an evolutionary precursor to DNA and RNA (48, 91). Phylogenetic analysis has determined that polyP scavenging is the older function associated with polyP metabolism, making PPK2 the older of the two PPKs (92).

The synthesis of polyP is not required for bacteria to utilize it. Even in bacteria that lack enzymes known to synthesize polyP, mechanisms still exist for its use. For example, *Bacillus subtilis* (*B. subtilis*) has neither PPK1 nor PPK2 (93). However, the NAD kinase encoded by the *yjbN* in *B. subtilis* is specifically adapted to utilize either polyP or ATP as a phosphate source (94). PolyP represents a high-value, easily scavenged energy resource readily available in the environment, which incentivizes the development of scavenging mechanisms, hence the earlier development of the PPK2 family of enzymes compared to the PPK1 family.

E. coli Polyphosphate Kinase: A Model

Kornberg's study of polyP predates the discovered of PPK by nearly 40 years, with the original works identifying "some enzyme" in *E. coli* that synthesized polyP and consumed ATP (1, 2). At this time, polyP was called "metaphosphate" and represented a novel biomolecule. Kornberg's studies led him to work on identifying and characterizing DNA polymerase, which ultimately earned him the 1959 Nobel Prize in Physiology or Medicine (95, 96). However, later in his career he returned to the study of metaphosphate – now called polyphosphate.

PPK was originally discovered, purified natively, and characterized in *E. coli* by Kornberg's group in 1990 (78). In this study, several fundamental characteristics of the enzyme were described. The enzyme was found to be a monomeric unit of ~69 kDa by SDS-PAGE analysis. However, fast liquid chromatography data and sedimentation studies indicated that PPK synthesized polyP as a homotetramer of ~270 kDa. Michaelis-Menten kinetics were calculated, with the K_m for ATP calculated at 2 mM with a V_{max} of $51 \mu\text{mol mg}^{-1} \text{min}^{-1}$. ADP, the substrate for the reverse reaction, acted as a competitive inhibitor ($K_i = 0.09 \text{ mM}$ with ATP at 1 mM in reaction). PPi and KCl also induced an inhibitory effect to varying degrees. Ammonium sulfate up to ~100 mM stimulated polyP production but inhibited it beyond that threshold. They found that at high concentrations of ATP (~1 mM) synthesis of polyP was immediate and proceeded in a linear manner for roughly 40 minutes. However, at low levels (~ 5 μM) there was no detectable activity for 20 minutes. The addition of polyP with a chain length of four units eliminated this lag, indicating a small polyP chain could potentially act as a primer at low substrate concentrations. They also showed that the enzyme experienced autophosphorylation and

that the autophosphorylated enzyme was an intermediary in the reaction. These observations became the foundational elements of PPK enzymology.

In 1992, the *ppk* gene was isolated, sequenced, and cloned into an expression vector for improved isolation (79). This study determined that there were roughly 850 molecules of the enzyme in each wild-type cell under normal conditions. They also found that PPK associates with the outer membrane.

In 1996, PPK characterization was greatly refined (15). PPK consistently produces polyP chains of around 750 units in length. They defined the relationship between phosphorylated PPK and ATP concentration, and that the concentration of ATP determines the amount of phosphorylated PPK in the reaction. They also introduced a new purification method that eliminated a great deal of the complicated purification techniques necessary for the previous studies. Perhaps most importantly, they identified two histidine residues, H435 and H454, which are essential for the autophosphorylation event required to initiate polyP synthesis. The H435 residue is autophosphorylated and that phosphate group becomes the first phosphate of a new polyP chain, while H454 acts as an attachment site for the chain as it grows. These results were further supplemented in 2000 with the characterization of the various oligomeric states of the enzyme and the reactions which they catalyze, with the tetramer having some polyP synthesis activity and the dimer being more efficient (97). There was a trimer form briefly discussed in the study as well, but that has not been studied further.

The crystal structure of PPK was resolved in 2003, giving new insight to how the enzyme functions (81). A more refined crystal structure designed to model the enzyme in its active form was resolved in 2005, at which point the enzyme was determined to

synthesize polyP as a dimer rather than a tetramer (80). Importantly, during the development of this set of experiments, the purification method for PPK isolation was changed to utilize a C-terminal polyhistidine tag. From 2003 until recently, this purification method has been the standard for PPK.

Many questions remain as to how polyP synthesis is regulated in response to stress. How PPK itself detects stress, for example, is entirely unknown. What signals occur in the cell following stress that activate PPK? How is polyP synthesis regulated during the stress response? Is PPK activity regulated by the amount of ATP and ADP present in its local environment? How is PPK inactivated once the stressor has been removed?

Here, we offer an in-depth exploration into the regulatory mechanisms controlling polyP synthesis in *E. coli*, identify key players in the activation of polyP biosynthesis, and clarify several elements of PPK1 activity previously obscured by purification artifacts. The aims of this project are two-fold. First, to identify regulatory elements that either trigger or suppress polyP production using genetic techniques. Secondly, to identify regulatory elements intrinsic to PPK through biochemical and biophysical techniques. The following is a body of manuscripts and unpublished research which reports the results of on how polyP production is regulated in *E. coli* which we have discovered through pursuing these aims. In the first chapter, we provide a comprehensive review of polyP biology in both host and microbe biology, which provides the basis for understanding the experimental aims of the project. The second chapter covers the first aim and details the role that nitrogen regulation plays in polyP production. The third chapter is a preprint that covers the second aim. This preprint manuscript first identifies a

problem with the field-standard PPK purification method, which produces an enzyme that is functionally different from the untagged enzyme. In it, we report a new purification method that produces a protein that is comparable to the WT enzyme. Using this enzyme, we describe new elements of PPK activity, oligomerization, and inhibition sensitivity. The fourth chapter details the development of PPK purification and detection methods, including the production of and optimization of a monoclonal antibody against purified PPK for future use in Western blotting and co-precipitation assays. The conclusion of this project increases the field's understanding of how certain stresses trigger polyP production, what regulatory elements are key players, and how further experiments can be designed to further identify regulatory elements of polyP biosynthesis.

INORGANIC POLYPHOSPHATE IN HOST AND MICROBE BIOLOGY

by

MARVIN Q BOWLIN AND MICHAEL J GRAY

Trends Microbiol. 2021 Nov;29(11):1013-1023.

Copyright

2021

By

Elsevier Ltd

Used by permission

Format adapted for dissertation and errata corrected

ABSTRACT

Inorganic polyphosphate (polyP) is produced by both bacteria and their eukaryotic hosts and appears to play multiple important roles in the interactions between those organisms. However, the detailed mechanisms of how polyP synthesis is regulated in bacteria and how it influences both bacterial and host biology remain largely unexplored. In this review, we examine recent developments in the understanding of how bacteria regulate the synthesis of polyP, what roles polyP plays in controlling virulence in pathogenic bacteria, and the effects of polyP on the mammalian immune system, as well as progress on developing drugs that may be able to target bacterial polyP synthesis as novel means of treating infectious disease.

Why Study Polyphosphate?

Inorganic polyphosphate (polyP) is a universally conserved biomolecule composed of covalently linked units of phosphate monomers, as depicted in Figure 1A, with functions as widely varied as life itself. In bacteria, polyP has been linked to a myriad of functions, including energy storage, metabolic regulation, stress responses, viability, colonization, pathogenicity, virulence, mobility, and antibiotic resistance [1–14]. PolyP is involved in the movement of large magnetotactic bacteria in suboxic zones of the Black Sea, and has recently been investigated as a basis for a photo-microbial fuel cell [15, 16]. In eukaryotes, polyP plays roles in everything from oxidative and divalent cation stress responses in *Saccharomyces cerevisiae* to blood coagulation, macrophage differentiation, leukocyte proliferation, neutrophil recruitment, and platelet functions in mammalian systems [17–22], as well as playing a protective role in neuronal signaling by preventing glutamate excitotoxicity [23]. PolyP is important in archaea, as well. In *Methanosarcina mazei*, for example, polyP has been shown to accumulate under phosphate starvation conditions, acting to regulate the transcription of multiple phosphate metabolism and transport genes including those encoding the *pstSCAB-phoU* complex [24], while in several species of *Sulfolobales*, polyP is involved in archaeal motility, adhesion, and biofilm formation in [25].

With such diverse functions, it is of little surprise that new studies are steadily discovering new and reimagined roles for polyP. It is the purpose of this review to discuss advances in the field of polyP biology over the past few years, emphasizing the

importance of understanding polyP functions in host-microbe interactions and how polyP represents a promising, but complicated target for clinical applications.

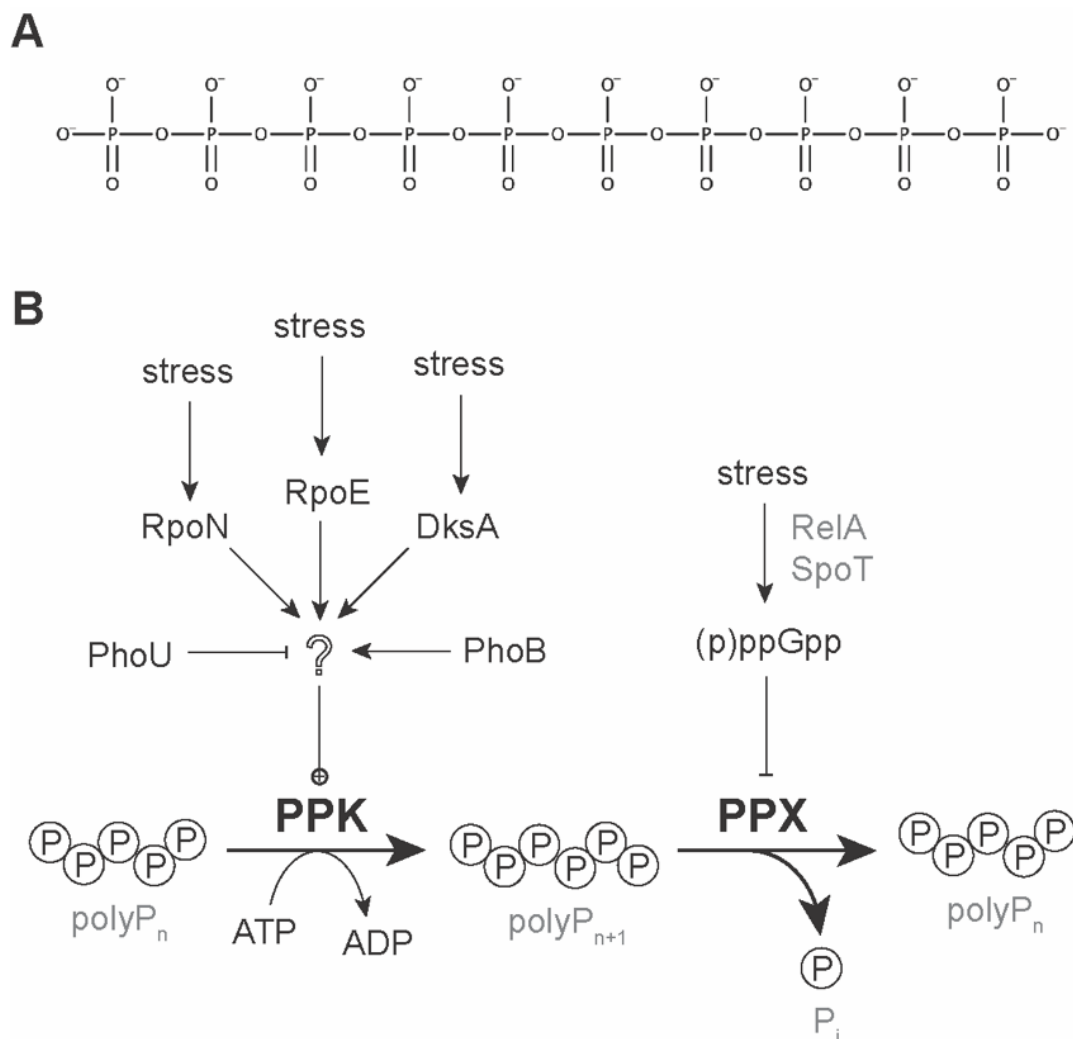


Figure 1. The Structure and Regulation of PolyP in Bacteria. (A) The structure of polyP. A short polyP molecule (polyP₁₀). Bacterial polyP can be up to 1000 phosphate units long, while eukaryotic polyP is usually substantially shorter. (B) The current model for polyP regulation in *Escherichia coli*. PolyP is synthesized by polyP kinase (PPK) and degraded by exo-polyPase (PPX). Starvation stress stimulates **RelA** and **SpoT** to synthesize (p)ppGpp, which inhibits PPX, but does not influence PPK activity and is not required for induction of polyP synthesis. Induction of polyP synthesis does depend on the transcription factors RpoN, RpoE, DksA, and PhoB, although none of these activate transcription of the *ppk* gene itself. PhoU is a negative regulator of both phosphate transport and polyP synthesis. None of the mechanism(s) by which these regulators affect PPK activity are currently known.

Overturing Established Models of Polyphosphate Regulation

There are two unrelated kinases utilized by many bacteria to synthesize polyP: **PPK1** or **PPK** (see Glossary) and **PPK2** [1]. PPK1 predominately catalyzes the synthesis of polyP from ATP. PPK2 is different in that it can efficiently use GTP or ATP to synthesize polyP and is more efficient at hydrolyzing polyP to synthesize nucleotide triphosphates [26]. Some bacteria possess **homologs** of both PPK1 and PPK2; others possess only one, or in some cases, neither. While this review focuses primarily on polyP synthesis by PPK1, it is important to note that some species (such as *Francisella tularensis*) have both PPK1 and PPK2 homologs, and that most studies we highlight only focus on one of these enzymes. For brevity, and because most recent studies examine PPK1 functions, it is the intent of this review to focus largely on PPK1. For clarity, however, we will take care to indicate when PPK2 is also present in a system.

Many bacteria, including the model Gram-negative bacterium *Escherichia coli* (*E. coli*), which has a single PPK1 homolog (called simply PPK) [27], activate polyP synthesis in response to environmental stress [28], and the many roles of polyP in stress tolerance [4, 6, 8, 9, 11, 12, 29–36] are central to the function of polyP in host-microbe interactions. Nevertheless, the molecular mechanisms of polyP regulation in bacteria have been largely ignored since early studies in *E. coli* by Arthur Kornberg's lab in the late 1990s [37, 38]. Those studies proposed a model in which the repression of polyP-degrading exopolyphosphatase (**PPX**) activity by the stringent response alarmone **(p)ppGpp** [39] was the key regulatory step in polyP synthesis [38, 40], and this idea was

generally accepted until very recently [41]. However, we have recently demonstrated that induction of polyP synthesis in *E. coli* is, in fact, independent of (p)ppGpp synthesis [42], although it does depend on the presence of the RNA polymerase-binding stringent transcription factor **DksA** as well as on the alternative sigma factors **RpoN** and **RpoE**, which are best known for their roles in responding to nitrogen starvation and cell envelope disruption stresses, respectively [42, 43]. We do not currently know what gene or genes regulated by these transcription factors directly influence polyP levels, since *ppk* transcription is not activated under stress conditions in *E. coli* [43], although there does appear to be transcriptional control of *ppk* in some other bacteria in response to stress [44, 45]. Our lab has also recently published a study describing point mutations in *E. coli* PPK that strongly activate polyP synthesis *in vivo* without affecting the enzyme's active site or *in vitro* activity [46] suggesting a role for some form of post-translational regulation of PPK activity, either by post-translational modification of PPK itself or by interaction with other proteins, but this remains to be tested. It has been known for some time that the phosphate transport regulators **PhoU** and **PhoB** regulate polyP accumulation in many bacteria [40, 47–49], but how they do so and whether they interact with other regulatory systems remains to be determined. In summary, as shown in Figure 1B, there is a great deal remaining to be discovered about the genes and proteins involved in controlling polyP accumulation, even in *E. coli*, which has a long history of polyP research.

Bacterial Polyphosphate and Lon Protease

One of the areas ripe for exploration is the relationship between bacterial polyP and **Lon** protease, one of the major protein-degrading enzymes of bacteria [50]. It is well

established, at least in *E. coli*, that polyP interacts with Lon. The effects of this interaction, though, remain incompletely understood. Early on, Kornberg reported that polyP activates Lon-mediated degradation of a subset of ribosomal proteins, contributing to recovery from amino acid starvation [51–53]. Recently, the Konieczny lab has shown that polyP regulates DNA replication initiation by acting on Lon during the stringent stress response in *E. coli* [54]. In this report, the researchers showed both *in vitro* and *in vivo* that polyP activates Lon protease to target and degrade the essential replication initiation protein DnaA. DnaA inhibits replication initiation when bound to ATP and stimulates replication when bound to ADP [55, 56]. Gross and Konieczny demonstrated that polyP associates with DnaA-ADP, but not with DnaA-ATP, and that this association is necessary for the Lon protease to degrade DnaA. This results in depletion of DnaA-ADP, while enriching the DnaA-ATP repressor pool. However, polyP inhibits the Lon-dependent degradation of some other proteins, including the model protein α -casein [57] and, notably, the cell division inhibitor SulA [53]. This suggests a general Lon-dependent network by which polyP accumulation inhibits cell division. PolyP, Lon, DnaA, and ribosomal proteins are all very highly conserved among bacteria, and DnaA is a conserved target for Lon degradation [58]. Importantly, Lon is implicated in multiple polyP-dependent functions, some of which will be discussed below. The mechanism by which polyP affects Lon targeting and activity is currently unknown. Further deciphering of the global effect of polyP on Lon targeting and activity, and therefore on the bacterial proteome, is essential for understanding polyP biology and represents an exciting area for future research.

Polyphosphate in pathogenic bacteria

Much of the research in the field focuses on pathogenic bacteria and how polyP is involved in disease. PolyP production is required for virulence in many pathogens [2, 3, 8, 12–14, 35], and recent research has now begun to establish more detailed molecular mechanisms for these roles. For example, one report found that polyP synthesis is essential for the virulence of *Salmonella enterica* serovar Typhimurium and its survival in *Dictyostelium discoideum*, a social amoeba used as a model for macrophage interactions [59]. The developmental cycle of *D. discoideum* progresses through three stages (aggregation, elevation, and culmination), which *S. enterica* sv. Typhimurium delays by inducing a starvation-like transcriptional response while selectively impairing expression of genes required for chemotaxis and aggregation [60–62]. *S. enterica* sv. Typhimurium, like *E. coli*, has only a single PPK1 homolog (called simply “PPK”) and lacks PPK2. The study by Varas et al found that Δppk *S. enterica* sv. Typhimurium were deficient in impairing developmental progress of *D. discoideum* [59]. Proteomic profiling of infected amoebae revealed that the WT strain triggered a robust response, including the expression of DNA repair enzymes, but the Δppk strain did not induce the expression of DNA repair enzymes. Importantly, while the WT strain was able to replicate and survive in the amoeba, the Δppk mutant was not, despite being internalized at significantly higher levels. This suggests that *S. enterica* sv. Typhimurium induces DNA damage through an unknown pathway that depends on continued bacterial survival, and that polyP synthesis is essential for this survival. What mechanisms are specifically regulated by polyP in *S. enterica* sv. Typhimurium and how those mechanisms allow it to

evade host defenses remain to be explored; however, *D. discoideum* is clearly a powerful model system for deciphering these kinds of bacterial eukaryotic interactions.

Another example of a newly-discovered role for polyP in bacterial pathogenesis is the recent report by Tang-Fichaux et al. showing that production of the DNA-damaging toxin colibactin by a variety of strains of *E. coli* is dependent on the presence of *ppk* [63]. The loss of polyP, either by deletion of *ppk* or by chemical inhibition of PPK activity with mesalamine (see The Discovery and Testing of Microbial Polyphosphate Kinase Inhibitors section below) decreased expression of the promoter driving the expression of colibactin synthesis genes, reducing the genotoxicity of *E. coli*.

There are many reports of polyP acting as a pro-virulence factor in bacteria. However, Rohlfing et al. tell a different story [64]. They investigated the role of PPK1 in *Francisella tularensis*, which possesses both PPK1 and PPK2. In *F. tularensis* major pathogenic elements are expressed from the *Francisella* Pathogenicity Island (**FPI**), which is regulated in a (p)ppGpp-dependent manner. Rohlfing et al. found that a *Appk1* mutant had higher expression of the FPI genes observed, suggesting that *ppk* expression actually antagonized *Francisella* pathogenicity. A Lon deletion strain (*Δlon*) also showed increased transcript levels of multiple virulence genes, though not to the level of the *Appk1* mutant. FPI expression in a *Δlon Appk* strain was comparable to the *Appk1* single mutant. **Western blots** revealed that the level of an FPI protein was higher in the *Δlon*, *Appk1*, and *Δlon Appk1* strains than in WT, further arguing that the expression of polyP represses the expression of FPI pathogenicity elements, likely through a Lon-dependent

mechanism. These results emphasize the importance of understanding both the polyP-Lon relationship and the individual mechanisms utilized by different pathogenic species.

Regulation of virulence gene expression and protein stability are not the only roles polyP may play in pathogenic bacteria's survival in a host. Roewe et al. have recently reported on the effect of bacterial polyP on innate host defense in an *E. coli* sepsis model in mice [34]. They found that polyP directly affects innate immune response in a chain-length dependent manner. Injecting long-chain polyP (lcPolyP, ~300–1000 phosphate units [31]), similar to that synthesized by bacterial PPK, into a host along with bacteria resulted in markedly increased mortality. High levels of polyP reduced the ability of neutrophils and macrophages to phagocytize bacteria while also reducing the expression of macrophage attracting chemokines (such as **CCL2** and **CXCL10**) and cytokines like **INF β** . Moreover, lcPolyP bound to the surfaces of macrophages and was internalized, resulting in drastic alterations to gene expression and macrophage polarization from an M1 (pro-inflammatory) to an M2 (anti-inflammatory) phenotype. Interestingly, lcPolyP not only drove a M2 phenotypic response, but it also overrode the LPS-induced M1 response by enhancing M2 genes in LPS-activated macrophages while simultaneously antagonizing M1 genes, even to the extent of impairing the expression of **iNOS** genes and the secretion of NO_2^- into the supernatant. LcPolyP also altered the type I interferon response to LPS, resulting in a less responsive macrophage population. As a final blow to the innate response, lcPolyP interfered with antigen presentation by suppressing the expression of the Major Histocompatibility Complex (**MHC**) invariant chain as well as the important costimulatory proteins **CD80** and **CD86**. Importantly, the reduction in the expression of the MHC-invariant chain was also seen *in vivo*,

demonstrating interference by lcPolyP in the interplay between the innate and adaptive immune systems.

Supporting the idea that bacterial polyP plays an important role in modulating innate immune responses, Rijal et al. have recently reported that pathogenic *Mycobacterium* species, including *M. tuberculosis* and *M. smegmatis* (both of which possess PPK1 and PPK2, although in this study only PPK1 was examined) secrete polyP and that this secreted bacterial polyP increases survival of these bacteria after phagocytosis by either human macrophages or *D. discoideum* amoeba [65]. In these experiments, polyP inhibited both phagosome acidification and lysosome activity. Intriguingly, in *D. discoideum*, the putative polyP receptor Gr1D was required for these effects, suggesting that eukaryotic cells may possess signaling pathways directly responsive to bacterial polyP. There is evidence that at least some other pro-inflammatory pathogenic bacteria can secrete or maintain substantial extracellular levels of polyP [66, 67] so, while important questions about physiological polyP concentration and sources during natural infections remain unresolved, the observation that bacterial-type polyP can repress the innate immune response is both important and informative for the study of polyP biology and suggests a molecular mechanism underlying the essentiality of polyP production for virulence in many pathogens.

Polyphosphate War: Clashing Functions in Host-Pathogen Interactions

PolyP is produced by both bacteria and eukaryotes. Not only does polyP play a role in bacterial survival, but it is also involved in host defense and repair mechanisms. For example, Suess et al. found that polyP plays multiple roles in wound healing and

leukocyte biology [22]. They demonstrated that fibrocyte differentiation depended on platelet-derived polyP and that low concentrations of polyP (1 – 2 pM) promoted fibrocyte differentiation in peripheral blood mononuclear cell (**PBMC**) cultures, while higher (30 – 125 pM) appeared to decrease fibrocyte differentiation while concurrently increasing macrophage differentiation in the absence of serum. Interestingly, they also found that 0 – 10 pM polyP gradients acted as chemoattractants for neutrophils, suggesting a novel role for recruiting neutrophils to sites of tissue damage. Finally, they found that extracellular polyP played a role in proliferation, as concentrations of 100 μ M or higher inhibited proliferation of PBMCs in vitro. In this study, Suess et al. convincingly demonstrated that polyP is highly involved in the innate response, playing roles in maturation of fibroblasts and macrophages while also acting as a chemoattractant for neutrophils into areas of inflammation.

The relationship between polyP and neutrophils takes on a new level of significance when considering neutrophilic responses to bacterial sepsis. In bacterial sepsis, neutrophils release traps composed of neutrophilic proteins (such as neutrophil elastase), DNA, and histones into the microvasculature in multiple tissues [68]. These Neutrophil Extracellular Traps (NETs) capture circulating bacteria while stimulating inflammation and coagulation in the surrounding tissue. While this serves as an effective mechanism to capture bacteria, the subsequent clotting and inflammation often cause significant tissue and organ damage.

In 2017, McDonald et al. investigated the role of NETs, **histone H4**, and polyP in sepsis induced intravascular coagulation [69]. To investigate the specific role of polyP in

the neutrophilic response and to determine if H4 histone-driven polyP release from platelet granules drove coagulation, they treated septic mice with a monoclonal blocking antibody against polyP. While blocking polyP did not affect the quantity of NETs or platelets in the microvasculature of the liver in septic mice, it significantly reduced the amount of thrombin cleavage activity and subsequent clotting, suggesting that polyP is a crucial factor in the platelet-NET-coagulation response. Taken with Suess et al.'s more recent results, a more informative - yet complicated - picture of polyP's role in the innate immune responses begins to emerge, where polyP both draws neutrophils to sites of infection to commence the innate response, while also driving the coagulation and inflammatory response in the area by regulating the activity of thrombin as well as the differentiation of macrophages and fibroblasts.

Given all of this, host polyP has become a target of great interest for potential medical treatments. One target of interest is inositol hexakisphosphate kinase I (**IP6K1**), which is known to regulate the levels of polyP produced by platelets in mice [70]. Recently, Hou et al. reported that impairing host IP6K1 substantially reduced the production of polyP from platelets, which resulted in enhanced host bacterial killing while reducing pulmonary neutrophil accumulation, thus minimizing tissue damage induced by highly active neutrophilic responses [71]. This reduction in lung damage was observed when mice were challenged with *E. coli*, *Staphylococcus aureus*, or purified LPS. The decrease in platelet-derived polyP resulted in fewer neutrophil-platelet aggregations (NPAs), which ultimately led to the reduction of neutrophil accumulation in the alveolar tissue. They found that by using an IP6K1-specific inhibitor they could induce the reduction of NPAs in both mice and a culture of human primary neutrophils

and platelets, demonstrating a clinical significance to their work. This identification of a polyP-driven immune mechanism that can be altered to enhance bacterial clearance and reduce host damage demonstrates the importance of understanding polyP on a larger scale.

In general, the data we have discussed in this section demonstrates multiple roles for polyP in host immune responses, including recruiting neutrophils, controlling fibroblast and macrophage differentiation, and altering the local microenvironmental chemistry. How this interacts with the immunomodulatory effects of polyP discussed in the previous section remains to be determined. There is clearly a delicate and complicated relationship between host and pathogen polyP usage, which has been summarized in Figure 2.

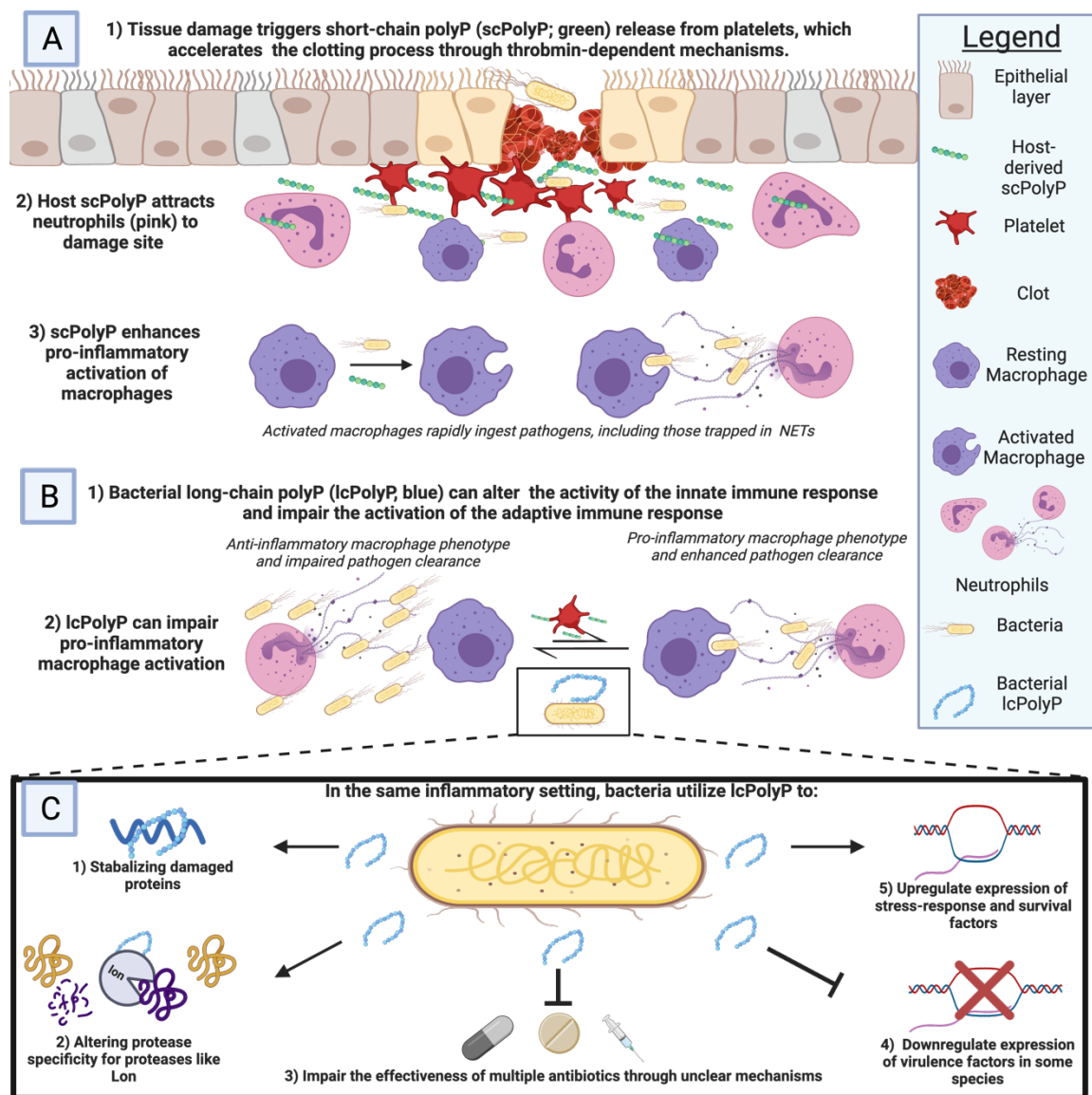


Figure 2. The PolyP Wars: The Struggle Between Host and Pathogen PolyP. A) Host polyP utilization begins as soon as damage is detected, with platelets releasing short-chain polyP (scPolyP) to accelerate thrombin-dependent clotting and neutrophil recruitment. Host polyP also drives macrophage differentiation into the pro-inflammatory M1 phenotype that facilitates rapid phagocytosis and clearance of pathogens. B) Meanwhile, pathogenic bacteria utilize long-chain polyP (lcPolyP) to impair the host immune response, driving the anti-inflammatory M2 activation of macrophages while also impairing the expression of MHC Class II molecules to hamper the adaptive immune response. C) Internally, bacteria utilize lcPolyP for a wide variety of functions from stabilizing damaged proteins to regulating expression of crucial stress response and virulence factors. The two sides clash in an age-old contest using an ancient biomolecule as their weapon of choice. Figure created using BioRender.

The Discovery and Testing of Microbial Polyphosphate Kinase Inhibitors

The enzymology of polyP production in mammals is not well understood (although one recent paper suggests that the mitochondrial **F1FO ATPase** synthesizes polyP [75]), but the well-characterized prokaryotic enzymes of microbial polyP metabolism [1] offer a unique opportunity to develop therapeutics targeting a multitude of infectious diseases. The idea that bacterial polyP metabolism could be a useful target for antimicrobial therapy is not new [76–79]. Several groups have recently reported substantial progress in this area and have identified a chemically diverse group of PPK1 inhibitors (Table 1), with exciting new data showing that bacterial polyP synthesis is targetable *in vivo* and that doing so may have useful anti-virulence effects. Only a small handful of studies have explored PPK2 as a target for inhibitors [77, 78, 80], and this remains an intriguing area for future work. Using *in silico* modeling in combination with an *in vivo* screen of *Pseudomonas aeruginosa* virulence with *D. discoideum* as a host, the Chavez lab identified five compounds that potently inhibit PPK1 *in vitro* ($IC_{50} < 10 \mu M$) and also reduce bacterial virulence, mimicking the effect of a *P. aeruginosa ppk1* knockout mutation [81], although this is complicated somewhat by the fact that *D. discoideum* is one of the few eukaryotes with a PPK1 homolog [82], and that polyP production by *D. discoideum* is involved in phagocytosis [83]. Usefully, however, the same compounds also inhibit *E. coli* PPK *in vitro* [84]. Another *in silico* screen for potential PPK inhibitors by the Bardaweel group identified two compounds that mimicked the effects of a *ppk* null mutation on both *E. coli* metabolism (as determined using the BiologTM platform) and reduced total biofilm production [85], but they did not report the effect of these compounds on *in vitro* PPK activity. In contrast, an *in vitro*

screen of bisphosphonic acid derivatives (a family of compounds which contains many clinically important enzyme inhibitors) by the Berlicki lab identified two compounds with IC50s for PPK1 of 50 – 60 μM , but did not test their effect on living bacteria [80]. Most recently, exciting new results from the Sun lab have identified two more PPK inhibitors, also from an initial *in silico* screen, that not only increase the stress sensitivity of uropathogenic *E. coli* (UPEC) under lab growth conditions, but also significantly reduce bacterial burden in an *in vivo* mouse model of UPEC infection [86]. Neither of these compounds are especially potent inhibitors of PPK activity *in vitro* (IC50 > 320 μM), but the fact that they are effective anti-virulence treatments *in vivo* is extremely encouraging. Surprisingly, none of the above studies directly measured the effect of inhibitors on bacterial polyP content, which will be an important control in future experiments.

By screening a library of FDA-approved drugs for inhibitory activity against *E. coli* PPK, the Jakob lab identified the front-line inflammatory bowel disease drug mesalamine (5-aminosalicylic acid) as a PPK inhibitor [87]. Although its inhibitory activity *in vitro* was also modest (increasing the K_m of PPK for ATP by 4-fold at 1 mM mesalamine), at concentrations comparable to those used therapeutically, mesalamine significantly reduced polyP accumulation by cultures of *E. coli*, *P. aeruginosa*, and *Vibrio cholerae*, as well as in the gut microbiota of mesalamine-treated mice and humans. The mechanism(s) by which mesalamine reduces inflammation have been debated for many years [88], but these results may suggest that, in fact, we actually have been using bacterial polyP as a therapeutic target for quite some time. It remains to be seen,

however, whether inhibiting polyP production will be a therapeutically useful strategy for dealing with other bacterial infections in humans, especially in light of the multiple roles of polyP in both host and microbe biology.

CONCLUDING REMARKS

Along with the renaissance of studies on the biology of polyP have come substantial improvements in the tools and assays for studying polyP in biological systems. These have been thoroughly reviewed recently [89], and include new and streamlined extraction and quantification techniques [90–93] as well as convenient biochemical methods for length determination and end-labeling of polyP [94, 95]. We expect that these and related technologies will be increasingly important as the community of researchers interested in polyP continues to grow.

The first description of polyP in living organisms was over a century ago [96], but our understanding of how it fits into cellular physiology has been slow in coming. There are no easy answers when studying polyP biology, but there is a bounty of questions to be explored (see Outstanding Questions), and a dynamic and growing community of researchers asking those questions. It's an exciting time for polyP, and we are eager to see what new insights will be revealed about this ancient molecule.

GLOSSARY

CCL2: C-C Motif Chemokine Ligand 2. One of several chemokine receptors utilized by monocytes and basophils to detect and direct migration towards areas with high C-C chemokine receptor 2 (CCR2) concentration.

CD80: An immunoglobulin expressed on antigen presenting cells that binds to a T cell's CD28 receptor to provide essential costimulatory signals for activation. Closely related to CD86.

CD86: An immunoglobulin expressed on antigen presenting cells that binds to a T cell's CD28 receptor to provide essential costimulatory signals for activation. Closely related to CD80.

CXCL10: A pro-inflammatory cytokine that binds to CXCR3 on monocytes, Natural Killer cells, and T cells to stimulate pleiotropic effects related to antimicrobial activity.

DksA: RNA polymerase-binding transcription factor involved in bacterial stringent response

F₁F₀ ATPase: protein complex responsible for ATP synthesis in mitochondria

FPI: *Francisella* Pathogenicity Island, genetic locus encoding multiple factors necessary for *F. tularensis* virulence

histone H4: one of the five histones involved in DNA packaging. Its presence outside of the host cell triggers immune activity as it should only be inside healthy cells.

homolog: a species-specific version of a gene or protein that is found among multiple species that share a common ancestor.

IC₅₀: concentration of an inhibitor which halves activity of the target

INF β : antiviral chemokine secreted by many immune cells. It stimulates macrophages and natural killer cells.

iNOS: inducible Nitric Oxide Synthase; produces nitric oxide which acts to regulate the host immune response

IP6K1: Canonically converts inositol hexakisphosphate to diphosphoinositol pentakisphosphate but has recently been shown to be involved in the production or regulation of mammalian polyP.

K_m: Michaelis-Menten constant; the concentration of substrate at which an enzyme acts at half its maximal velocity

Lon: major bacterial protease involved in protein turnover and regulation

LPS: lipopolysaccharide; strongly immuno-stimulatory outer membrane lipid of Gram-negative bacteria

MHC: major histocompatibility complex; utilized by cells to present antigen fragments to T and B cells

PBMC: the portion of blood cells containing the mononuclear lineages, which include the lymphocytes (T cells, B cells, NK cells) and monocytes.

PhoB: bacterial transcription factor that positively regulates phosphate uptake

PhoU: negative regulator of phosphate uptake in bacteria

(p)ppGpp: guanosine penta- and tetraphosphate; second messengers that are global regulators of starvation stress response

PPK1: or PPK, family of polyphosphate kinases, synthesizes polyP from ATP

PPK2: family of polyphosphate kinases, synthesizes polyP from NTPs

PPX: exopolyphosphatase; breaks down polyP to orthophosphate

RelA: (p)ppGpp synthase

RpoE: global regulator of bacterial cell envelope stress responses

RpoN: global regulator of bacterial nitrogen starvation stress response

RpoS: global regulator of bacterial general stress response

SpoT: (p)ppGpp synthase/hydrolase

Stringent response: bacterial starvation stress response mediated by (p)ppGpp and DksA

Western blot: technique for detecting and quantifying proteins using specific antibodies

REFERENCES

1. Achbergerova, L. and Nahalka, J. (2011) Polyphosphate--an ancient energy source and active metabolic regulator. *Microb Cell Fact* 10, 63.
2. Candon, H.L. et al. (2007) Polyphosphate kinase 1 is a pathogenesis determinant in *Campylobacter jejuni*. *J Bacteriol* 189 (22), 8099-108.
3. Cha, S.B. et al. (2012) Generation and envelope protein analysis of internalization defective *Brucella abortus* mutants in professional phagocytes, RAW 264.7. *FEMS Immunol Med Microbiol* 64 (2), 244-54.
4. Kim, K.S. et al. (2002) Inorganic polyphosphate is essential for long-term survival and virulence factors in *Shigella* and *Salmonella* spp. *Proc Natl Acad Sci U S A* 99 (11), 7675-80.
5. Kornberg, A. et al. (1999) Inorganic polyphosphate: a molecule of many functions. *Annu Rev Biochem* 68, 89-125.
6. Ogawa, N. et al. (2000) Inorganic polyphosphate in *Vibrio cholerae*: genetic, biochemical, and physiologic features. *J Bacteriol* 182 (23), 6687-93.
7. Ortiz-Severin, J. et al. (2015) Multiple antibiotic susceptibility of polyphosphate kinase mutants (ppk1 and ppk2) from *Pseudomonas aeruginosa* PAO1 as revealed by global phenotypic analysis. *Biol Res* 48, 22.
8. Peng, L. et al. (2012) Polyphosphate kinase 1 is required for the pathogenesis process of meningitic *Escherichia coli* K1 (RS218). *Future Microbiol* 7 (3), 411-23.
9. Rao, N.N. et al. (2009) Inorganic polyphosphate: essential for growth and survival. *Annu Rev Biochem* 78, 605-47.
10. Rao, N.N. and Kornberg, A. (1996) Inorganic polyphosphate supports resistance and survival of stationary-phase *Escherichia coli*. *J Bacteriol* 178 (5), 1394-400.
11. Rashid, M.H. et al. (2000) Inorganic polyphosphate is required for motility of bacterial pathogens. *J Bacteriol* 182 (1), 225-7.
12. Tunpiboonsak, S. et al. (2010) Role of a *Burkholderia pseudomallei* polyphosphate kinase in an oxidative stress response, motilities, and biofilm formation. *J Microbiol* 48 (1), 63-70.
13. Jenal, U. and Hengge-Aronis, R. (2003) Regulation by proteolysis in bacterial cells. *Curr Opin Microbiol* 6 (2), 163-72.
14. Zygmunt, M.S. et al. (2006) Identification of *Brucella melitensis* 16M genes required for bacterial survival in the caprine host. *Microbes Infect* 8 (14-15), 2849-54.
15. Schulz-Vogt, H.N. et al. (2019) Effect of large magnetotactic bacteria with polyphosphate inclusions on the phosphate profile of the suboxic zone in the Black Sea. *ISME J* 13 (5), 1198-1208.

16. Lai, Y.C. et al. (2017) Polyphosphate metabolism by purple non-sulfur bacteria and its possible application on photo-microbial fuel cell. *J Biosci Bioeng* 123 (6), 722-730.
17. Trilisenko, L. et al. (2019) The Reduced Level of Inorganic Polyphosphate Mobilizes Antioxidant and Manganese-Resistance Systems in *Saccharomyces cerevisiae*. *Cells* 8 (5).
18. Travers, R.J. et al. (2015) Polyphosphate, platelets, and coagulation. *Int J Lab Hematol* 37 Suppl 1, 31-5.
19. Morrissey, J.H. et al. (2012) Polyphosphate: an ancient molecule that links platelets, coagulation, and inflammation. *Blood* 119 (25), 5972-9.
20. Puy, C. et al. (2016) Platelet-Derived Short-Chain Polyphosphates Enhance the Inactivation of Tissue Factor Pathway Inhibitor by Activated Coagulation Factor XI. *PLoS One* 11 (10), e0165172.
21. Smith, S.A. et al. (2010) Polyphosphate exerts differential effects on blood clotting, depending on polymer size. *Blood* 116 (20), 4353-9.
22. Suess, P.M. et al. (2019) Extracellular Polyphosphate Promotes Macrophage and Fibrocyte Differentiation, Inhibits Leukocyte Proliferation, and Acts as a Chemotactic Agent for Neutrophils. *J Immunol* 203 (2), 493-499.
23. Maiolino, M. et al. (2019) Inorganic Polyphosphate Regulates AMPA and NMDA Receptors and Protects Against Glutamate Excitotoxicity via Activation of P2Y Receptors. *J Neurosci* 39 (31), 6038-6048.
24. Paula, F.S. et al. (2019) The potential for polyphosphate metabolism in Archaea and anaerobic polyphosphate formation in *Methanosarcina mazei*. *Sci Rep* 9 (1), 17101.
25. Recalde, A. et al. (2021) The Role of Polyphosphate in Motility, Adhesion, and Biofilm Formation in Sulfolobales. *Microorganisms* 9 (1).
26. Zhang, H. et al. (2002) A polyphosphate kinase (PPK2) widely conserved in bacteria. *Proc Natl Acad Sci U S A* 99 (26), 16678-83.
27. Ahn, K. and Kornberg, A. (1990) Polyphosphate kinase from *Escherichia coli*. Purification and demonstration of a phosphoenzyme intermediate. *J Biol Chem* 265 (20), 11734-9.
28. Albi, T. and Serrano, A. (2016) Inorganic polyphosphate in the microbial world. Emerging roles for a multifaceted biopolymer. *World J Microbiol Biotechnol* 32 (2), 27.
29. Kuroda, A. and Kornberg, A. (1997) Polyphosphate kinase as a nucleoside diphosphate kinase in *Escherichia coli* and *Pseudomonas aeruginosa*. *Proc Natl Acad Sci U S A* 94 (2), 439-42.
30. Kuroda, A. et al. (1999) Inorganic polyphosphate kinase is required to stimulate protein degradation and for adaptation to amino acid starvation in *Escherichia coli*. *Proc Natl Acad Sci U S A* 96 (25), 14264-9.

31. Moreno, S.N. and Docampo, R. (2013) Polyphosphate and its diverse functions in host cells and pathogens. *PLoS Pathog* 9 (5), e1003230.
32. Rashid, M.H. and Kornberg, A. (2000) Inorganic polyphosphate is needed for swimming, swarming, and twitching motilities of *Pseudomonas aeruginosa*. *Proc Natl Acad Sci U S A* 97 (9), 4885-90.
33. Rashid, M.H. et al. (2000) Polyphosphate kinase is essential for biofilm development, quorum sensing, and virulence of *Pseudomonas aeruginosa*. *Proc Natl Acad Sci U S A* 97 (17), 9636-41.
34. Roewe, J. et al. (2020) Bacterial polyphosphates interfere with the innate host defense to infection. *Nat Commun* 11 (1), 4035.
35. Srisanga, K. et al. (2019) Polyphosphate kinase 1 of *Burkholderia pseudomallei* controls quorum sensing, RpoS and host cell invasion. *J Proteomics* 194, 14-24.
36. Tiwari, P. et al. (2019) Inorganic polyphosphate accumulation suppresses the dormancy response and virulence in *Mycobacterium tuberculosis*. *J Biol Chem* 294 (28), 10819-10832.
37. Ault-Riche, D. et al. (1998) Novel assay reveals multiple pathways regulating stress-induced accumulations of inorganic polyphosphate in *Escherichia coli*. *J Bacteriol* 180 (7), 1841-7.
38. Kuroda, A. et al. (1997) Guanosine tetra- and pentaphosphate promote accumulation of inorganic polyphosphate in *Escherichia coli*. *J Biol Chem* 272 (34), 21240-3.
39. Gourse, R.L. et al. (2018) Transcriptional Responses to ppGpp and DksA. *Annu Rev Microbiol* 72, 163-184.
40. Rao, N.N. et al. (1998) Inorganic polyphosphate in *Escherichia coli*: the phosphate regulon and the stringent response. *J Bacteriol* 180 (8), 2186-93.
41. Van Melderen, L. and Wood, T.K. (2017) Commentary: What Is the Link between Stringent Response, Endoribonuclease Encoding Type II Toxin-Antitoxin Systems and Persistence? *Front Microbiol* 8, 191.
42. Gray, M.J. (2019) Inorganic Polyphosphate Accumulation in *Escherichia coli* Is Regulated by DksA but Not by (p)ppGpp. *J Bacteriol* 201 (9), e00664-18.
43. Gray, M.J. (2020) Interactions between DksA and stress-responsive alternative sigma factors control inorganic polyphosphate accumulation in *Escherichia coli*. *J Bacteriol*.
44. Munevar, N.F. et al. (2017) Differential regulation of polyphosphate genes in *Pseudomonas aeruginosa*. *Mol Genet Genomics* 292 (1), 105-116.
45. Sanyal, S. et al. (2013) Polyphosphate kinase 1, a central node in the stress response network of *Mycobacterium tuberculosis*, connects the two-component systems MprAB and SenX3-RegX3 and the extracytoplasmic function sigma factor, sigma E. *Microbiology (Reading)* 159 (Pt 10), 2074-2086.

46. Rudat, A.K. et al. (2018) Mutations in *Escherichia coli* Polyphosphate Kinase That Lead to Dramatically Increased In Vivo Polyphosphate Levels. *J Bacteriol* 200 (6), e00697-17.
47. Morohoshi, T. et al. (2002) Accumulation of inorganic polyphosphate in *phoU* mutants of *Escherichia coli* and *Synechocystis* sp. strain PCC6803. *Appl Environ Microbiol* 68 (8), 4107-10.
48. de Almeida, L.G. et al. (2015) *phoU* inactivation in *Pseudomonas aeruginosa* enhances accumulation of ppGpp and polyphosphate. *Appl Environ Microbiol* 81 (9), 3006-15.
49. Grillo-Puertas, M. et al. (2016) *PhoB* activation in non-limiting phosphate condition by the maintenance of high polyphosphate levels in the stationary phase inhibits biofilm formation in *Escherichia coli*. *Microbiology (Reading)* 162 (6), 1000-1008.
50. Cho, Y. et al. (2015) Individual and collective contributions of chaperoning and degradation to protein homeostasis in *E. coli*. *Cell Rep* 11 (2), 321-33.
51. Kuroda, A. (2006) A polyphosphate-lon protease complex in the adaptation of *Escherichia coli* to amino acid starvation. *Biosci Biotechnol Biochem* 70 (2), 325-31.
52. Kuroda, A. et al. (2001) Role of inorganic polyphosphate in promoting ribosomal protein degradation by the Lon protease in *E. coli*. *Science* 293 (5530), 705-8.
53. Nomura, K. et al. (2004) Effects of inorganic polyphosphate on the proteolytic and DNA-binding activities of Lon in *Escherichia coli*. *J Biol Chem* 279 (33), 34406-10.
54. Gross, M.H. and Konieczny, I. (2020) Polyphosphate induces the proteolysis of ADP-bound fraction of initiator to inhibit DNA replication initiation upon stress in *Escherichia coli*. *Nucleic Acids Res* 48 (10), 5457-5466.
55. Kurokawa, K. et al. (1999) Replication cycle-coordinated change of the adenine nucleotide-bound forms of DnaA protein in *Escherichia coli*. *EMBO J* 18 (23), 6642-52.
56. Speck, C. et al. (1999) ATP- and ADP-dnaA protein, a molecular switch in gene regulation. *EMBO J* 18 (21), 6169-76.
57. Osbourne, D.O. et al. (2014) Polyphosphate, cyclic AMP, guanosine tetraphosphate, and c-di-GMP reduce in vitro Lon activity. *Bioengineered* 5 (4), 264-8.
58. Liu, J. et al. (2019) Lon recognition of the replication initiator DnaA requires a bipartite degon. *Mol Microbiol* 111 (1), 176-186.
59. Varas, M.A. et al. (2018) Inorganic Polyphosphate Is Essential for *Salmonella Typhimurium* Virulence and Survival in *Dictyostelium discoideum*. *Front Cell Infect Microbiol* 8, 8.
60. Bozzaro, S. and Eichinger, L. (2011) The professional phagocyte *Dictyostelium discoideum* as a model host for bacterial pathogens. *Curr Drug Targets* 12 (7), 942-54.
61. Loomis, W.F. (1996) Genetic networks that regulate development in *Dictyostelium* cells. *Microbiol Rev* 60 (1), 135-50.

62. Sillo, A. et al. (2011) Salmonella typhimurium is pathogenic for Dictyostelium cells and subverts the starvation response. Cell Microbiol 13 (11), 1793-811.
63. Tang-Fichaux, M. et al. (2020) The Polyphosphate Kinase of Escherichia coli Is Required for Full Production of the Genotoxin Colibactin. mSphere 5 (6).
64. Rohlfing, A.E. et al. (2018) Polyphosphate Kinase Antagonizes Virulence Gene Expression in Francisella tularensis. J Bacteriol 200 (3).
65. Rijal, R. et al. (2020) Polyphosphate is an extracellular signal that can facilitate bacterial survival in eukaryotic cells. Proceedings of the National Academy of Sciences, 202012009.
66. Neilands, J. and Kinnby, B. (2020) Porphyromonas gingivalis initiates coagulation and secretes polyphosphates - A mechanism for sustaining chronic inflammation? Microb Pathog, 104648.
67. Noegel, A. and Gotschlich, E.C. (1983) Isolation of a high molecular weight polyphosphate from Neisseria gonorrhoeae. J Exp Med 157 (6), 2049-60.
68. Brinkmann, V. et al. (2004) Neutrophil extracellular traps kill bacteria. Science 303 (5663), 1532-5.
69. McDonald, B. et al. (2017) Platelets and neutrophil extracellular traps collaborate to promote intravascular coagulation during sepsis in mice. Blood 129 (10), 1357-1367.
70. Ghosh, S. et al. (2013) Inositol hexakisphosphate kinase 1 maintains hemostasis in mice by regulating platelet polyphosphate levels. Blood 122 (8), 1478-86.
71. Hou, Q. et al. (2018) Inhibition of IP6K1 suppresses neutrophil-mediated pulmonary damage in bacterial pneumonia. Sci Transl Med 10 (435).
72. Almeida, V.H. et al. (2019) Novel Aspects of Extracellular Vesicles as Mediators of Cancer-Associated Thrombosis. Cells 8 (7).
73. Kulakovskaya, E.V. et al. (2018) Inorganic Polyphosphate and Cancer. Biochemistry (Mosc) 83 (8), 961-968.
74. Zhang, C.M. et al. (2019) Possible mechanisms of polyphosphate-induced amyloid fibril formation of beta2-microglobulin. Proc Natl Acad Sci U S A 116 (26), 12833-12838.
75. Baev, A.Y. et al. (2020) Inorganic polyphosphate is produced and hydrolyzed in F0F1-ATP synthase of mammalian mitochondria. Biochem J 477 (8), 1515-1524.
76. Kornberg, A., Novel Antimicrobial Therapies, KORNBERG ARTHUR, US, 2002.
77. Shum, K.T. et al. (2011) Aptamer-mediated inhibition of Mycobacterium tuberculosis polyphosphate kinase 2. Biochemistry 50 (15), 3261-71.
78. Singh, M. et al. (2016) Establishing Virulence Associated Polyphosphate Kinase 2 as a drug target for Mycobacterium tuberculosis. Sci Rep 6, 26900.

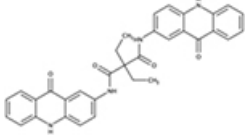
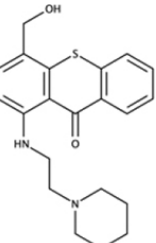
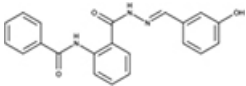
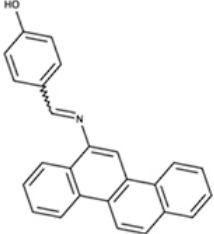
79. Gautam, L.K. et al. (2019) Bacterial Polyphosphate Kinases Revisited: Role in Pathogenesis and Therapeutic Potential. *Curr Drug Targets* 20 (3), 292-301.
80. Burda-Grabowska, M. et al. (2019) Bisphosphonic acids and related compounds as inhibitors of nucleotide- and polyphosphate-processing enzymes: A PPK1 and PPK2 case study. *Chem Biol Drug Des* 93 (6), 1197-1206.
81. Bravo-Toncio, C. et al. (2016) *Dictyostelium discoideum* as a surrogate host-microbe model for antivirulence screening in *Pseudomonas aeruginosa* PAO1. *Int J Antimicrob Agents* 47 (5), 403-9.
82. Gomez-Garcia, M.R. and Kornberg, A. (2004) Formation of an actin-like filament concurrent with the enzymatic synthesis of inorganic polyphosphate. *Proc Natl Acad Sci U S A* 101 (45), 15876-80.
83. Zhang, H. et al. (2005) Inorganic polyphosphate in *Dictyostelium discoideum*: influence on development, sporulation, and predation. *Proc Natl Acad Sci U S A* 102 (8), 2731-5.
84. Campos, F. et al. (2019) Fluorescence enzymatic assay for bacterial polyphosphate kinase 1 (PPK1) as a platform for screening antivirulence molecules. *Infect Drug Resist* 12, 2237-2242.
85. Bashatwah, R.M. et al. (2018) Discovery of potent polyphosphate kinase 1 (PPK1) inhibitors using structure-based exploration of PPK1 Pharmacophoric space coupled with docking analyses. *J Mol Recognit* 31 (10), e2726.
86. Peng, L. et al. (2020) Discovery and antibacterial study of potential PPK1 inhibitors against uropathogenic *E. coli*. *J Enzyme Inhib Med Chem* 35 (1), 1224-1232.
87. Dahl, J.U. et al. (2017) The anti-inflammatory drug mesalamine targets bacterial polyphosphate accumulation. *Nat Microbiol* 2, 16267.
88. Hauso, O. et al. (2015) 5-Aminosalicylic acid, a specific drug for ulcerative colitis. *Scand J Gastroenterol* 50 (8), 933-41.
89. Christ, J.J. et al. (2020) Methods for the Analysis of Polyphosphate in the Life Sciences. *Anal Chem* 92 (6), 4167-4176.
90. Christ, J.J. and Blank, L.M. (2018) Enzymatic quantification and length determination of polyphosphate down to a chain length of two. *Anal Biochem* 548, 82-90.
91. Christ, J.J. and Blank, L.M. (2018) Analytical polyphosphate extraction from *Saccharomyces cerevisiae*. *Anal Biochem* 563, 71-78.
92. Pokhrel, A. et al. (2019) Assaying for Inorganic Polyphosphate in Bacteria. *J Vis Exp* (143).
93. Dahl, J.-U. et al. (2018) Extraction and Quantification of Polyphosphate (polyP) from Gram-negative Bacteria. *Bioprotocol* 8 (18), e3011.

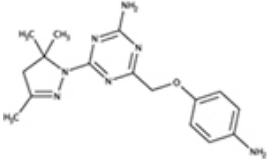
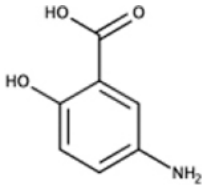
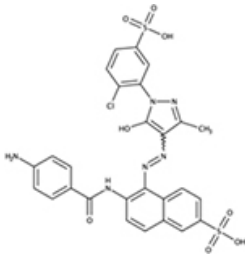
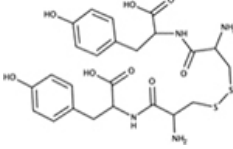
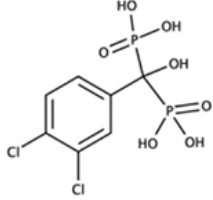
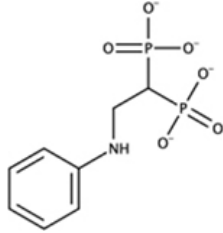
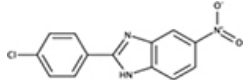
94. Smith, S.A. et al. (2018) DNA ladders can be used to size polyphosphate resolved by polyacrylamide gel electrophoresis. *Electrophoresis*.
95. Baker, C.J. et al. (2020) Diversification of polyphosphate end-labeling via bridging molecules. *PLoS One* 15 (8), e0237849.
96. Meyer, A. (1904) Orientierende Untersuchungen ueber Verbreitung, Morphologie, und Chemie des Volutins. *Bot Zeit.* 62, 113-152.

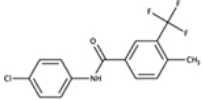
TABLES

Table 1. Structures and Activities of PPK1 Inhibitors

^a+++ = IC₅₀ < 10 μM, ++ = IC₅₀ < 70 μM, + = IC₅₀ > 100 μM, ND = not determined.

Structure	Chemical ID	Target Species	<i>In Vitro</i> PPK1 Inhibition ^a	<i>In Vivo</i> Effects
	NSC618160	<i>P. aeruginosa</i>	+++	modestly reduced virulence in <i>D. discoideum</i> [81]
	NSC166366	<i>P. aeruginosa</i>	+++	reduced virulence in <i>D. discoideum</i> [81]
	NSC205574	<i>P. aeruginosa</i>	+++	strongly reduced virulence in <i>D. discoideum</i> [81]
	NSC141672	<i>P. aeruginosa</i>	+++	strongly reduced virulence in <i>D. discoideum</i> [81]

Structure	Chemical ID	Target Species	<i>In Vitro</i> PPK1 Inhibition ^a	<i>In Vivo</i> Effects
	NSC696924	<i>P. aeruginosa</i>	+++	strongly reduced virulence in <i>D. discoideum</i> [81]
	mesalamine (5-amino-salicylic acid)	<i>E. coli</i>	+	reduced polyP, mimics <i>ppk</i> phenotypes [87]
	NSC75963	<i>E. coli</i>	ND	mimics <i>ppk</i> phenotypes [85]
	NSC333714	<i>E. coli</i>	ND	mimics <i>ppk</i> phenotypes [85]
	[(3,4-dichlorophenyl)(hydroxy)phosphonomethyl]phosphonate	<i>E. coli</i>	++	ND [80]
	[2-(phenylamino)-1-phosphonoethyl]phosphonate	<i>E. coli</i>	++	ND [80]
	2-(4-chlorophenyl)-5-nitro-1H-benzo[d]imidazole	<i>E. coli</i>	+	mimics <i>ppk</i> phenotypes, treats UPEC infections [86]

Structure	Chemical ID	Target Species	<i>In Vitro</i> PPK1 Inhibition ^a	<i>In Vivo</i> Effects
	N-(4-chlorophenyl)-4-methyl-3-(trifluoromethyl)benzamide	<i>E. coli</i>	+	mimics <i>ppk</i> phenotypes, treats UPEC infections [86]

THE ROLE OF NITROGEN-RESPONSIVE REGULATORS IN CONTROLLING
INORGANIC POLYPHOSPHATE SYNTHESIS IN ESCHERICHIA COLI

by

MARVIN Q BOWLIN, ABAGAIL R LONG, JOSHUA T HUFFINES, AND MICHAEL
J GRAY

Microbiology 2022;168:001185

Copyright

2022

By

The Authors

Used by permission

Format adapted for dissertation and errata corrected

ABSTRACT

Inorganic polyphosphate (polyP) is synthesized by bacteria under stressful environmental conditions and acts by a variety of mechanisms to promote cell survival. While the kinase that synthesizes polyP (PPK, encoded by the *ppk* gene) is well known, *ppk* transcription is not activated by environmental stress and little is understood about how environmental stress signals lead to polyP accumulation. Previous work has shown that the transcriptional regulators DksA, RpoN (σ^{54}) and RpoE (σ^{24}) positively regulate polyP production, but not *ppk* transcription, in *Escherichia coli*. In this work, we examine the role of the alternative sigma factor RpoN and nitrogen starvation stress response pathways in controlling polyP synthesis. We show that the RpoN enhancer binding proteins GlnG and GlnR impact polyP production, and uncover a new role for the nitrogen phosphotransferase regulator PtsN (EIIA^{Ntr}) as a positive regulator of polyP production, acting upstream of DksA, downstream of RpoN and apparently independently of RpoE. However, neither these regulatory proteins nor common nitrogen metabolites appear to act directly on PPK, and the precise mechanism(s) by which polyP production is modulated after stress remain(s) unclear. Unexpectedly, we also found that the genes that impact polyP production vary depending on the composition of the rich media in which the cells were grown before exposure to polyP-inducing stress. These results constitute progress towards deciphering the regulatory networks driving polyP production under stress, and highlight the remarkable complexity of this regulation and its connections to a broad range of stress-sensing pathways.

INTRODUCTION

Inorganic polyphosphate (polyP) is a linear polymer of 3–1000 phosphate units that is produced by organisms of all domains of life [1–3]. Bacterial polyP is well known to be important for stress response through diverse mechanisms, including roles in metal chelation [4, 5], resistance to oxidants [6], unfolded and damaged protein stabilization [7], and DNA metabolism [8–10], and plays a major role in virulence in many pathogens [6, 11, 12]. Recent work has also begun to decipher the molecular mechanisms by which bacterial polyP directly disrupts phagocytic cell functions important in the host immune response to bacterial infections [13–17]. These results have led to a growing interest in polyP metabolism and the recent identification of a range of chemicals that inhibit the bacterial polyP kinases (PPKs) responsible for polyP synthesis as promising potential anti-virulence drug candidates [13, 18–21].

Despite this, relatively little is known about how polyP production is regulated in bacteria. In the model organism *Escherichia coli*, polyP is undetectable during exponential growth in rich media, but is synthesized rapidly upon exposure to a variety of stress conditions, including severe oxidative stress, heat shock, salt stress and multiple types of starvation stresses [22–24]. Early work identified a few regulators in *E. coli* that affected polyP synthesis under different conditions, but did not establish the mechanisms by which these acted [22, 25, 26]. In *E. coli*, PPK and the polyP-degrading enzyme exopolyPase (PPX) are encoded in a bicistronic *ppk–ppx* operon [27] whose transcription does not increase upon stress treatment [23, 28, 29].

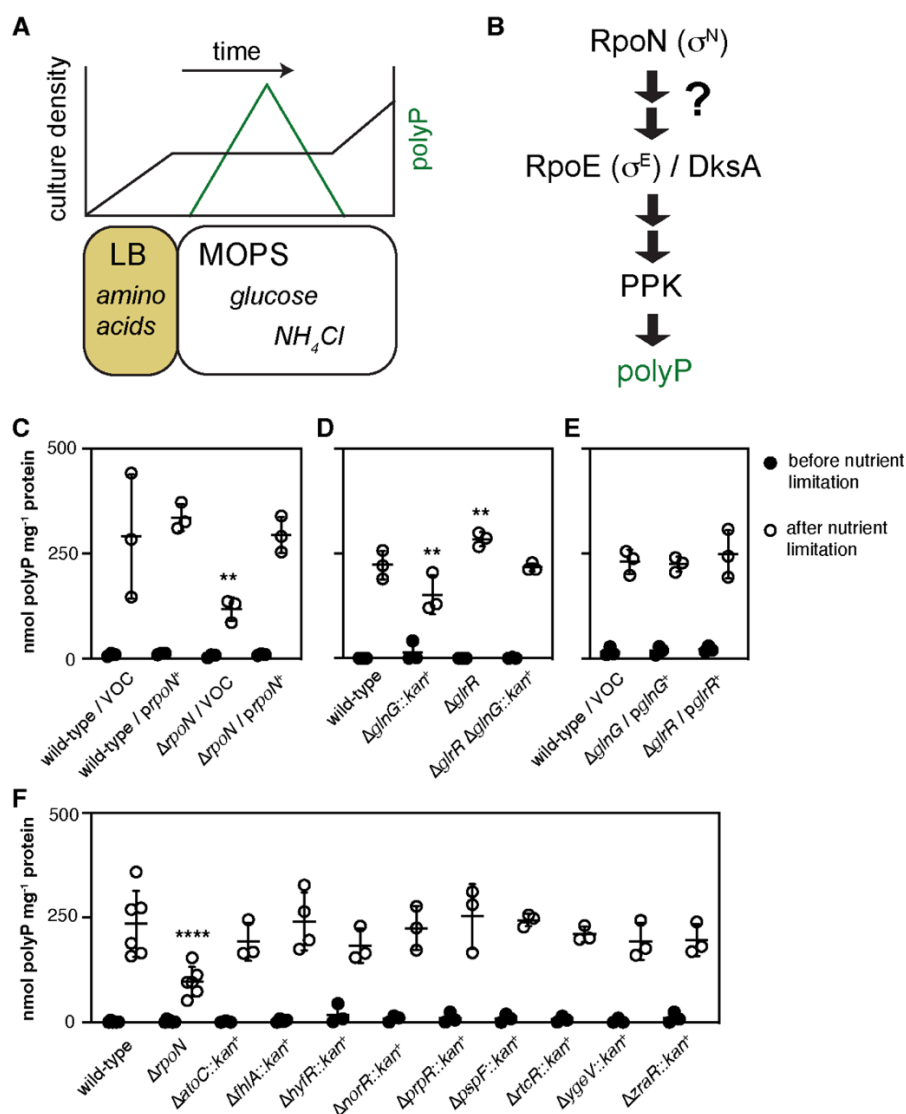


Fig. 1. The RpoN bEBPs GlnG and GlrR Influence PolyP Production. (a) Illustration of the polyP-inducing nutrient limitation protocol. (b) Relationships between known regulators of polyP production in *E. coli*. (c) PolyP concentrations in *E. coli* MG1655 wild-type or Δ rpoN730 containing either pBAD24 (Vector Only Control, VOC) or pRpoN (prpoN⁺) plasmids before (black circles) or 2 h after (white circles) nutrient limitation (n=3, mean±sd). (d) PolyP concentrations in MG1655 wild-type, Δ glnG730::kan⁺, Δ glrR728 or Δ glrR728 Δ glnG730::kan⁺ before (black circles) or 2h after (white circles) nutrient limitation (n=3, mean±sd). (f) PolyP concentrations in MG1655 wild-type, Δ rpoN730, Δ atoC774::kan⁺, Δ hyfR739::kan⁺, Δ norR784::kan⁺, Δ prpR772::kan⁺, Δ pspF739::kan⁺, Δ rtcR755::kan⁺, Δ ygeV720::kan⁺ or Δ zraR775::kan⁺ before (black circles) or 2 h after (white circles) nutrient limitation (n=3–6, mean±sd). Asterisks indicate polyP levels significantly different from those of the wild-type control for a given experiment (two-way repeated-measures ANOVA with Holm–Sidak’s multiple comparisons test; **P<0.01, ****P<0.0001).

One of the most robust polyP-inducing stresses is nutrient limitation (Fig. 1a) [22, 28–30]. In this procedure, exponentially growing cells in LB rich medium, in which the primary carbon and nitrogen sources are amino acids, are resuspended in MOPS minimal medium with glucose as the sole carbon source and ammonium chloride as the sole nitrogen source. As with other polyP- inducing stresses, this results in growth arrest and accumulation of polyP, followed by degradation of polyP and resumption of growth some hours later [22, 23, 30]. Although nutrient limitation is technically straightforward, transcriptomics reveal sweeping genome-wide gene expression changes [28], and reverse genetic approaches have identified roles for multiple stress response regulators in polyP accumulation under these conditions. These include the RNA polymerase-binding protein DksA [30] and the stress-responsive alternative sigma factors RpoE and RpoN (Fig. 1b) [28]. These observations led us to hypothesize that these transcription factors regulate the expression of genes or proteins responsible for directly activating PPK under stress conditions.

The experiments described in this paper were aimed at deciphering the role of RpoN-dependent genes in polyP regulation. RpoN is the *E. coli* σ^{54} -family sigma factor, and is notable for requiring additional ATPase proteins for activation of transcription at specific promoters [31, 32]. These bacterial enhancer binding proteins (bEBPs) control specific and well-defined regulons in *E. coli* [33], and we hypothesized that by determining which bEBP(s) were necessary for polyP production we would be able to identify relevant polyP-inducing signals and potential RpoN-dependent polyP regulators.

In the course of testing this hypothesis, we discovered that the bEBP GlnG, involved in the classical nitrogen starvation response in *E. coli* [34], is a positive regulator of polyP synthesis, but that this activity and the effect of RpoN on polyP synthesis are suppressed by the presence of glutamine or other preferred nitrogen sources in the rich medium before nutrient limitation, growth conditions under which polyP is not being produced. The cell envelope stress-sensing bEBP GlnR [35–37], by contrast, acted as a negative regulator of polyP synthesis. By examining additional RpoN-linked nitrogen-responsive regulatory systems in *E. coli*, we identified an important role for the nitrogen phosphotransferase regulator PtsN (EIIA^{Ntr}) [38] as an activator of polyP synthesis that acts downstream of RpoN, upstream of DksA and apparently independently of RpoE.

METHODS

Bacterial strains, growth conditions and molecular methods

All strains and plasmids used in this study are listed in Table 1. We carried out DNA manipulations by standard methods [39, 40] in the *E. coli* cloning strain DH5 α (Invitrogen) and grew *E. coli* at 37°C in Lysogeny Broth (LB) [41] containing 5g NaCl l⁻¹ and, where indicated, l-glutamine, l-glutamate or NH₄Cl (5mM unless otherwise indicated), Starvation Medium (SM) with or without 20mM NH₄Cl [22], or M9 minimal medium (pH 5.8) [40, 42]. LB supplemented with glutamine is referred to as LBQ. We prepared fresh glutamine stock solutions each day. We added antibiotics when appropriate: ampicillin (100 μ g ml⁻¹), chloramphenicol (17 or 35 μ g ml⁻¹) or kanamycin (25 or 50 μ g ml⁻¹). We constructed, maintained, and tested all *rpoE* mutant strains in media containing erythromycin at 10 μ g ml⁻¹ [43].

Databases and primer design

We obtained information about *E. coli* genes, proteins and regulatory networks from the Integrated Microbial Genomes database [44], EcoCyc [33] and RegulonDB [45]. We designed PCR and sequencing primers with Web Primer (www.candidagenome.org/cgi-bin/compute/web-primer) or SnapGene version 5.3.2 (Insightful Science), and mutagenic primers with PrimerX (www.bioinformatics.org/primerx/index.htm). We designed all primers used for quantitative (q)PCR with Primer Quest [www.idtdna.com; parameter set ‘qPCR 2 primers intercalating dyes’ for quantitative reverse transcriptase (qRT)-PCR primer design] and confirmed specificity and amplification efficiencies for each primer pair of close to 1. These primers are listed in Table 2.

Strain Construction

Unless otherwise indicated, all *E. coli* strains were derivatives of wild-type strain MG1655 ($F^- \lambda^-$, *rph-1 ilvG⁻ rfb-50*) [46], and we confirmed all chromosomal mutations by PCR.

We used P1 vir transduction [30, 47] to move gene knockout alleles from the Keio collection [48] into MG1655, generating strains MJG1955 ($\Delta glrR728::kan^+$), MJG1956 ($\Delta atoC774::kan^+$), MJG1969 ($\Delta hyfR739::kan^+$), MJG1970 ($\Delta spsF739::kan^+$), MJG1971 ($\Delta norR784::kan^+$), MJG1972 ($\Delta ygeV720::kan^+$), MJG1973 ($\Delta rtcR755::kan^+$), MJG1974 ($\Delta prpR772::kan^+$), MJG1975 ($\Delta zraR775::kan^+$), MJG1976 ($\Delta fhIA735::kan^+$), MJG2058 ($\Delta glnB727::kan^+$), MJG2061 ($\Delta glnK736::kan^+$), MJG2064 ($\Delta glnG730::kan^+$), MJG2086 ($\Delta ptsN732::kan^+$), MJG2090 ($\Delta npr-734::kan^+$), MJG2091 ($\Delta ptsP753::kan^+$) and MJG2112

($\Delta rapZ733::kan^+$). We resolved the insertions [49] in MJG1955, MJG2058, MJG2086 and MJG2112 to give strains MJG2065 ($\Delta glrR728$), MJG2082 ($\Delta glnB727$), MJG2089 ($\Delta ptsN732$) and MJG2114 ($\Delta rapZ733$), then transduced MJG2065 and MJG2082 with $\Delta glnG730::kan^+$ and $\Delta glnK736::kan^+$, respectively, to yield strains MJG2068 ($\Delta glrR728 \Delta glnG730::kan^+$) and MJG2083 ($\Delta glnB727 \Delta glnK736::kan^+$). Strains lacking both *glnB* and *glnK* are glutamine auxotrophs [50] and were constructed and maintained on LBQ.

We replaced the *glmZ* and *glmY* genes of strain MG1655 with pKD3-derived chloramphenicol resistance cassettes by recombineering [49], using primers 5' AAGTGTTAAGGGATGTTATTTCCCGATTCTCTGTGGCATAATAAACGAGTAGT GTA GGCTGGAGCTGCTTC 3' and 5' CTTCTGATACATAAAAAACGCCTGCTCTTATTACGGAGCAGGCGTTAAAC ATAT GAATATCCTCCTTAG 3', or 5' TTACCAAACACTATTTTCTTTATTGGCACAGTTACTGCATAATAGTAACCAGTGT GTA GGCTGGAGCTGCTTC 3' and 5' TCGTCAGACGCGAATAGCCTGATGCTAACCGAGGGGAAGTTCAGATACAACC ATAT GAATATCCTCCTTAG 3', to yield strains MJG2151 ($\Delta glmZ1000::cat^+$) and MJG2155 ($\Delta glmY1000::cat^+$).

We fused a 3xFLAG tag to the C terminus of the chromosomal *ptsN* gene by recombineering [51]. We amplified the 3xFLAG sequence and kanamycin resistance cassette from plasmid pSUB11 [51] with primers 5' GAAGAGCTGTATCAAATCAT TACGGATACCGAAGGTACTCCGGATGAAGCGGACTACAAAGACCATGACGG 3' and 5' TACCATGTACTGTTC

TCCTCACAACGTCTAAAAGAGACATTACCGAATAACATATGAATATCCTCCTT
 AG 3' and electroporated the resulting PCR product into MG1655 expressing λ Red
 recombinase from plasmid pKD46 [49], generating strain MJG2179 (*ptsN-3xFLAG*
kan⁺). We then resolved the kanamycin resistance cassette in MJG2179 with plasmid
 pCP20 [49] to yield strain MJG2191 (*ptsN-3xFLAG*). We used P1vir transduction [30,
 47] to move the Δ *phoP790::kan⁺* allele from the Keio collection [48] into MJG2191,
 generating strain MJG2193 (*ptsN-3xFLAG* Δ *phoP790::kan⁺*). We amplified the
 Δ *rpoN730::kan⁺* allele from strain MJG1763 with primers 5'
 TACAAGACGAACACGTTA 3' and 5' TTTGGCAAATTTGGCTGT 3' and used
 recombineering [49] to insert this locus into strain MJG2191, generating strain MJG2200
 (Δ *rpoN730::kan⁺* *ptsN-3xFLAG*), which we then resolved [49] to generate strain
 MJG2202 (Δ *rpoN730* *ptsN-3xFLAG*).

Plasmid construction

Plasmid pRpoN was a gift from Dr Joseph Wade (NY State Department of
 Health) [52].

We amplified the *glnK* CDS (339 bp) plus 20 bp of upstream sequence from *E.*
coli MG1655 genomic DNA with primers 5' TTCG
 AATTCATTCTGACCGGAGGGGATCTAT 3' and 5'
 CTTAAGCTTTTACAGCGCCGCTTCGTC 3' and cloned it into the EcoRI and HindIII
 sites of plasmid pBAD18 [53] to generate plasmid pGLNK1. We amplified the *glnB*
 coding sequence (CDS) (339 bp) plus 11 bp of upstream sequence and the *glnS* CDS
 (1830 bp) plus 25 bp of upstream sequence from *E. coli* MG1655 genomic DNA with

primers 5' TTTGGGCTAGCGAATTCCAAGGAATAGCATGAAAAAGATTGA 3' and 5' CAAAACAG CCAAGCTTTTAAATTGCCGCGTCGTC 3' or 5' TTTGGGCTAGCGAATTCACGATATAAATCGGAATCAAAAACACTATG 3' and 5' CAAAACAGCCAAGCTTTTACTCAACCGTAACCGATTTTGC 3' and then inserted each gene between the EcoRI and HindIII sites of plasmid pBAD18 (amplified with primers 5' AAGCTTGGCTGTTTTGGC 3' and 5' GAATTCGCTAGC CCAAAAAAAC 3') by *in vivo* assembly cloning [54] to generate plasmids pGLNB1 and pGLMS1, respectively. We amplified the *glnG* CDS (1410 bp) plus 20 bp of upstream sequence from *E. coli* MG1655 genomic DNA with primers 5' TTTGGGCTAGCG AATTCAGGAAATAAAGGTGACGTTTATGC 3' and 5' CAAAACAGCCAAGCTTTCCTCCATCCCCAGCTCTTTTA 3'. We amplified the *glrR* CDS (1335 bp) plus 20 bp of upstream sequence from *E. coli* MG1655 genomic DNA with primers 5' TTTG GGCTAGCGAATTCCACCCATGAGGTCCTCCTGA 3' and 5' CAAAACAGCCAAGCTTTCATTCCTTGAATCGTTTG C 3'. We then cloned the resulting products between the EcoRI and HindIII sites of plasmid pBAD18 (amplified with primers 5' AAGCTTGGCTGTTTTGGC 3' and 5' GAATTCGCTAGCCCAAAAAA C 3') by *in vivo* assembly cloning [54] to generate plasmids pGLNG1 and pGLRR1, respectively.

Plasmid pPPK33, encoding PPK with a C-terminal GAAEPEA peptide tag for affinity purification [55] between the NdeI and HindIII sites of plasmid pET-21b(+)(Novagen) was synthesized by GenScript.

We amplified the *ptsN* CDS (492bp) plus 20bp of upstream sequence from *E. coli* MG1655 genomic DNA with primers 5'

CTCTCTACTGTTTCTCCATACCCGTTTTTTTTGGGCTAGCGGCAGGTTCTTAGGT
GAAATTATGACAAATAATGATACA 3' and 5'

TATCAGGCTGAAAATCTTCTCTCATCCGCCAAAACAGCCACTACGCTTCATCC
GGAGTACCT 3' and inserted it between the EcoRI and HindIII sites of plasmid

pBAD18 by *in vivo* assembly cloning [54] to generate plasmid pPTSN1. We used single
primer site-directed mutagenesis [56] to mutate pPTSN1 with primers 5'

CAATGGTATTGCCATTCCGGAAGGCAAA CTGGAAGAAGATAC 3' or 5'

GGTATTGCCATTCCGGCGGGCAAACCTGGAAGAAG 3'. This yielded pPTSN2,

containing a *ptsN*^{C217G, T219A} allele (encoding PtsN^{H73E}), and pPTSN3, containing a

ptsN^{C217G, A218C, T219G} allele (encoding PtsN^{H73A}).

We amplified the dimerizing leucine zipper domain of GCN4 (105 bp) from

Saccharomyces cerevisiae genomic DNA with primers 5'

TCCGGATCCCTTGCAAAGAATGAAACAACCTTGAAG 3' and 5'

ACCGGTACCCGGCGTTCGCCAACTAATTTCT 3' and cloned it into the BamHI and
KpnI sites of plasmid pKT25 [57] to yield plasmid pGCN4zip1 and into the BamHI and

KpnI sites of plasmid pUT18 [57] to yield plasmid pGCN4zip3. We amplified the *ppk*
CDS with no stop codon (2084 bp) from *E. coli* MG1655 genomic DNA with primers 5'

CAGCTGCAGGGATGGGTCAGGAAAAGCTATAACATCG 3' and 5' TCCGGATC

CTCTTCAGGTTGTTTCGAGTGATTTG 3' and cloned it into the PstI and BamHI sites

of plasmid pKNT25 [57] to yield plasmid pPPK12 or into the PstI and BamHI sites of

plasmid pKT25 [57] to yield plasmid pPPK13. We amplified the *ptsN* CDS (493 bp)

from plasmid pPTSN1 with primers 5'

CACTGCAGGATGACAAATAATGATACAACCTCTACAGCTTA 3' and 5'

TGAATTCG ACTACGCTTCATCCGGAGTAC 3', amplified pUT18C [57] with primers 5' GAAGCGTAGTCGAATTCATCGATATAAC TAAGTAATATGGTG 3' and 5' TATTTGTCATCCTGCAGTGGCGTTCCAC 3', and joined the resulting products by *in vivo* assembly [54], yielding plasmid pPTS_{N5}.

In vivo polyphosphate assay

We extracted and quantified polyP from bacterial cultures as previously described [58]. To induce polyP synthesis by nutrient limitation [22, 28], we grew *E. coli* strains in 10 mL rich medium (LB with or without additional supplements as indicated) at 37°C with shaking (200r.p.m.) to A_{600} of 0.2–0.4, then harvested 1 mL samples by centrifugation, resuspended them in 250 μ L of 4 M guanidine isothiocyanate and 50 mM Tris-HCl (pH 7), lysed by incubation for 10 min at 95 °C, then immediately froze them at –80 °C. We harvested 5 mL of each LB culture by centrifugation (5 min at 4696 g at room temperature), rinsed once with 5 mL PBS, then re-centrifuged and resuspended in 5 mL MOPS minimal medium (Teknova) [59] containing 0.1 mM K_2HPO_4 , and 0.1 mM uracil and 4 g glucose l^{-1} [30]. We incubated these cultures for 2 h at 37 °C with shaking, then collected additional samples as described above. For experiments involving arabinose-inducible plasmids, we added arabinose (2 g l^{-1}) to both the rich and minimal media. We determined the protein concentrations of thawed samples by a Bradford assay (Bio-Rad), then mixed with 250 μ L of 95% ethanol, applied to an EconoSpin silica spin column (Epoch Life Science), rinsed with 750 μ L 5 mM Tris-HCl, pH 7.5, 50 mM NaCl, 5 mM EDTA, 50% ethanol, and eluted with 150 μ L 50 mM Tris-HCl, pH 8. We brought the eluate to 20 mM Tris-HCl, pH 7.5, 5 mM $MgCl_2$, 50 mM ammonium acetate with 1

μg of *Saccharomyces cerevisiae* exopolyphosphatase PPX1 [60] in a final volume of 200 μl , incubated for 15 min at 37 °C, then measured the resulting polyP-derived orthophosphate using a colorimetric assay [61] and normalized to total protein content. For all figures, we report polyP concentrations in terms of individual phosphate monomers.

Quantitative RT-PCR

At the indicated time points after nutrient limitation, we harvested 1 ml of cells by centrifugation and resuspended in RNAlater (ThermoFisher) for storage at -20 °C. We extracted RNA using the RiboPure RNA Purification Kit for bacteria (Ambion) following the manufacturer's instructions, including DNase treatment to remove contaminating genomic DNA, then used the SuperScript IV VILO kit (ThermoFisher) to reverse transcribe cDNA from mRNA, following the manufacturer's instructions and including a no-RT control for each reaction. We calculated changes in gene expression using the $2^{-\Delta\Delta C_t}$ method [62], normalizing to *yqfB*, whose expression does not change under these polyP induction conditions [28], as an internal expression control.

PPK overexpression and purification

C-tagged PPK was overexpressed and purified by a modification of a previously published protocol [23]. Overnight cultures (50 ml) of BL21(DE3) containing pPPK33 were subcultured into 1 l of Protein Expression Medium (PEM; 12 g tryptone l^{-1} , 24 g yeast extract l^{-1} , 4% v/v glycerol, 2.314 g KH_2PO_4 l^{-1} , 12.54 g l^{-1} K_2HPO_4)

supplemented with 10 mM MgCl₂ and 100 µg ampicillin ml⁻¹. The culture was grown at 37 °C with shaking until an A₆₀₀ of 0.8, then shifted to 20 °C and cooled for 1 h.

Following the cool-down period, PPK expression was induced by the addition of 150 µM IPTG. Overexpression was allowed to proceed overnight at 20 °C with shaking. The overexpression culture was pelleted at 6000 g, resuspended in 100 ml of Buffer A (50 mM Tris-HCl pH 7.5, 10% w/v sucrose) with 300 µg lysozyme ml⁻¹, and incubated on ice for 45 min, pelleted at 16000 g for 10 min, and then the pellet was resuspended in 50 ml of Buffer B (Buffer A+5 mM MgCl₂ +30 U ml⁻¹ Pierce Universal Nuclease + 1 Pierce Protease Inhibitor cocktail tablet) and lysed by sonication (5s on, 5s off for 5min at 50% amplitude). The sonicated lysate was pelleted at 20,000 g for 1 h at 4 °C, and the pellet was resuspended in 25 ml of C-tag Binding Buffer (20 mM Tris-HCl, pH 7.4) plus solid KCl to 1 M final concentration. 1 M Na₂CO₃ was added at a 1:10 dilution to the resuspension, and the salt extraction was incubated at 4 °C for 30 min with stirring. Following incubation, the solution was sonicated in 5 s pulses for 2 min, then pelleted at 20,000 g for 1 h at 4°C. The supernatant was diluted 1:1 with cold H₂O and loaded onto a C-tag Affinity Column (ThermoFisher) equilibrated with C-tag Binding Buffer. The column was washed with 10 column volumes of C-tag Binding Buffer and PPK was eluted with a gradient of 0–100% C-tag Elution Buffer (20 mM Tris-HCl pH 7.4, 2 M MgCl₂) with an ÄKTA Start FPLC (Cytiva Life Sciences). Fractions containing pure PPK were pooled and dialysed against PPK Storage Buffer (20 mM HEPES-KOH pH 8.0, 150 mM NaCl, 15% glycerol, 1 mM EDTA) at 4 °C and stored at -80 °C.

In vitro assay of PPK activity

We determined the specific activity for polyP synthesis by PPK as previously described [29]. Reactions (125 μ l total volume) contained 5 nM PPK, 50 mM HEPES-KOH (pH 7.5), 50 mM ammonium sulphate, 5 mM MgCl₂, 20 mM creatine phosphate and 60 μ g creatine kinase ml⁻¹. Where indicated, reactions also contained 100 mM freshly prepared l-glutamate (pH 7.5), 10 mM l-glutamine (pH 7.5), 1 mM fructose 6-phosphate, 1mM glucosamine 6-phosphate, or 5 or 10mM α -ketoglutarate (pH 7.5), concentrations chosen to represent the high end of the physiological range for each compound in *E. coli* [63]. We prewarmed reactions to 37 °C, then started them by addition of MgCl₂ and ATP to final concentrations of 6 mM. We removed aliquots (20 μ l) at 1, 2, 3 and 4 min and diluted them into 80 μ l of a stop solution containing 62.5 mM EDTA and 50 μ M DAPI in black 96-well plates, then measured steady-state polyP-DAPI fluorescence of these samples (ex. 415 nm, em. 600 nm) [21] in an Infinite M1000 Pro microplate reader (Tecan Group). We determined the polyP content of each sample (calculated in terms of individual phosphate monomers) by comparison to a standard curve of commercially available polyP (Acros Organics) (0–150 μ M) prepared in the buffer described above containing 6 mM MgATP and calculated rates of polyP synthesis by linear regression (Prism 9; GraphPad Software).

Bacterial two-hybrid protein interaction assay

We assessed protein interactions *in vivo* using the BACTH procedure [57]. Briefly, we grew derivatives of *E. coli cya* strain BTH101 containing plasmids expressing fusions of proteins of interest to the T18 or T25 complementary fragments of *Bordetella*

pertussis adenylate cyclase overnight in LB and then evaluated β -galactosidase activity of these strains either by spotting overnight cultures on LB plates containing ampicillin, kanamycin, 0.5 mM IPTG, and 40 μg X-Gal ml^{-1} and incubating for 2 days at 30 °C or, for quantitative measurements, using a single-step assay [64]: after 24 h of growth at 37 °C in LB broth containing ampicillin, kanamycin, and 0.5 mM IPTG we harvested 80 μl of cells by centrifugation, resuspended them in 200 μl of 60 mM Na_2HPO_4 , 40 mM NaH_2PO_4 , 10 mM KCl, 1 mM MgSO_4 , 36 mM β -mercaptoethanol, 1.1 mg ONPG ml^{-1} , 1.25 mg lysozyme ml^{-1} and 6.7% PopCulture reagent (Novagen) in a 96-well plate, and then measured A_{600} and A_{420} over time at 24 °C in an Infinite M1000 Pro microplate reader (Tecan Group). We calculated Miller Units according to the formula $(1000 \times (A_{420}/\text{min})) / (\text{initial } A_{600} \times \text{culture volume (ml)})$.

Quantitative western blotting

E. coli strains with chromosomal ptsN-3xFLAG fusions were grown and stressed by nutrient limitation as described above. At the indicated time points, 1 ml aliquots were harvested by centrifugation and resuspended in 100 μl of 50 mM Tris-HCl (pH 8), 150 mM NaCl, 1 % Triton X-100 containing 1 \times HALT protease inhibitor cocktail (ThermoFisher), then incubated at 95 °C for 10 min to lyse the cells. Lysates were stored at -80 °C until use. Aliquots of each sample were thawed on ice, mixed 1:1 with fresh lysis buffer, then mixed 4:1 with reducing loading dye (250 mM Tris-HCl pH 6.8, 10 % SDS, 0.008 % bromophenol blue, 40% glycerol, 2.8 M β -mercaptoethanol). Western blots were prepared and analyzed as described previously [65, 66] with few exceptions. Briefly, lysate samples were loaded on an AnykDa Stain-Free SDS-PAGE gel (BioRad)

and run until the dye front neared the bottom of the gel. Gels were then transferred to a PVDF membrane (BioRad) using a TurboBlot semi-dry transfer system, then blocked in StartingBlock T20 TBS blocking buffer (ThermoFisher) overnight. Blots were blocked for 30 min at room temperature, then incubated in a 1:25000 dilution of rabbit anti-RecA antibody (Abcam Cat. no. ab63797) in the blocking buffer for 1 h at room temperature. Blots were washed in three times in TBST, then incubated for 1h at room temperature in blocking buffer containing a 1:10000 dilution of goat anti-rabbit IgG H+L HRP-conjugated (Abcam Cat. no. ab63797). Blots were washed again in 3× TBST then incubated in blocking buffer containing a 1:5000 dilution of rabbit anti-DDDDK horseradish peroxidase (HRP)-conjugated antibody (Abcam Cat. no. ab2493). Blots were washed three times with TBST and once with TBS, then developed using the BioRad Clarity ECL Substrate kit and imaged on a BioRad Gel Doc. Images were analyzed in ImageJ [67] by taking same-area measurements of each RecA band or PtsN band, blank correcting the mean grey values (signal) using same-area measurements matched to the respective band, and normalizing the PtsN signal to RecA signal.

Statistical analyses

We used GraphPad Prism version 9.2 (GraphPad Software) to perform statistical analyses, including two-way repeated- measures ANOVA with Holm–Sidak’s multiple comparison tests. Repeated-measures ANOVA cannot handle missing values, so we analyzed data sets with samples having different n numbers (e.g. Fig. 1f) with an equivalent mixed model which uses a compound symmetry covariance matrix and is fit

using Restricted Maximum Likelihood (REML) (without Geisser–Green-House correction).

Data Availability

All strains and plasmids generated in the course of this work are available from the authors upon request.

RESULTS

Nutrient limitation activates the nitrogen starvation response

Nitrogen starvation, which has been studied extensively in *E. coli* and other enterobacteria, decreases the ratio of intracellular glutamine to glutamate and triggers accumulation of α -ketoglutarate [34, 68, 69]. This leads to a characteristic RpoN- and GlnG-dependent activation of transcription of the PII protein gene *glnK* [34, 70, 71]. Strong upregulation of *glnK* after nutrient limitation (Fig. S1, available in the online version of this article) indicates that our polyP-inducing nutrient limitation protocol (Fig. 1a) activated this response, although it is notable that nitrogen starvation alone does not robustly induce polyP accumulation (Fig. S2) [22], reinforcing the multifactorial nature of polyP regulation. We have previously shown that ectopic expression of *dksA* or *rpoE* rescue polyP production in a $\Delta rpoN$ mutant, but not vice versa [28], indicating that RpoN acts upstream of DksA and RpoE in polyP regulation (Fig. 1b), but the RpoN-regulated genes involved are not yet known.

The RpoN bEBPs GlnG and GlrR influence polyP production

As we have previously reported [28], $\Delta rpoN$ mutant *E. coli* had a significant defect in polyP synthesis upon nutrient limitation stress (Fig. 1c). Expression of *rpoN* from a plasmid rescued this phenotype, but did not increase polyP production in a wild-type strain (Fig. 1c). RpoN-dependent promoters require bEBPs [31, 32], so to narrow down the identity of the RpoN-dependent gene(s) involved in polyP synthesis, we measured polyP production in mutants lacking each of the 11 bEBPs present in *E. coli* MG1655 [33] (Fig. 1d, f). Mutants lacking *glnG* (also known as *ntrC*) [34] had a defect in polyP production comparable to that of a $\Delta rpoN$ mutant and mutants lacking *glrR* produced significantly more polyP than the wild-type (Fig. 1d). These phenotypes cancelled each other out, and a $\Delta glrR \Delta glnG$ double mutant produced an amount of polyP indistinguishable from the wild-type.

Notably, although the $\Delta glrR$ mutant produced significantly more polyP after nutrient limitation than the wild-type, it did not accumulate detectable polyP before nutrient limitation. This is similar to the phenotype of a Δppx mutant, which lacks the dominant polyP-degrading enzyme of *E. coli* [30], and suggests a model in which there is a factor or factors dominant to *glrR* and *ppx* that represses polyP accumulation and/or PPK activity during growth in rich media.

Complementation of either the $\Delta glnG$ or the $\Delta glrR$ mutants with plasmids encoding the respective knocked out genes restored wild-type polyP levels (Fig. 1e), but overexpressing *glnG* or *glrR* in wild-type *E. coli* had no significant effect on polyP accumulation (Fig. S3). No other bEBP mutations affected the extent of polyP synthesis under these conditions (Fig. 1f).

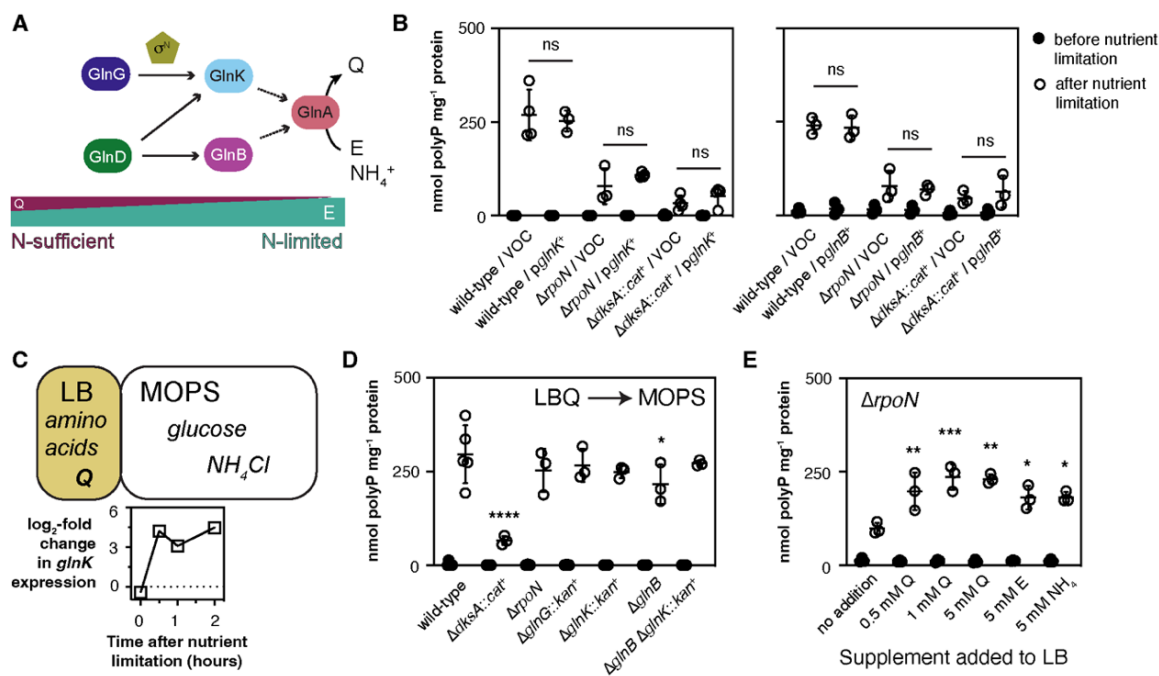


Fig. 2. RpoN-Dependent Regulation of PolyP Synthesis Is Dependent on Cellular Nitrogen Status, but Not on GlnB or GlnK. (a) Simplified model of the regulation of GlnA (glutamine synthetase) activity in response to changes in the intracellular glutamate (E) to glutamine (Q) ratio. (b) PolyP concentrations in *E. coli* MG1655 wild-type, $\Delta rpoN730$ or $\Delta dksA1000::cat^+$ containing either pBAD18 (+), pGLNK1 (*glnK*⁺) or pGLNB1 (*glnB*⁺) plasmids before (black circles) or 2 h after (white circles) nutrient limitation ($n=3-4$, mean \pm sd). (c) Illustration of polyP-inducing nutrient limitation protocol modified to add 5 mM glutamine (Q) to the LB broth. Small bottom panel shows qRT-PCR measurement of *glnK* expression after Q-enriched nutrient limitation. (d) PolyP concentrations in MG1655 wild-type, $\Delta dksA1000::cat^+$, $\Delta rpoN732$, $\Delta glnG730::kan^+$, $\Delta glnK736::kan^+$, $\Delta glnB727$ or $\Delta glnB727 \Delta glnK736::kan^+$ before (black circles) or 2 h after (white circles) Q-enriched nutrient limitation ($n=3-5$, mean \pm sd). (e) PolyP concentrations in $\Delta rpoN732$ before (black circles) or 2 h after (white circles) nutrient limitation from LB media supplemented with glutamine (Q), glutamate (E), or NH₄Cl as indicated ($n=3$, mean \pm sd). Asterisks indicate polyP levels significantly different from those of the wild-type or untreated control for a given experiment (two-way repeated-measures ANOVA with Holm-Sidak's multiple comparisons test, ns=not significant, * $P<0.05$, ** $P<0.01$, *** $P<0.001$, **** $P<0.0001$).

RpoN-dependent regulation of polyP synthesis is dependent on cellular nitrogen status, but not on GlnB or GlnK directly

The involvement of GlnG in polyP synthesis implicates the cellular response to nitrogen starvation in polyP regulation [34], which was not unexpected based on previous

reports in the literature [8, 22]. Under nitrogen limitation conditions, glutamine synthase (GlnA) is activated by a pathway involving the PII signalling proteins GlnB and GlnK [34, 50, 71–73] (Fig. 2a). Transcription of *glnB* is constitutive, but *glnK* transcription is activated by RpoN and GlnG [34, 70, 71] (Fig. 2a). We therefore hypothesized that GlnK or GlnB, which regulate the activity of a variety of proteins by direct interaction [34, 72, 74–76], might be activators of polyP synthesis. To test this idea and to determine whether any such regulation might bypass or be independent of the requirement for DksA in polyP production (Fig. 1b), we expressed *glnB* and *glnK* from arabinose-inducible plasmids, but found that neither *glnB* nor *glnK* overexpression increased polyP production in wild-type, $\Delta rpoN$ or $\Delta dksA$ mutant strains (Fig. 2b).

Mutants lacking both *glnB* and *glnK* are glutamine auxotrophs [77], and LB, the rich medium used for the ‘before stress’ growth condition (Fig. 1a) [22], is naturally very low in glutamine (Fig. S4) [78], so we tested whether $\Delta glnB$, $\Delta glnK$ or $\Delta glnBK$ mutations affected polyP production after nutrient shift from rich media supplemented with glutamine (LBQ; Fig. 2c). A shift from LBQ to minimal media activated *glnK* expression even more strongly than a shift from LB (Fig. 2c, bottom panel). There was a very slight defect in polyP production in the $\Delta glnB$ mutant under these conditions, but the more surprising result was that, although the extent of polyP production after shift from LBQ into minimal medium was very similar to that after shift from LB (Fig. 2d), neither *rpoN* nor *glnG* mutants had any defect in polyP synthesis under these conditions. This was unexpected and showed that cellular nitrogen status affects the regulatory pathway by which polyP synthesis is activated. This observation suggests that the very high variability in polyP production we have previously reported in a $\Delta glnG$ mutant [30] may

be due to different glutamine concentrations in different batches of LB medium. This was not true for the $\Delta dksA$ mutant [28, 30], which was defective in polyP synthesis regardless of whether the LB was supplemented with glutamine (Fig. 2d). PolyP accumulation by the $\Delta rpoN$ mutant also increased after nutrient shift from LB supplemented with lower concentrations of glutamine (0.5 or 1 mM) and also from LB supplemented with 5 mM of either glutamate or NH_4Cl (Fig. 2e), albeit to a lesser extent, indicating that growth on other high-quality nitrogen sources could also rescue this phenotype.

GlmS regulation has minimal impact on polyP production

The bEBP GlrR is activated by GlrK, a histidine kinase that responds to cell envelope disruptions [35]. In *E. coli* MG1655, whose transcriptome has been extensively characterized [45], GlrR is only known to regulate the expression of two promoters, that of the operon encoding the alternative sigma factor RpoE and that of the sRNA *glmY* [36, 37] (Fig. 3a). We have previously reported that $\Delta rpoE$ mutants have significant defects in polyP synthesis, indicating that RpoE is a positive regulator of polyP production [28]. Regulation of the *rpoE* operon is complex [37, 79, 80], but GlrR is an activator of *rpoE* expression [37], so it is difficult to reconcile a model in which this explains the increase in polyP production in the $\Delta glrR$ mutant (Fig. 1d). We therefore turned our attention to *glmY*, which, in a pathway involving the RNA-binding protein RapZ and the sRNA *glmZ*, is responsible for increasing GlmS (glutamine–fructose 6-phosphate aminotransferase) synthesis under conditions where intracellular glucosamine 6-phosphate (GlcN6P) becomes limiting [36, 81, 82] (Fig. 3a).

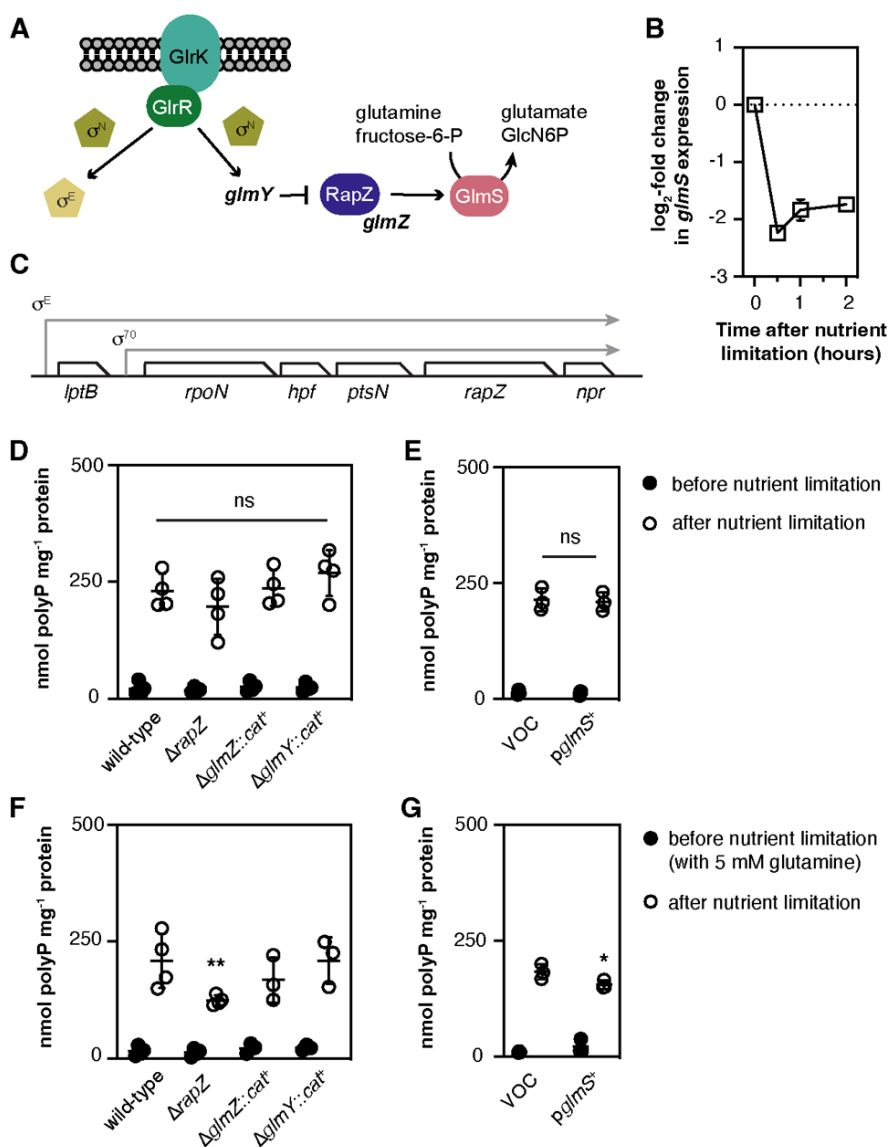


Fig. 3. GlmS Regulation Has Minimal Impact on PolyP Production. (a) Diagram of GlrR-dependent regulation in *E. coli*. (b) qRT-PCR measurement of *glmS* expression after nutrient limitation ($n=3$, mean \pm sd). (c) Diagram of the *rpoN* operon in *E. coli*. (d) PolyP concentrations in *E. coli* MG1655 wild-type, $\Delta rapZ733$, $\Delta glmZ1000::cat^+$ or $\Delta glmY1000::cat^+$ before (black circles) or 2 h after (white circles) nutrient limitation ($n=4$, mean \pm sd). (e) PolyP concentrations in MG1655 wild-type containing plasmids pBAD18 (VOC) or pGLMS1 ($pglmS^+$) before (black circles) or 2 h after (white circles) nutrient limitation ($n=3$, \pm sd). (f, g) Identical to panels (d) and (e), except for the addition of glutamine to the LB medium. Asterisks indicate polyP levels significantly different from those of the wild-type or VOC for a given experiment (two-way repeated-measures ANOVA with Holm–Sidak’s multiple comparisons test, ns=not significant, $*P<0.05$, $**P<0.01$).

GlcN6P, synthesized by GlmS from glutamine and fructose 6-phosphate (F6P), is an essential precursor of the peptidoglycan cell wall [83, 84], and so is linked to both cell envelope stress and cellular nitrogen status. Nutrient limitation led to a 4-fold decrease in *glmS* expression (Fig. 3b). The *rapZ* gene is part of the *rpoN* operon (Fig. 3c). However, deletion of *rapZ*, *glmY* or *glmZ* had no impact on polyP synthesis after nutrient limitation (Fig. 3d), and neither did overexpression of *glmS* in wild-type *E. coli* (Fig. 3e). PolyP production was slightly but significantly reduced in the $\Delta rapZ$ mutant and the *glmS* overexpression strain after nutrient limitation of cells grown in LBQ (Fig. 3f, g), but neither *glmZ* nor *glmY* mutations had any effect, suggesting that GlmS regulation has, at most, indirect effects on polyP synthesis.

Ptsn positively regulates polyP synthesis, acting upstream of dksA and downstream of Rpon

The nitrogen phosphotransferase system (PTS^{Ntr}) is a regulatory cascade that responds to nitrogen limitation and regulates the activity of multiple proteins in *Enterobacteriaceae* (Fig. 4a) [42, 85–89]. The genes encoding PtsN (also known as EIIA^{Ntr}) and NPr, homologues of the EIIA and HPr proteins of the well-characterized carbon PTS [90], are encoded in the *rpoN* operon (Fig. 3c) [38]. PtsP (also known as EI^{Ntr}), which is homologous to EI of the carbon PTS [38, 90], responds to both glutamine and α -ketoglutarate as signals of cellular nitrogen limitation by autophosphorylation [69, 91], ultimately resulting in phosphorylation of NPr and PtsN [92]. Both NPr and PtsN interact with and regulate the activity of a variety of proteins, typically depending on their phosphorylation states [42, 85–89]. Mutants lacking *ptsN* were defective in polyP synthesis, regardless of glutamine supplementation (Fig. 4b, c).

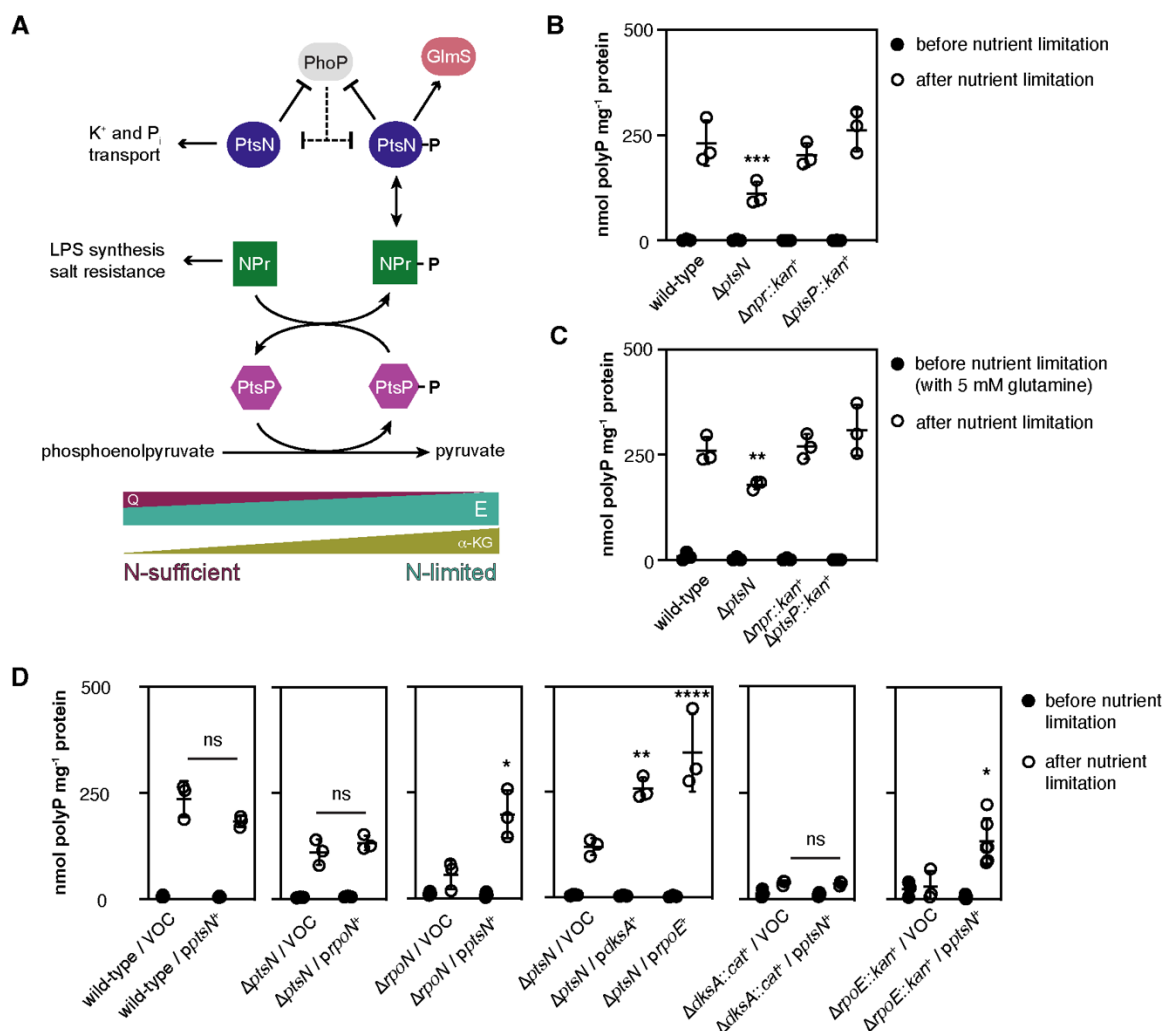


Fig. 4. PtsN Positively Regulates PolyP Production. (a) Diagram of the nitrogen phosphotransferase system of *E. coli*. (b) PolyP concentrations in MG1655 wild-type, $\Delta ptsN732$, $\Delta npr-734::kan^+$ or $\Delta ptsP753::kan^+$ before (black circles) or 2h after (white circles) nutrient limitation (n=3, mean \pm sd). (c) Identical to panel (b), except for the addition of glutamine to the LB medium. (d) PolyP concentrations in MG1655 wild-type, $\Delta ptsN732$, $\Delta rpoN730$, $\Delta dksA1000::cat^+$ or $\Delta rpoE1000::kan^+$ +the indicated plasmids [VOC is pBAD24 for pRpoN (*prpoN*⁺) and pBAD18 for all other experiments; *pptsN*⁺ is pPTS_{N1}, *pdksA*⁺ is pDKSA1, and *prpoE*⁺ is pRPOE1] before (black circles) or 2h after (white circles) nutrient limitation (n=3–6, mean \pm sd). Asterisks indicate polyP levels significantly different from those of the wild-type or VOC for a given experiment (two-way repeated-measures ANOVA with Holm–Sidak’s multiple comparisons test, ns=not significant, *P<0.05, **P<0.01, ***P<0.001, ****P<0.0001).

Ectopic expression of *ptsN* in wild-type *E. coli* had no effect on polyP accumulation (Fig. 4d). Ectopic expression of *rpoN* in a $\Delta ptsN$ mutant, as we saw in a

wild-type background (Fig. 1c), also did not increase polyP production, but expression of *ptsN* did increase polyP production in a $\Delta rpoN$ mutant, indicating that PtsN acts downstream of RpoN (Fig. 4d). Similar experiments with *dksA* and *rpoE*, aimed at determining the relationships between regulators of polyP, indicate that PtsN acts upstream of DksA, and apparently independently of RpoE, since expression of PtsN can increase polyP production in a $\Delta rpoE$ mutant and expression of RpoE increases polyP production in a $\Delta ptsN$ strain (Fig. 4d). We have previously shown that ectopic expression of either *dksA* or *rpoE* increases polyP accumulation in wild-type *E. coli* [28, 30].

Ptsn regulation of polyP synthesis is not dependent on Ptsn phosphorylation state, changes in Ptsn abundance or direct interaction with PPK

The fact that the defect in polyP production in a $\Delta ptsN$ mutant was not seen in Δnpr or $\Delta ptsP$ mutants (Fig. 4b, c) suggested that PtsN phosphorylation was not important for this phenotype. Indeed, both the non-phosphorylatable PtsN^{H73A} variant and the phosphorylated form-mimicking PtsN^{H73E} variant [93, 94] complemented the polyP defect of a $\Delta ptsN$ mutant as well as did wild-type PtsN (Fig. 5a). In *Salmonella*, PtsN inhibits PhoP binding to DNA, and in turn, PhoP regulates the proteolytic degradation of PtsN, leading to a decrease in PtsN protein concentration under PhoP-activating conditions [42]. Both abundance and phosphorylation of PtsN are therefore potential variables in any PtsN-dependent regulatory system. We constructed strains encoding chromosomal fusions of the 3xFLAG epitope tag to the C terminus of PtsN [42] to allow us to determine whether our polyP-inducing stress conditions led to changes in PtsN abundance in *E. coli*, normalized to the abundance of RecA, which does not change after nutrient limitation (Fig. S5). There was no significant change in PtsN abundance after

nutrient limitation in either wild-type or $\Delta phoP$ strains (Fig. 5b, c). There was a small, but significant increase in PtsN abundance 2 h after nutrient limitation in a $\Delta rpoN$ mutant (Fig. 5d), but this increase did not correlate with polyP accumulation, which is lower in this strain (Fig. 1c). These results argue against a role for PtsN abundance in polyP regulation in *E. coli*. PtsN regulates other proteins by direct physical interaction [42, 85–89], so we used a bacterial two-hybrid assay [57] to test whether PtsN interacts with PPK *in vivo*, and found no evidence for such an interaction (Fig. 5e). Proteomic assessments of the *E. coli* protein interactome have also not identified any such interactions [95–98].

Nitrogen metabolites do not allosterically regulate PPK activity

The data above show that RpoN, GlnG and PtsN, all of which are known to respond to changes in cellular nitrogen status, impact polyP production, but do not clearly identify regulatory links with PPK. One possibility we considered is that the observed changes in polyP accumulation might be due to direct allosteric regulation of PPK by nitrogen metabolites and that changes in polyP in various nitrogen response mutants might be due to indirect impacts of changes in these metabolites. However, the specific activity of purified PPK *in vitro* was not affected by physiological concentrations [63] of glutamate, glutamine (Fig. S7a), F6P, GlcN6P (Fig. S7b) or α -ketoglutarate (Fig. S7c), eliminating this possibility.

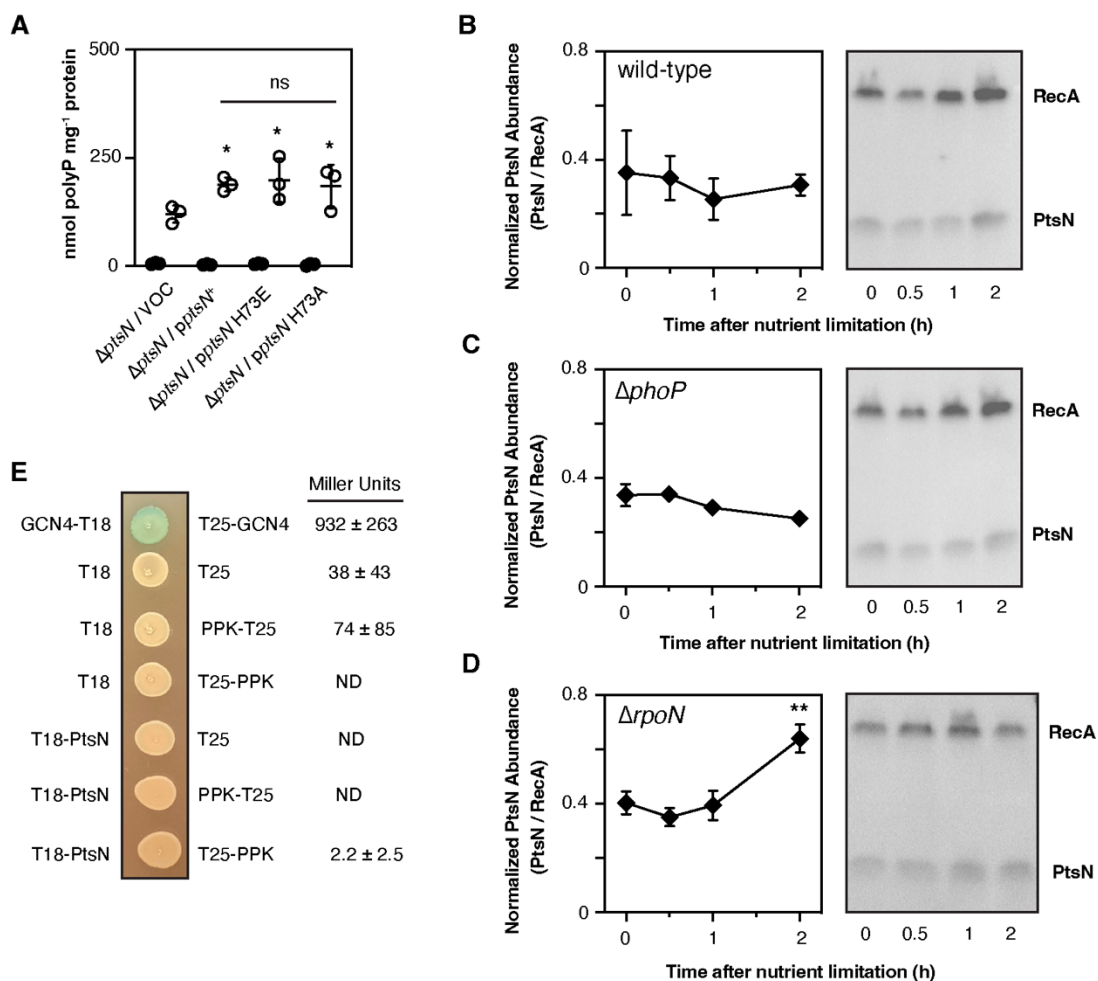


Fig. 5. PtsN Regulation of PolyP Synthesis Is Not Dependent on PtsN Phosphorylation State, Changes in PtsN Abundance or Direct Interaction with PPK. (a) PolyP concentrations in *E. coli* $\Delta ptsN732$ containing either pBAD18 (VOC), pPTNS1 (*pptsN*⁺), pPTNS2 (*pptsN* H73E) or pPTNS3 (*pptsN* H73A) before (black circles) or 2 h after (white circles) nutrient limitation ($n=3$, mean \pm sd). Asterisks indicate polyP levels significantly different from those of the VOC; there were no significant differences among the other three strains (two-way repeated-measures ANOVA with Holm–Sidak’s multiple comparisons test, ns=not significant * $P<0.05$). (b) *ptsN*-3xFLAG, (c) $\Delta phoP$ *ptsN*-3xFLAG, and (d) $\Delta rpoN$ *ptsN*-3xFLAG strains were subjected to nutrient limitation. At the indicated time points, protein samples ($n=3$, mean \pm sd) were collected and immunoblotted to quantify the ratio of PtsN-3xFLAG to control protein RecA. Representative blots are shown. Full gels are shown in Fig. S6. Asterisks indicate normalized PtsN levels significantly different from those of the wild-type at the indicated time point (two-way repeated-measures ANOVA with Holm–Sidak’s multiple comparisons test, ** $P<0.01$). (e) *E. coli* BTH101 (*cya*⁻) containing plasmids expressing the indicated protein fusions were grown overnight in LB and either spotted on LB medium containing 0.5 mM IPTG and 40 μ g X-Gal ml⁻¹ or lysed for quantitative assay of β -galactosidase activity ($n=3$, mean \pm sd; ND=not detectable).

DISCUSSION

It is perhaps unsurprising that the regulation of polyP synthesis is complex, given the ancient evolutionary roots of polyP [3, 6, 99, 100] and the intricacy of the regulatory networks for other general stress response pathways in bacteria. In *E. coli*, for example, there are at least 20 regulators of the stress-responsive sigma factor RpoS known at the time of writing, acting at the transcriptional, post-transcriptional and post-translational levels [33, 101, 102]. Cell envelope stress responses are equally complex and involve a variety of interacting and overlapping pathways and regulons, the details of which are still not fully understood [80, 103].

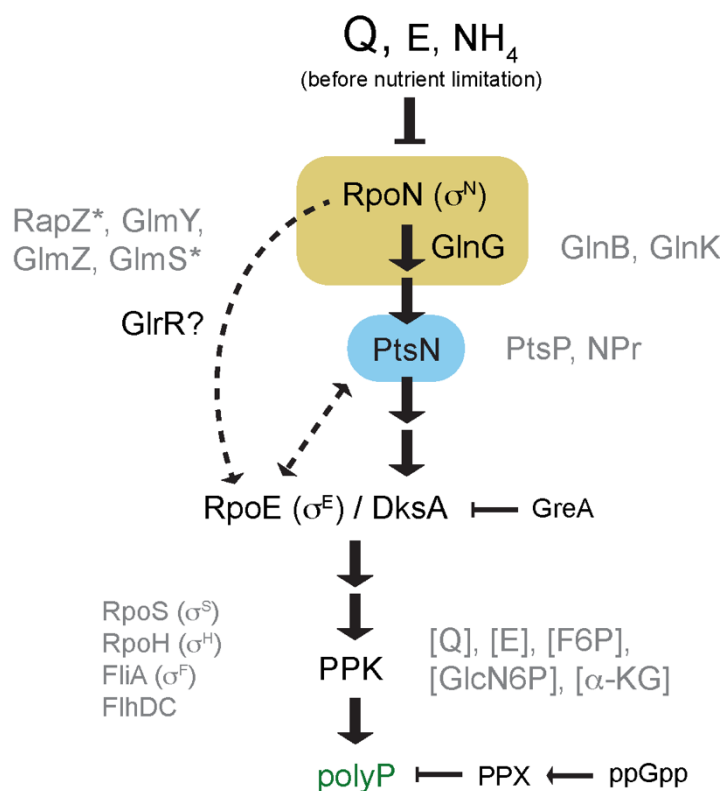


Fig. 6. Current Model for PolyP Regulation in *E. coli*. Proteins and metabolites indicated in grey are now known to not play roles in regulating polyP synthesis after nutrient limitation, with asterisks indicating proteins that may have minor conditional effects (RapZ and GlmS). Dashed lines indicate possible polyP-impacting regulatory relationships between RpoN/GlnR, PtsN and RpoE.

Work from our lab and others [22, 23, 26, 28–30, 104] has nevertheless made considerable progress towards understanding polyP regulation in *E. coli*, although much of that progress has been, like Thomas Edison’s famous comment on the invention of the light bulb, in identifying a large number of ways in which polyP regulation doesn’t work (Fig. 6). PolyP regulation, for example, does not require the sigma factors RpoS, RpoH or FliA, or the global regulator FlhDC [28], and the stringent response alarmone ppGpp is involved only in modulating PPX activity and is not required for induction of polyP production [26, 28].

The experiments presented in this paper were intended to identify the gene or genes regulated by RpoN that contribute to polyP production [22, 28], and while we did successfully identify previously unknown roles for the RpoN-related proteins GlnG, GlrR and PtsN in modulating polyP production (Figs. 1, 4 and 5), and clarify the relative relationships between RpoN, PtsN, DksA and RpoE (Fig. 4d), we did not find a simple RpoN-dependent activator of polyP production. GlnG regulates at least 50 genes in *E. coli*, including other regulators [33]. The role of GlrR in polyP regulation is unclear, although it appears unlikely to involve GlnS (Fig. 3). Future work will be needed to clarify the roles of RpoE and RpoE-regulating proteins (like GlrR) in polyP regulation. Since the defects of $\Delta rpoE$ and $\Delta ptsN$ mutants can each be rescued by expression of the other gene (Fig. 4d), the simplest interpretation is that they regulate polyP production by independent mechanisms. However, *ptsN* is both a member of the RpoE regulon [105] and a multicopy suppressor of the growth defect of a $\Delta rpoE$ mutant [106], so these results must be interpreted cautiously. The impact of supplementing LB with glutamine, glutamate and NH_4 on polyP regulation (Fig. 2c–e) was surprising, and remains to be

fully explained. However, it does mean that growth in LB medium [78] cannot simply be considered a ‘non-stress’ condition that contrasts with ‘stressful’ nutrient limitation, and that in order to fully understand polyP regulation we must also consider the cell’s physiological state under conditions when it is not producing detectable amounts of polyP.

The exact function of PTS^{Ntr} has been debated for some time [34, 38], but it is clear from our results that PtsN has a phosphorylation-independent positive effect on polyP synthesis (Figs. 4 and 5). What is less clear is how this occurs. PtsN does not appear to interact directly with PPK *in vivo* (Fig. 5e) [95–98]. Overexpression of PtsN is known to generally reduce cell envelope stress in *E. coli*, although the mechanism by which it does so is not well understood [106]. Known targets of PtsN regulation in enterobacteria include proteins involved in phosphate transport [107], potassium transport [108–110], GlcN6P synthesis [86] and environmental sensing [42]. While phosphate transport is certainly important for polyP synthesis [22, 25, 111, 112] and PtsN-dependent changes in potassium levels are known to impact sigma factor specificity [109], which may also play a role in polyP regulation [28], both of these phenotypes are dependent on the phosphorylation state of PtsN, as is the interaction between PtsN and GlmS [86]. Gravina *et al.* [113] recently reported multiple new possible PtsN interaction candidates in *E. coli*. Fortunately, we have already tested many of these for potential roles in polyP accumulation [28], including proteins involved in flagellar motility and glycerol metabolism, and found that those pathways have minimal effects on polyP accumulation. However, there are additional candidates, including proteins of unknown

function (e.g. YeaG, YcgR, and YcjN) and enzymes of central metabolism (e.g. AceAB, PpsA, SucC), that remain to be tested.

Our results illustrate previously unknown connections among a variety of well-conserved environmental stress response pathways and show that even as well-studied an organism as *E. coli* still has plenty of capacity to surprise us and confound our expectations.

FUNDING INFORMATION

This project was supported by United States National Institutes of Health grant R35GM124590 (to M.J.G.).

AUTHOR CONTRIBUTIONS

M.Q.B., formal analysis, investigation, methodology, visualization, writing – review and editing. A.R.L., investigation, methodology, visualization, writing – review and editing. J.T.H., investigation, methodology, visualization. M.J.G., conceptualization, formal analysis, funding acquisition, investigation, methodology, project administration, supervision, visualization, writing – original draft, writing – review and editing.

CONFLICTS OF INTEREST

The authors declare that there are no conflicts of interest.

REFERENCES

1. Denoncourt A, Downey M. Model systems for studying polyphosphate biology: a focus on microorganisms. *Curr Genet* 2021;67:331–346.
2. Desfougères Y, Saiardi A, Azevedo C. Inorganic polyphosphate in mammals: where's Wally? *Biochem Soc Trans* 2020;48:95–101.
3. Albi T, Serrano A. Inorganic polyphosphate in the microbial world. Emerging roles for a multifaceted biopolymer. *World J Microbiol Biotechnol* 2016;32:27.
4. Beaufay F, Quarles E, Franz A, Katamanin O, Wholey WY, et al. Polyphosphate functions in vivo as an iron chelator and Fenton reaction inhibitor. *mBio* 2020;11:e01017-20.
5. Dai S, Xie Z, Wang B, Yu N, Zhao J, et al. Dynamic polyphosphate metabolism coordinating with manganese ions defends against oxidative stress in the extreme bacterium *Deinococcus radiodurans*. *Appl Environ Microbiol* 2021;87:e02785-20.
6. Gray MJ, Jakob U. Oxidative stress protection by polyphosphate--new roles for an old player. *Curr Opin Microbiol* 2015;24:1–6.
7. Xie L, Jakob U. Inorganic polyphosphate, a multifunctional poly-anionic protein scaffold. *J Biol Chem* 2019;294:2180–2190.
8. Racki LR, Tocheva EI, Dieterle MG, Sullivan MC, Jensen GJ, et al. Polyphosphate granule biogenesis is temporally and functionally tied to cell cycle exit during starvation in *Pseudomonas aeruginosa*. *Proc Natl Acad Sci U S A* 2017;114:E2440–E2449.
9. Gross MH, Konieczny I. Polyphosphate induces the proteolysis of ADP-bound fraction of initiator to inhibit DNA replication initiation upon stress in *Escherichia coli*. *Nucleic Acids Res* 2020;48:5457–5466.
10. Beaufay F, Amemiya HM, Guan J, Basalla J, Meinen BA, et al. Polyphosphate drives bacterial heterochromatin formation. *Sci Adv* 2021;7:eabk0233.
11. Gautam LK, Sharma P, Capalash N. Bacterial polyphosphate kinases revisited: role in pathogenesis and therapeutic potential. *Curr Drug Targets* 2019;20:292–301.
12. Rao NN, Gómez-García MR, Kornberg A. Inorganic polyphosphate: essential for growth and survival. *Annu Rev Biochem* 2009;78:605–647.
13. Bowlin MQ, Gray MJ. Inorganic polyphosphate in host and microbe biology. *Trends Microbiol* 2021;29:1013–1023.
14. Suess PM, China LE, Pilling D, Gomer RH. Extracellular polyphosphate promotes macrophage and fibrocyte differentiation, inhibits leukocyte proliferation, and acts as a chemotactic agent for neutrophils. *J Immunol* 2019;203:493–499.
15. Roewe J, Stavrides G, Strueve M, Sharma A, Marini F, et al. Bacterial polyphosphates interfere with the innate host defense to infection. *Nat Commun* 2020;11:4035.

16. Rijal R, Cadena LA, Smith MR, Carr JF, Gomer RH. Polyphosphate is an extracellular signal that can facilitate bacterial survival in eukaryotic cells. *Proc Natl Acad Sci U S A* 2020;117:31923–31934.
17. McDonald B, Davis RP, Kim S-J, Tse M, Esmon CT, et al. Platelets and neutrophil extracellular traps collaborate to promote intravascular coagulation during sepsis in mice. *Blood* 2017;129:1357–1367.
18. Peng L, Zeng L, Jin H, Yang L, Xiao Y, et al. Discovery and antibacterial study of potential PPK1 inhibitors against uropathogenic *E. coli* J Enzyme Inhib Med Chem 2020;35:1224–1232.
19. Neville N, Roberge N, Ji X, Stephen P, Lu JL, et al. A dual-specificity inhibitor targets polyphosphate kinase 1 and 2 enzymes to attenuate virulence of *Pseudomonas aeruginosa*. *mBio* 2021;12:e0059221.
20. Bravo-Toncio C, Álvarez JA, Campos F, Ortiz-Severín J, Varas M, et al. *Dictyostelium discoideum* as a surrogate host-microbe model for antivirulence screening in *Pseudomonas aeruginosa* PAO1. *Int J Antimicrob Agents* 2016;47:403–409.
21. Dahl J-U, Gray MJ, Bazopoulou D, Beaufay F, Lempart J, et al. The anti-inflammatory drug mesalamine targets bacterial polyphosphate accumulation. *Nat Microbiol* 2017;2:16267.
22. Ault-Riché D, Fraley CD, Tzeng CM, Kornberg A. Novel assay reveals multiple pathways regulating stress-induced accumulations of inorganic polyphosphate in *Escherichia coli*. *J Bacteriol* 1998;180:1841–1847.
23. Gray MJ, Wholey W-Y, Wagner NO, Cremers CM, Mueller-Schickert A, et al. Polyphosphate is a primordial chaperone. *Mol Cell* 2014;53:689–699.
24. Yoo NG, Dogra S, Meinen BA, Tse E, Haefliger J, et al. Polyphosphate stabilizes protein unfolding intermediates as soluble amyloid-like oligomers. *J Mol Biol* 2018;430:4195–4208.
25. Morohoshi T, Maruo T, Shirai Y, Kato J, Ikeda T, et al. Accumulation of inorganic polyphosphate in *phoU* mutants of *Escherichia coli* and *Synechocystis* sp. strain PCC6803. *Appl Environ Microbiol* 2002;68:4107–4110.
26. Kuroda A, Murphy H, Cashel M, Kornberg A. Guanosine tetra- and pentaphosphate promote accumulation of inorganic polyphosphate in *Escherichia coli*. *J Biol Chem* 1997;272:21240–21243.
27. Akiyama M, Crooke E, Kornberg A. An exopolyphosphatase of *Escherichia coli*. The enzyme and its *ppx* gene in a polyphosphate operon. *J Biol Chem* 1993;268:633–639.
28. Gray MJ. Interactions between DksA and stress-responsive alternative sigma factors control inorganic polyphosphate accumulation in *Escherichia coli*. *J Bacteriol* 2020;202:e00133-20.

29. Rudat AK, Pokhrel A, Green TJ, Gray MJ. Mutations in *Escherichia coli* polyphosphate kinase that lead to dramatically increased in vivo polyphosphate levels. *J Bacteriol* 2018;200:e00697-17.
30. Gray MJ. Inorganic polyphosphate accumulation in *Escherichia coli* is regulated by DksA but not by (p)ppGpp. *J Bacteriol* 2019;201:e00664-18.
31. Danson AE, Jovanovic M, Buck M, Zhang X. Mechanisms of σ ⁵⁴-dependent transcription initiation and regulation. *J Mol Biol* 2019;431:3960–3974.
32. Riordan JT, Mitra A. Regulation of *Escherichia coli* pathogenesis by alternative sigma factor N. *EcoSal Plus* 2017;7.
33. Keseler IM, Mackie A, Santos-Zavaleta A, Billington R, Bonavides-Martínez C, et al. The EcoCyc database: reflecting new knowledge about *Escherichia coli* K-12. *Nucleic Acids Res* 2017;45:D543–D550.
34. van Heeswijk WC, Westerhoff HV, Boogerd FC. Nitrogen assimilation in *Escherichia coli*: putting molecular data into a systems perspective. *Microbiol Mol Biol Rev* 2013;77:628–695.
35. Göpel Y, Görke B. Interaction of lipoprotein QseG with sensor kinase QseE in the periplasm controls the phosphorylation state of the two-component system QseE/QseF in *Escherichia coli*. *PLoS Genet* 2018;14:e1007547.
36. Reichenbach B, Göpel Y, Görke B. Dual control by perfectly overlapping sigma 54- and sigma 70- promoters adjusts small RNA GlnY expression to different environmental signals. *Mol Microbiol* 2009;74:1054–1070.
37. Klein G, Stupak A, Biernacka D, Wojtkiewicz P, Lindner B, et al. Multiple transcriptional factors regulate transcription of the *rpoE* gene in *Escherichia coli* under different growth conditions and when the lipopolysaccharide biosynthesis is defective. *J Biol Chem* 2016;291:22999–23019.
38. Pflüger-Grau K, Görke B. Regulatory roles of the bacterial nitrogen-related phosphotransferase system. *Trends Microbiol* 2010;18:205–214.
39. Guo B, Bi Y. Cloning PCR products. an overview. *Methods Mol Biol* 2002;192:111–119.
40. Sambrook J, Fritsch EF, Maniatis T. *Molecular Cloning: A Laboratory Manual*. 2nd ed. Cold Spring Harbor, NY: Cold Spring Harbor Laboratory Press; 1989.
41. Bertani G. Studies on lysogenesis. I. The mode of phage liberation by lysogenic *Escherichia coli*. *J Bacteriol* 1951;62:293–300.
42. Choi J, Kim H, Chang Y, Yoo W, Kim D, et al. Programmed delay of a virulence circuit promotes *Salmonella* pathogenicity. *mBio* 2019;10:e00291-19.
43. Daimon Y, Narita S, Akiyama Y. Activation of toxin-antitoxin system toxins suppresses lethality caused by the loss of σ ^E in *Escherichia coli*. *J Bacteriol* 2015;197:2316–2324.

44. Chen I-MA, Chu K, Palaniappan K, Ratner A, Huang J, et al. The IMG/M data management and analysis system v.6.0: new tools and advanced capabilities. *Nucleic Acids Res* 2021;49:D751–D763.
45. Santos-Zavaleta A, Salgado H, Gama-Castro S, Sánchez-Pérez M, Gómez-Romero L, et al. RegulonDB v 10.5: tackling challenges to unify classic and high throughput knowledge of gene regulation in *E. coli* K-12. *Nucleic Acids Res* 2019;47:D212–D220.
46. Blattner FR, Plunkett G, Bloch CA, Perna NT, Burland V, et al. The complete genome sequence of *Escherichia coli* K-12. *Science* 1997;277:1453–1462.
47. Silhavy TJ, Berman ML, Enquist LW. *Experiments with Gene Fusions*. Cold Spring Harbor, NY: Cold Spring Harbor Laboratory; 1984.
48. Baba T, Ara T, Hasegawa M, Takai Y, Okumura Y, et al. Construction of *Escherichia coli* K-12 in-frame, single-gene knockout mutants: the Keio collection. *Mol Syst Biol* 2006;2:0008.
49. Datsenko KA, Wanner BL. One-step inactivation of chromosomal genes in *Escherichia coli* K-12 using PCR products. *Proc Natl Acad Sci USA* 2000;97:6640–6645.
50. Blauwkamp TA, Ninfa AJ. Physiological role of the GlnK signal transduction protein of *Escherichia coli*: survival of nitrogen starvation. *Mol Microbiol* 2002;46:203–214.
51. Uzzau S, Figueroa-Bossi N, Rubino S, Bossi L. Epitope tagging of chromosomal genes in *Salmonella*. *Proc Natl Acad Sci U S A* 2001;98:15264–15269.
52. Bonocora RP, Smith C, Lapierre P, Wade JT. Genome-scale mapping of *Escherichia coli* σ 54 reveals widespread, conserved intragenic binding. *PLoS Genet* 2015;11:10.
53. Guzman LM, Belin D, Carson MJ, Beckwith J. Tight regulation, modulation, and high-level expression by vectors containing the arabinose PBAD promoter. *J Bacteriol* 1995;177:4121–4130.
54. Watson JF, García-Nafria J. In vivo DNA assembly using common laboratory bacteria: A re-emerging tool to simplify molecular cloning. *J Biol Chem* 2019;294:15271–15281.
55. De Genst EJ, Guilleams T, Wellens J, O’Day EM, Waudby CA, et al. Structure and properties of a complex of α -synuclein and a single-domain camelid antibody. *J Mol Biol* 2010;402:326–343.
56. Huang Y, Zhang L. An in vitro single-primer site-directed mutagenesis method for use in biotechnology. *Methods Mol Biol* 2017;1498:375–383.
57. Karimova G, Pidoux J, Ullmann A, Ladant D. A bacterial two-hybrid system based on a reconstituted signal transduction pathway. *Proc Natl Acad Sci U S A* 1998;95:5752–5756.
58. Pokhrel A, Lingo JC, Wolschendorf F, Gray MJ. Assaying for inorganic polyphosphate in bacteria. *J Vis Exp* 2019;2019:143.

59. Neidhardt FC, Bloch PL, Smith DF. Culture medium for entero- bacteria. *J Bacteriol* 1974;119:736–747.
60. Wurst H, Kornberg A. A soluble exopolyphosphatase of *Saccha- romyces cerevisiae*. purification and characterization. *J Biol Chem* 1994;269:10996–11001.
61. Christ JJ, Blank LM. Enzymatic quantification and length deter- mination of polyphosphate down to a chain length of two. *Anal Biochem* 2018;548:82–90.
62. Schmittgen TD, Livak KJ. Analyzing real-time PCR data by the comparative C(T) method. *Nat Protoc* 2008;3:1101–1108.
63. Bennett BD, Kimball EH, Gao M, Osterhout R, Van Dien SJ, et al. Absolute metabolite concentrations and implied enzyme active site occupancy in *Escherichia coli*. *Nat Chem Biol* 2009;5:593–599.
64. Schaefer J, Jovanovic G, Kotta-Loizou I, Buck M. Single-step method for β -galactosidase assays in *Escherichia coli* using a 96-well microplate reader. *Anal Biochem* 2016;503:56–57.
65. Pillai-Kastoori L, Schutz-Geschwender AR, Harford JA. A systematic approach to quantitative Western blot analysis. *Anal Biochem* 2020;593:113608.
66. Kurien BT, Scofield RH. Introduction to protein blotting. *Methods Mol Biol* 2009;536:9–22.
67. Schneider CA, Rasband WS, Eliceiri KW. NIH image to imagej: 25 years of image analysis. *Nat Methods* 2012;9:671–675.
68. Ikeda TP, Shauger AE, Kustu S. *Salmonella typhimurium* apparently perceives external nitrogen limitation as internal glutamine limitation. *J Mol Biol* 1996;259:589–607.
69. Huergo LF, Dixon R. The emergence of 2-oxoglutarate as a master regulator metabolite. *Microbiol Mol Biol Rev* 2015;79:419–435.
70. Atkinson MR, Blauwkamp TA, Ninfa AJ. Context-dependent func- tions of the PII and glnK signal transduction proteins in *Escheri- chia coli*. *J Bacteriol* 2002;184:5364–5375.
71. Gosztolai A, Schumacher J, Behrends V, Bundy JG, Heydenreich F, et al. GlnK facilitates the dynamic regulation of bacterial nitrogen assimilation. *Biophys J* 2017;112:2219–2230.
72. Forchhammer K, Lüddecke J. Sensory properties of the PII signalling protein family. *FEBS J* 2016;283:425–437.
73. Maeda K, Westerhoff HV, Kurata H, Boogerd FC. Ranking network mechanisms by how they fit diverse experiments and deciding on *E. coli*'s ammonium transport and assimilation network. *NPJ Syst Biol Appl* 2019;5:14.
74. Blauwkamp TA, Ninfa AJ. Antagonism of PII signalling by the AmtB protein of *Escherichia coli*. *Mol Microbiol* 2003;48:1017–1028.

75. Rodionova IA, Goodacre N, Babu M, Emili A, Uetz P, et al. The nitrogen regulatory PII protein (GlnB) and N-acetylglucosamine 6-phosphate epimerase (NanE) allosterically activate glucosamine 6-phosphate deaminase (NagB) in *Escherichia coli*. *J Bacteriol* 2018;200:e00691-17.
76. Schubert C, Zedler S, Strecker A, Uden G. L-Aspartate as a high-quality nitrogen source in *Escherichia coli*: Regulation of L-aspartase by the nitrogen regulatory system and interaction of L-aspartase with GlnB. *Mol Microbiol* 2021;115:526–538.
77. Atkinson MR, Ninfa AJ. Role of the glnK signal transduction protein in the regulation of nitrogen assimilation in *Escherichia coli*. *Mol Microbiol* 1998;29:431–447.
78. Sezonov G, Joseleau-Petit D, D’Ari R. *Escherichia coli* physiology in luria-bertani broth. *J Bacteriol* 2007;189:8746–8749.
79. Yakhnin H, Aichele R, Ades SE, Romeo T, Babitzke P. Circuitry linking the global csr- and sigma(E)-dependent cell envelope stress response systems. *J Bacteriol* 2017;199:23.
80. Hews CL, Cho T, Rowley G, Raivio TL. Maintaining integrity under stress: envelope stress response regulation of pathogenesis in gram-negative bacteria. *Front Cell Infect Microbiol* 2019;9:313.
81. Khan MA, Durica-Mitic S, Göpel Y, Heermann R, Görke B. Small RNA-binding protein RapZ mediates cell envelope precursor sensing and signaling in *Escherichia coli*. *EMBO J* 2020;39:e103848.
82. Durica-Mitic S, Göpel Y, Amman F, Görke B. Adaptor protein RapZ activates endoribonuclease RNase E by protein-protein interaction to cleave a small regulatory RNA. *RNA* 2020;26:1198–1215.
83. Teplyakov A, Leriche C, Obmolova G, Badet B, Badet-Denisot MA. From Lobry de Bruyn to enzyme-catalyzed ammonia channeling: molecular studies of D-glucosamine-6P synthase. *Nat Prod Rep* 2002;19:60–69.
84. Mouilleron S, Badet-Denisot MA, Badet B, Golinelli-Pimpaneau B. Dynamics of glucosamine-6-phosphate synthase catalysis. *Arch Biochem Biophys* 2011;505:1–12.
85. Yoo W, Choi J, Park B, Byndloss MX, Ryu S. A nitrogen metabolic enzyme provides *Salmonella* fitness advantage by promoting utilization of microbiota-derived carbon source. *ACS Infect Dis* 2021;7:1208–1220.
86. Yoo W, Yoon H, Seok YJ, Lee CR, Lee HH, et al. Fine-tuning of amino sugar homeostasis by EIIA^{Ntr} in *Salmonella Typhimurium*. *Sci Rep* 2016;6:33055.
87. Kim HJ, Lee CR, Kim M, Peterkofsky A, Seok YJ. Dephosphorylated npr of the nitrogen PTS regulates lipid A biosynthesis by direct interaction with lpxd. *Biochem Biophys Res Commun* 2011;409:556–561.
88. Lee J, Park YH, Kim YR, Seok YJ, Lee CR. Dephosphorylated NPr is involved in an envelope stress response of *Escherichia coli*. *Microbiology (Reading)* 2015;161:1113–1123.

89. Choi J, Ryu S. Regulation of iron uptake by fine-tuning the iron responsiveness of the iron sensor Fur. *Appl Environ Microbiol* 2019;85:e03026-18.
90. Deutscher J, Aké FMD, Derkaoui M, Zébré AC, Cao TN, et al. The bacterial phosphoenolpyruvate:carbohydrate phospho-transferase system: regulation by protein phosphorylation and phosphorylation-dependent protein-protein interactions. *Microbiol Mol Biol Rev* 2014;78:231–256.
91. Lee C-R, Park Y-H, Kim M, Kim Y-R, Park S, et al. Reciprocal regulation of the autophosphorylation of enzyme INtr by glutamine and α -ketoglutarate in *Escherichia coli*. *Mol Microbiol* 2013;88:473–485.
92. Rabus R, Reizer J, Paulsen I, Saier MH. Enzyme I(Ntr) from *Escherichia coli*. A novel enzyme of the phosphoenolpyruvate-dependent phosphotransferase system exhibiting strict specificity for its phosphoryl acceptor, NPr. *J Biol Chem* 1999;274:26185–26191.
93. Karstens K, Zschiedrich CP, Bowien B, Stülke J, Görke B. Phosphotransferase protein EIIANtr interacts with SpoT, a key enzyme of the stringent response, in *Ralstonia eutropha* H16. *Microbiology (Reading)* 2014;160:711–722.
94. Mörk-Mörkenstein M, Heermann R, Göpel Y, Jung K, Görke B. Non-canonical activation of histidine kinase KdpD by phosphotransferase protein PtsN through interaction with the transmitter domain. *Mol Microbiol* 2017;106:54–73.
95. Rajagopala SV, Sikorski P, Kumar A, Mosca R, Vlasblom J, et al. The binary protein-protein interaction landscape of *Escherichia coli*. *Nat Biotechnol* 2014;32:285–290.
96. Hu P, Janga SC, Babu M, Díaz-Mejía JJ, Butland G, et al. Global functional atlas of *Escherichia coli* encompassing previously uncharacterized proteins. *PLoS Biol* 2009;7:e96.
97. Alonso-López D, Campos-Laborie FJ, Gutiérrez MA, Lambourne L, Calderwood MA, et al. APID database: redefining protein-protein interaction experimental evidences and binary interactomes. *Database (Oxford)* 2019;2019.
98. Arifuzzaman M, Maeda M, Itoh A, Nishikata K, Takita C, et al. Large-scale identification of protein-protein interaction of *Escherichia coli* K-12. *Genome Res* 2006;16:686–691.
99. Wang L, Yan J, Wise MJ, Liu Q, Asenso J, et al. Distribution patterns of polyphosphate metabolism pathway and its relationships with bacterial durability and virulence. *Front Microbiol* 2018;9:782.
100. Achbergerová L, Nahálka J. Polyphosphate--an ancient energy source and active metabolic regulator. *Microb Cell Fact* 2011;10:63.
101. Gottesman S. Trouble is coming: signaling pathways that regulate general stress responses in bacteria. *J Biol Chem* 2019;294:11685–11700.
102. Schellhorn HE. Function, evolution, and composition of the RpoS regulon in *Escherichia coli*. *Front Microbiol* 2020;11:560099.

103. Saha S, Lach SR, Konovalova A. Homeostasis of the Gram-negative cell envelope. *Curr Opin Microbiol* 2021;61:99–106.
104. Rao NN, Liu S, Kornberg A. Inorganic polyphosphate in *Escherichia coli*: the phosphate regulon and the stringent response. *J Bacteriol* 1998;180:2186–2193.
105. Rhodius VA, Suh WC, Nonaka G, West J, Gross CA. Conserved and variable functions of the sigmaE stress response in related genomes. *PLoS Biol* 2006;4:e2.
106. Hayden JD, Ades SE. The extracytoplasmic stress factor, sigmaE, is required to maintain cell envelope integrity in *Escherichia coli*. *PloS one* 2008;3:e1573.
107. Lüttmann D, Göpel Y, Görke B. The phosphotransferase protein EIIA^{Ntr} modulates the phosphate starvation response through interaction with histidine kinase PhoR in *Escherichia coli*. *Mol Microbiol* 2012;86:96–110.
108. Lüttmann D, Heermann R, Zimmer B, Hillmann A, Rampp IS, et al. Stimulation of the potassium sensor KdpD kinase activity by interaction with the phosphotransferase protein IIA^{Ntr} in *Escherichia coli*. *Mol Microbiol* 2009;72:978–994.
109. Lee CR, Cho SH, Kim HJ, Kim M, Peterkofsky A, et al. Potassium mediates *Escherichia coli* enzyme IIA^{Ntr}-dependent regulation of sigma factor selectivity. *Mol Microbiol* 2010;78:1468–1483.
110. Lee CR, Cho SH, Yoon MJ, Peterkofsky A, Seok YJ. *Escherichia coli* enzyme IIA^{Ntr} regulates the K⁺ transporter trkA. *Proc Natl Acad Sci USA* 2007;104:4124–4129.
111. Grillo-Puertas M, Rintoul MR, Rapisarda VA. PhoB activation in non-limiting phosphate condition by the maintenance of high polyphosphate levels in the stationary phase inhibits biofilm formation in *Escherichia coli*. *Microbiology (Reading)* 2016;162:1000–1008.
112. Hirota R, Motomura K, Nakai S, Handa T, Ikeda T, et al. Stable polyphosphate accumulation by a pseudo-revertant of an *Escherichia coli* phoU mutant. *Biotechnol Lett* 2013;35:695–701.
113. Gravina F, Degaut FL, Gerhardt ECM, Pedrosa FO, Souza EM, et al. The protein-protein interaction network of the *Escherichia coli* EIIA^{Ntr} regulatory protein reveals a role in cell motility and metabolic control. *Res Microbiol* 2021;172:103882.

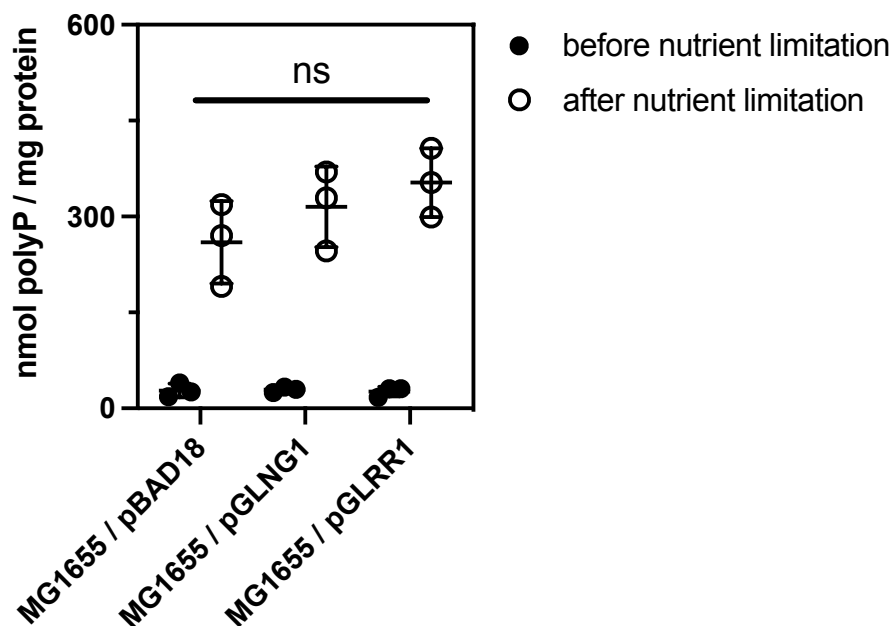
TABLES

Table 1. Strains and Plasmids Used to Identify the Role of Nitrogen-Responsive Regulators in Controlling Inorganic Polyphosphate Synthesis in *E. coli*. Unless otherwise indicated, all strains and plasmids were generated in the course of this work. Ap^R, ampicillin resistance; Cm^R, chloramphenicol resistance; Em^D, erythromycin dependence; Kn^R, kanamycin resistance; Sp^R, spectinomycin resistance; Sm^R, streptomycin resistance.

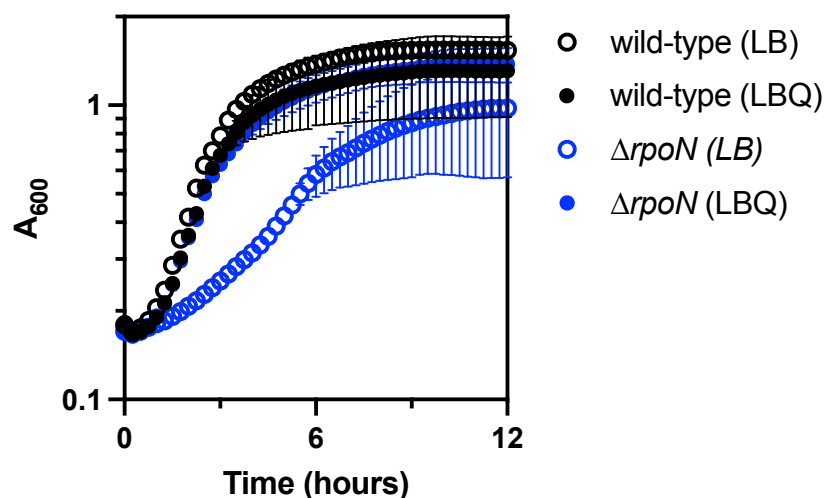
Strain	Markers	Relevant genotype	Source
<i>E. coli</i> strains			
DH5 α		F ⁻ , λ , ϕ 80 <i>lacZ</i> Δ M15 Δ (<i>lacZYA-argF</i>)U169 <i>recA1 endA1 hsdR17</i> (r _K ⁻ , m _K ⁺) <i>phoA supE44 thi-1 gyrA96 relA1</i>	Invitrogen
BL21(DE3)		F ⁻ , <i>ompT gal dem lon hsdSB</i> (r _B ⁻ m _B ⁻) λ (DE3 [<i>lacI lacUV5-T7 gene 1 ind1 sam7 nin5</i>])	EMD Millipore
BTH101	Sm ^R	F ⁻ , <i>cya-99 araD139 galE15 galK16 rpsL1 hsdR2 mcrA1 mcrB1</i>	[57]
MG1655		F ⁻ , λ , <i>rph-1 ilvG⁻ rfb-50</i>	[46]
MJG1419	Cm ^R	MG1655 Δ <i>dkaA1000::kan</i> ⁺	[30]
MJG1763		MG1655 Δ <i>rpoN730::kan</i> ⁺	[28]
MJG1766		MG1655 Δ <i>rpoN730</i>	[28]
MJG1767	Em ^D Kn ^R	MG1655 Δ <i>rpoE1000::kan</i> ⁺	[28]
MJG1955	Kn ^R	MG1655 Δ <i>glrR728::kan</i> ⁺	
MJG1956	Kn ^R	MG1655 Δ <i>atoC774::kan</i> ⁺	
MJG1969	Kn ^R	MG1655 Δ <i>hyfR739::kan</i> ⁺	
MJG1970	Kn ^R	MG1655 Δ <i>pspF739::kan</i> ⁺	
MJG1971	Kn ^R	MG1655 Δ <i>norR784::kan</i> ⁺	
MJG1972	Kn ^R	MG1655 Δ <i>ygeV720::kan</i> ⁺	
MJG1973	Kn ^R	MG1655 Δ <i>rtcR755::kan</i> ⁺	
MJG1974	Kn ^R	MG1655 Δ <i>prpR772::kan</i> ⁺	
MJG1975	Kn ^R	MG1655 Δ <i>zraR775::kan</i> ⁺	
MJG1976	Kn ^R	MG1655 Δ <i>fhlA735::kan</i> ⁺	
MJG2058	Kn ^R	MG1655 Δ <i>glnB727::kan</i> ⁺	
MJG2061	Kn ^R	MG1655 Δ <i>glnK736::kan</i> ⁺	
MJG2064	Kn ^R	MG1655 Δ <i>glnG730::kan</i> ⁺	
MJG2065		MG1655 Δ <i>glrR728</i>	
MJG2068	Kn ^R	MG1655 Δ <i>glrR728 glnG730::kan</i> ⁺	
MJG2082		MG1655 Δ <i>glnB727</i>	
MJG2083	Kn ^R	MG1655 Δ <i>glnB727 glnK736::kan</i> ⁺	

Strain	Markers	Relevant genotype	Source
MJG2086	Kn ^R	MG1655 $\Delta ptsN732::kan^+$	
MJG2089		MG1655 $\Delta ptsN732$	
MJG2090	Kn ^R	MG1655 $\Delta npr-734::kan^+$	
MJG2091	Kn ^R	MG1655 $\Delta ptsP753::kan^+$	
MJG2112	Kn ^R	MG1655 $\Delta rapZ733::kan^+$	
MJG2114		MG1655 $\Delta rapZ733$	
MJG2151	Cm ^R	MG1655 $\Delta glmZ1000::cat^+$	
MJG2155	Cm ^R	MG1655 $\Delta glmY1000::cat^+$	
MJG2179	Kn ^R	MG1655 $ptsN-3xFLAG::kan^+$	
MJG2191		MG1655 $ptsN-3xFLAG$	
MJG2193	Kn ^R	MG1655 $ptsN-3xFLAG \Delta phoP790::kan^+$	
MJG2200	Kn ^R	MG1655 $ptsN-3xFLAG \Delta rpoN730::kan^+$	
MJG2202		MG1655 $ptsN-3xFLAG \Delta rpoN730$	
Plasmids			
pBAD18	Ap ^R	<i>bla</i> ⁺	[53]
pBAD24	Ap ^R	<i>bla</i> ⁺	[53]
pCP20	Ap ^R Cm ^R	Flp ⁺ <i>bla</i> ⁺ <i>cat</i> ⁺	[49]
pDKSA1	Ap ^R	<i>dksA</i> ⁺ <i>bla</i> ⁺	[30]
pET-21b(+)	Ap ^R	<i>bla</i> ⁺	Novagen
pGCN4zip1	Kn ^R	T25-GCN4zip <i>kan</i> ⁺	
pGCN4zip3	Ap ^R	GCN4zip-T18 <i>bla</i> ⁺	
pGLMS1	Ap ^R	<i>glmS</i> ⁺ <i>bla</i> ⁺	
pGLNB1	Ap ^R	<i>glnB</i> ⁺ <i>bla</i> ⁺	
pGLNG1	Ap ^R	<i>glnG</i> ⁺ <i>bla</i> ⁺	
pGLNK1	Ap ^R	<i>glnK</i> ⁺ <i>bla</i> ⁺	
pGLRR1	Ap ^R	<i>glrR</i> ⁺ <i>bla</i> ⁺	
pKD3	Cm ^R	<i>cat</i> ⁺	[49]
pKD46	Ap ^R	λ Red ⁺ <i>bla</i> ⁺	[49]
pKNT25	Kn ^R	T25 <i>kan</i> ⁺	[57]
pKT25	Kn ^R	T25 <i>kan</i> ⁺	[57]
pPPK12	Kn ^R	<i>ppk-T25 kan</i> ⁺	
pPPK13	Kn ^R	T25- <i>ppk kan</i> ⁺	
pPPK33	Ap ^R	<i>ppk-GAAEPEA bla</i> ⁺	
pPTSN1	Ap ^R	<i>ptsN</i> ⁺ <i>bla</i> ⁺	
pPTSN2	Ap ^R	<i>ptsN</i> ^{C217G, T219A} (encoding PtsN ^{H73E}) <i>bla</i> ⁺	
pPTSN3	Ap ^R	<i>ptsN</i> ^{C217G, A218C, T219G} (encoding PtsN ^{H73A}) <i>bla</i> ⁺	

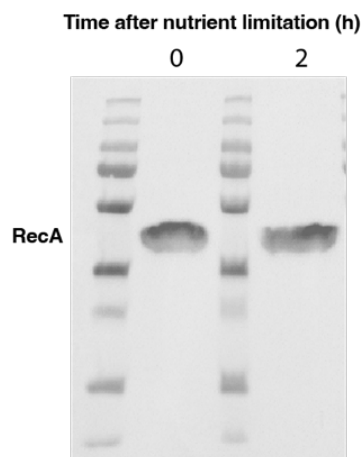
Strain	Markers	Relevant genotype	Source
pPTSN5	Ap ^R	T18- <i>ptsN</i> <i>bla</i> ⁺	
pRPOE1	Ap ^R	<i>rpoE</i> ⁺ <i>bla</i> ⁺	[28]
pRpoN	Ap ^R	<i>rpoN</i> ⁺ <i>bla</i> ⁺	[52]
pSUB11	Ap ^R Kn ^R	3xFLAG <i>kan</i> ⁺ <i>bla</i> ⁺	[51]
pUT18	Ap ^R	T18 <i>bla</i> ⁺	[57]
pUT18C	Ap ^R	T18 <i>bla</i> ⁺	[57]



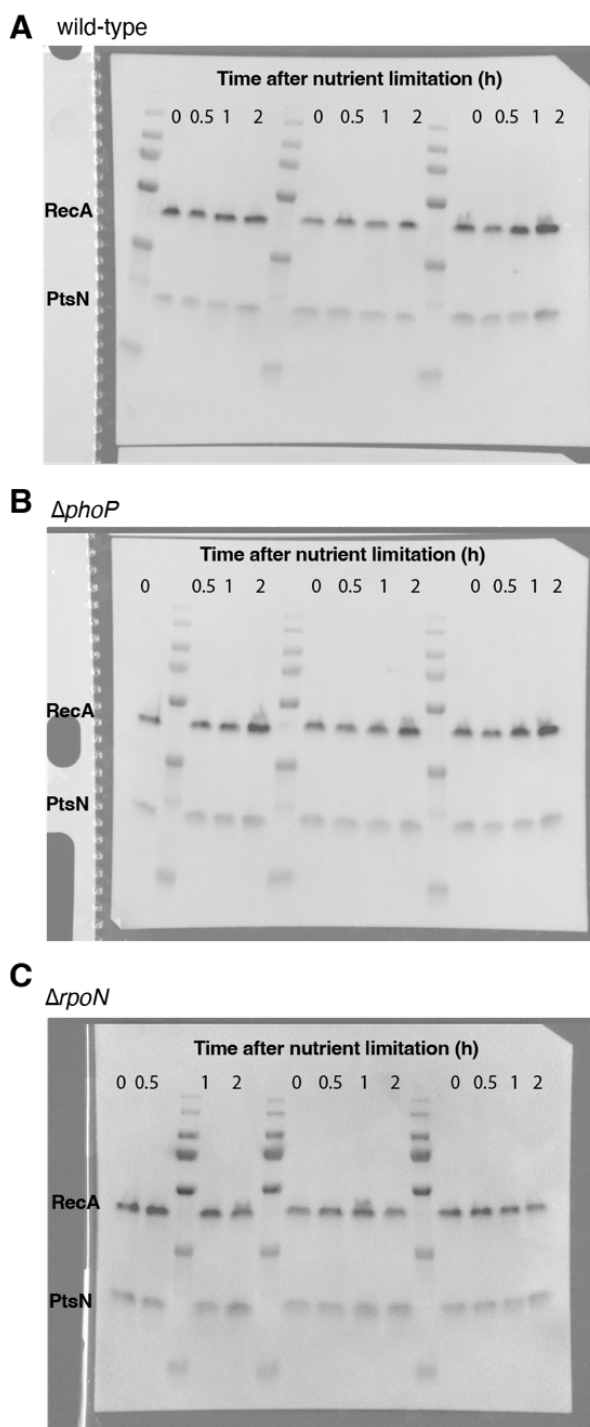
SUPPLEMENTAL FIGURE S3. Overexpressing GlnG Or GlnR Does Not Significantly Impact PolyP Production in Wild-Type *E. coli*. PolyP concentrations in *E. coli* MG1655 wild-type containing the indicated plasmids before (black circles) or 2 hours after (white circles) nutrient limitation (n=3, mean±SD). There were no significant differences among the strains (two-way repeated measures ANOVA with Holm-Sidak's multiple comparisons test, ns=not significant).



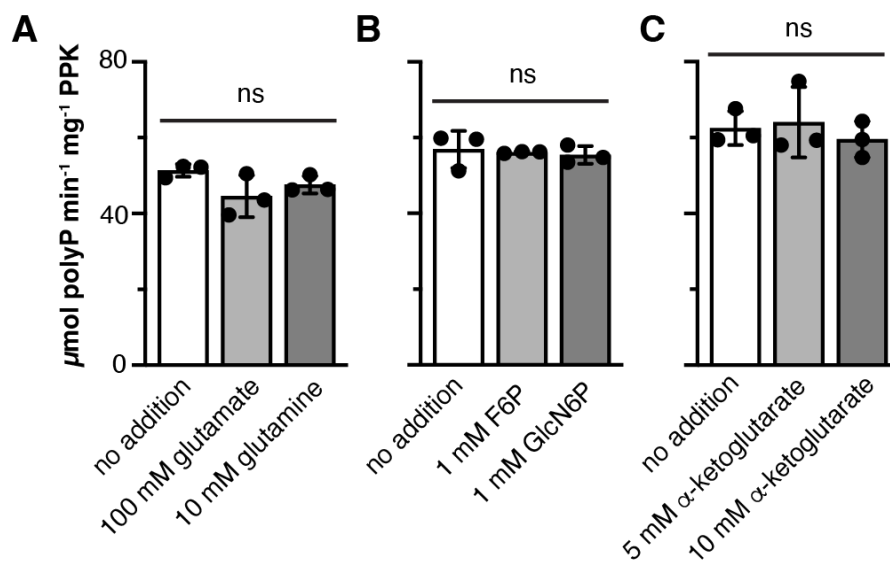
SUPPLEMENTAL FIGURE S4. Glutamine Limitation Explains the Growth Defect of an *rpoN* Mutant in LB Medium. *E. coli* MG1655 wild-type (black symbols) or $\Delta rpoN730$ (blue symbols) containing plasmid pBAD18 were grown at 37°C with shaking in LB (open circles) or LBQ (supplemented with 5 mM glutamine, closed circles) containing ampicillin in a Sunrise microplate reader (Tecan, Ltd.)(n=3, mean±SD).



SUPPLEMENTAL FIGURE S5. RecA Protein Concentration Does Not Change in Response to PolyP-Inducing Nutrient Limitation Stress. 6 μ g of total protein harvested from pre-stress (t = 0 h) or post-stress (t = 2 h) cultures were mixed 3:1 with 4X reducing loading dye and separated on an SDS-PAGE gel. The gel was blotted on a PVDF membrane and probed with a 1:12,500 dilution of rabbit anti-RecA antibody, washed, then probed with a 1:10 dilution of a goat anti-rabbit HRP secondary antibody. Ladder is PageRuler™ Plus Prestained Protein Ladder, 10 to 250 kDa (ThermoFisher).



SUPPLEMENTAL FIGURE S6. PolyP-Inducing Nutrient Limitation Does Not Affect PtsN Protein Levels *In Vivo*. Complete gels for data shown in Fig. 5B. *E. coli* MG1655 (A) *ptsN*-3xFLAG, (B) $\Delta phoP790::kan^+$ *ptsN*-3xFLAG, or (C) $\Delta rpoN730::kan^+$ strains were grown at 37°C to $A_{600}=0.2-0.4$ in LB and then shifted to minimal medium for 2 hours. At the indicated timepoints, protein samples (n=3) were collected and immunoblotted to quantify PtsN-3xFLAG (18 kDa) and RecA (38 kDa). Ladder is PageRuler™ Plus Prestained Protein Ladder, 10 to 250 kDa (ThermoFisher).



SUPPLEMENTAL FIGURE S7. Nitrogen Metabolites Do Not Allosterically Regulate PPK Activity. Specific activity of purified PPK in the presence of the indicated compounds, with statistical comparison of reactions containing additives to the reaction without those additives from the same set of experiments (n=3, mean \pm SD; one-way ANOVA, ns=not significant).

A C-TERMINAL POLY-HISTIDINE TAG ALTERS POLYPHOSPHATE KINASE
ACTIVITY AND MASKS POTENTIAL REGULATORY EFFECTS

by

MARVIN Q. BOWLIN, AVERY D. LIEBER, ABAGAIL R. LONG, AND MICHAEL J.
GRAY

Manuscript Under Preparation
Format adapted for dissertation and eratta corrected

ABSTRACT

In *Escherichia coli*, many environmental stressors trigger polyphosphate (polyP) synthesis by polyphosphate kinase (PPK), including heat, nutrient restriction, toxic compounds, and osmotic imbalances. PPK is essential for virulence in many pathogens, and has been the target of multiple screens for small molecule inhibitors that might serve as new anti-virulence drugs. However, the mechanisms by which PPK activity and polyP synthesis are regulated are poorly understood. Our previous attempts to uncover PPK regulatory elements resulted in the discovery of PPK* mutants, which accumulate more polyP *in vivo*, but do not produce more *in vitro*. In attempting to further characterize these mutant enzymes, we discovered that the most commonly-used PPK purification method – Ni-affinity chromatography using a C-terminal poly-histidine tag – altered intrinsic aspects of the PPK enzyme, including specific activity, oligomeric state, and kinetic values. We developed an alternative purification strategy using the C-terminal C-tag system which did not have these effects. Using this strategy, we were able to demonstrate major differences in the *in vitro* response of PPK to 5-aminosalicylic acid, a known PPK inhibitor, and observed several key differences between the wild-type and PPK* enzymes, including changes in oligomeric distribution, increased enzymatic activity, increased resistance to substrate inhibition, and increased resistance to product and substrate inhibition, that help to explain their *in vivo* effects. Importantly, our results indicate that the C-terminal poly-histidine tag is inappropriate for purification of PPK, and that any *in vitro* studies or inhibitor screens performed with such tags need to be reconsidered in that light.

INTRODUCTION

Inorganic polyphosphate (polyP, **Figure 1A**) is an evolutionarily conserved biomolecule utilized by all domains of life for a myriad of functions (1). In bacteria, the synthesis of polyP is a stress response mechanism triggered in response to environmental stressors such as reactive chemical species, nutrient starvation, osmotic imbalances, antibiotics, and host immune responses. In many species of bacteria, polyP synthesis is catalyzed by the enzyme polyP kinase (PPK), which hydrolyzes ATP and transfers the γ -phosphate unit to the elongating chain of high-energy phosphoanhydride bonds (2-4). Two unrelated families of PPK enzymes have been described: PPK1, originally discovered in *Escherichia coli* (where it is called simply 'PPK'), and PPK2, discovered in *Pseudomonas aeruginosa* (5, 6). Both enzymes can catalyze both the synthesis and hydrolysis of polyP (**Figure 1B**). However, PPK1 preferentially catalyzes the synthesis of polyP while PPK2 preferentially catalyzes the reverse reaction to replenish the nucleotide triphosphate pool. Importantly, while polyP is universally conserved, there are no universally conserved homologs of either PPK (5-7). While neither PPK1 nor PPK2 is found in mammals, a wide number of bacterial species, including many pathogens, possess homologs of one or both PPK enzymes, making polyP metabolism a promising target for therapeutic development (6, 8). In fact, 5-aminosalicylic acid (5-ASA, a.k.a. mesalamine), a known PPK1 inhibitor (9), is the gold standard in treatment for ulcerative colitis and irritable bowel syndrome (10). *In vivo* studies determined that 5-ASA reduces bacterial polyP levels in the human intestine and sensitizes bacteria in the gut to oxidative stress, impairing their ability to colonize and persist in chronically inflamed environments (9). In many bacterial species that express PPK homologs, PPK activity is directly

associated with aspects of bacterial survival and pathogenesis, including tissue invasion, colonization, expression of virulence factors, biofilm formation, migration, chemotaxis, gene regulation, antibiotic resistance, and defense against host immune responses (1, 11-20). Collectively, these data suggest that PPK represents a unique opportunity to manipulate a target heavily linked to bacterial pathogenesis while avoiding any potential effect on host metabolism by targeting an enzyme exclusive to bacteria.

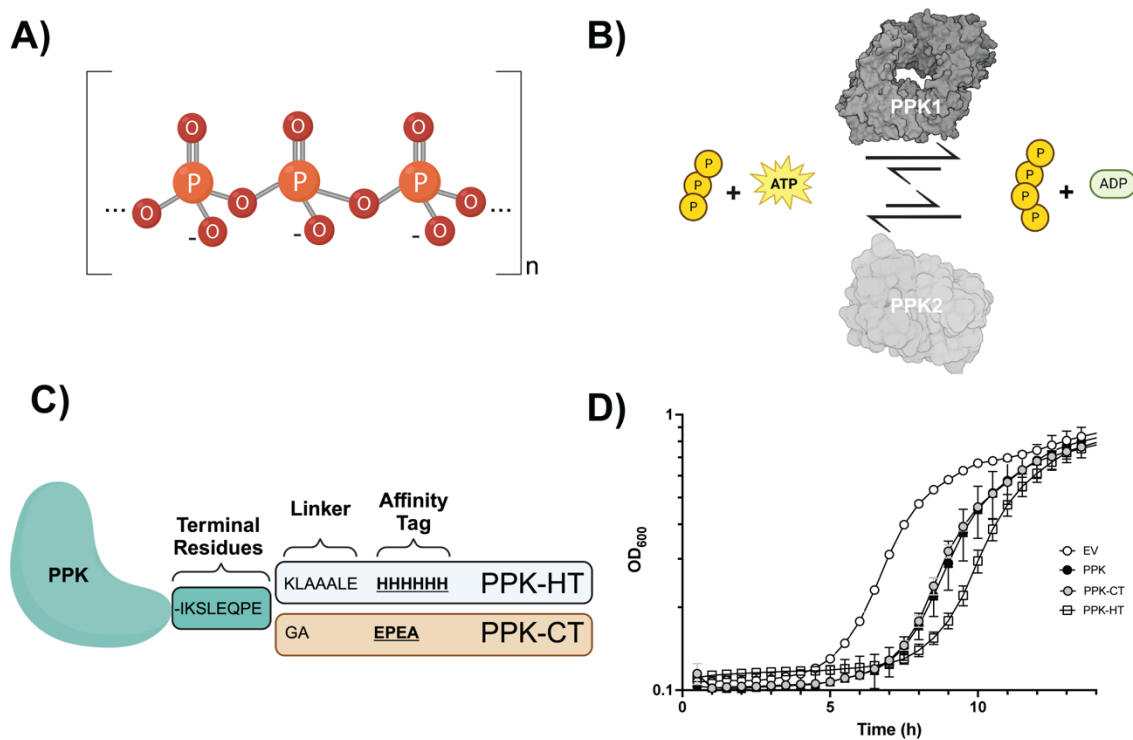


Figure 1 | PolyP, PPK, and Protein Purification Methods. **A)** Structural representation of a polyphosphate polymer. **B)** PPK activity exists in an equilibrium, where a PPK enzyme can drive either the synthesis of polyP from ATP, or the degradation of polyP into ATP and a polyP molecule or pyrophosphate. PPK1 preferentially catalyzes the forward reaction, while PPK2 preferentially catalyzes the reverse. **C)** Diagram of PPK constructs used in this paper. PPK-HT has a thirteen residue tag, while PPK-CT has a six residue tag. Untagged PPK has the full sequence with no tag. **D)** Δppk strains transformed with either pET21b (empty vector, EV), pPPK35 (PPK), pPPK33 (PPK-CT), or pPPK29 (PPK-HT) were grown to stationary phase, diluted to an OD_{600} of 0.01, and cultured for 24 hours at 37°C with shaking.

Despite the wide array of studies done on PPK1, PPK2, and polyP, very little is known about the regulation of the polyP synthesis response. In the 30 or more years *E. coli* PPK has been studied, it has been characterized as a dimer, trimer, and a tetramer synthesizing polyP, degrading polyP, or generating guanosine-5'-tetrphosphate (pppp(G)) (3, 4, 21-23). Understanding the regulation of PPK activity is key to understanding how the entire polyP response is regulated. In previous works, we have attempted to answer this question with a top-down genetics approach, identifying a variety of transcription factors that act in the pathway leading to polyP synthesis (24, 25). Unfortunately, while highlighting several steps in the response cascade that triggers polyP synthesis, none of these studies have yielded a clear understanding of the full regulatory pathway. Importantly, none of the regulators identified so far directly affect PPK1 activity, which suggests that there is an enzyme-specific regulatory feature that we have not identified yet with genetic studies. In an attempt to understand regulatory activity targeting PPK directly, we isolated a series of mutations in *ppk* which produce PPK* variants that resulted in significantly higher levels of polyP accumulation *in vivo* (26). While this represented the first report of mutations in *ppk* that increase polyP accumulation, surprisingly, *in vitro* analysis of these mutant enzymes revealed no substantial difference in their activities under any tested condition, further emphasizing how much remains to be learned about the regulation of polyP production.

In the present study, we have identified an issue that, in addition to affecting our previous observations, has important implications for any studies done using PPK1 enzymes purified with the field-standard C-terminal poly-histidine affinity tag (9, 22, 23,

27-30). To address this issue, we developed a novel protein purification strategy that allows us to purify *E. coli* PPK with minimal effects on the enzyme's structure or functions, allowing us to make more rigorous conclusions about the regulation of PPK activity in *in vitro* experiments. We found, for example, that PPK purified in this way is more sensitive to 5-ASA than poly-histidine tagged PPK *in vitro*, indicating that choice of protein purification method is an important variable in any experiment aimed at identifying PPK1 inhibitors for potential therapeutic use (8, 9, 29, 30). Using our new purification strategy, we have also found distinct differences in PPK* enzyme properties that were previously unseen in the poly-histidine tagged enzymes, including effects on oligomeric states, enzymatic activity, and inhibitor sensitivity, with important implications for understanding the mechanisms by which these mutations lead to an increase *in vivo* polyP production. Our results demonstrate a straightforward method of purifying PPK protein with the essential properties of the native enzyme and provide novel insight into the activities of PPK1 enzymes, while also highlighting the complicated and still incompletely understood regulation of polyP synthesis.

RESULTS

C-terminal poly-histidine tagging alters the intrinsic properties of PPK

A major question that remained from our previous work was how the PPK* mutations resulted in a significantly higher accumulation of polyP *in vivo* without altering the specific activity of the enzymes or their sensitivities to substrate concentration or endogenous inhibitors *in vitro*. PPK1 is known to have different activities based on its oligomeric state (21). At first, due to the position of the amino acids changed in the PPK*

proteins in predicted monomer interfaces in the PPK tetramer (26), we suspected the mutations could be affecting the oligomerization of the monomers, but this presented new challenges.

Previous reports indicated that PPK1, when purified from a native expression culture, purifies as a tetramer with an ATP in the active site (3, 4, 21). Conversely, crystallography studies suggested that PPK1 purified using a C-terminal 6X poly-histidine tag formed a dimer with a non-hydrolyzable ATP analog in the active site (22, 23). The 2003 structure study reported that the C-terminally His-tagged enzyme had comparable activity to untagged enzyme, and since that time nickel affinity chromatography of the C-terminally His-tagged enzyme has become the field standard technique for both PPK1 and PPK2 purification (9, 22, 23, 27-30).

This presents a multitude of potential issues. First, poly-histidine purification tags are not uniform across laboratories. Some constructs produce a short tag of 6 or 8 residues while others utilize a longer tag of upwards to 16 residues. One reason for tag length variations is that tag flexibility is often used to improve purification yields and solubility, which is a known issue with PPK (4, 22, 23). Second, it has been well-established that terminal poly-histidine tags can alter enzymatic structure, function, solubility, stability, oligomeric state, and activity of a variety of different proteins (31-35). Indeed, in the same report that established the C-terminal His-tag method of PPK purification, an N-terminal 6X poly-histidine tag resulted in the near total loss of activity (22). Recently, polyP has been observed to strongly modify poly-histidine sequences by

an ionic mechanism, inducing a significant shift in NuPAGE and SEC migration for enzymes with a poly-histidine tag and producing a pH-sensitive association that requires extremely high ionic strength to disrupt (36). These known issues with the poly-histidine tag led us to question whether our purified PPK* mutant enzymes were being affected by the purification tag itself.

To address these issues, we developed a purification construct using the C-tag system, which uses a four residue tag (E-P-E-A) that binds to a commercially available nanobody-based resin for purification (37). To allow for flexibility, we included a two residue linker for a total length of six residues (G-A-E-P-E-A, **Figure 1C**), making our final tag on par with the shortest His-tags used in the field. We refer to this construct hereafter as PPK-CT, in contrast to C-terminally His-tagged PPK-HT. We also developed and optimized a new purification method for untagged recombinant PPK based on the original native purification process (**Supporting Information Figure S1**) (3).

Our PPK purification method involves inoculating a rich overexpression medium with an overnight culture and allowing the cells to grow into late log phase before inducing overexpression of the recombinant enzyme. In preparing overexpression cultures for purification, we observed that both the untagged PPK and PPK-CT cultures took roughly 3.5 hours to reach the target OD₆₀₀ of 0.8. Conversely, PPK-HT cultures required longer incubations to reach the target OD, upwards of 5 hours (data not shown). Previously, we reported that magnesium supplementation rescues polyP-associated toxicity (26). Addition of 10 mM MgCl₂ in the overexpression media improved the

incubation time of our overexpression strains so that each strain reached the target OD in around 3 hours (data not shown), suggesting the effect was due to polyP. Full plasmid sequencing showed no changes in the backbone of the expression vector between the three plasmids. This led us to question whether PPK-HT expression had significant effects on bacterial growth and recovery. To test this, we transformed the same overexpression plasmids into an *E. coli* Δppk (DE3) strain. We set up growth curves in rich protein expression media with 150 μ M IPTG and 10 mM MgCl₂ and compared their growth to an empty-vector control. As expected, the empty vector strain had a very short lag phase (**Figure 1D**) as there was no polyP synthesis to impair growth. Strains expressing either PPK and PPK-CT had similar growth delays of approximately 7 hours. However, the PPK-HT strain had a more severely delayed onset of growth compared to the other two strains, indicating that PPK-HT resulted in a more severe delay of recovery from stationary phase and, most importantly, that PPK-HT behaves differently *in vivo* from either untagged PPK or PPK-CT.

Using purified PPK, PPK-CT, and PPK-HT enzymes, we tested polyP kinase activity *in vitro* at 6 mM ATP, which is the concentration at which polyP synthesis is maximized without the effect of substrate inhibition being observed (9, 26). We also tested polyP synthesis at 20 mM ATP, a concentration that induces strong substrate inhibition. This allowed us to compare the specific activities of our PPK tag variants at either the optimal (**Figure 2A**) or inhibitory (**Figure 2B**) substrate concentrations. In both situations, untagged PPK and PPK-CT had comparable activities. Conversely, PPK-HT had significantly higher activity at both optimal and inhibitory concentrations. This

indicated that PPK-HT has an altered enzymatic profile with distinctly different activities compared to the untagged enzyme, but that PPK-CT is more comparable to the native enzyme.

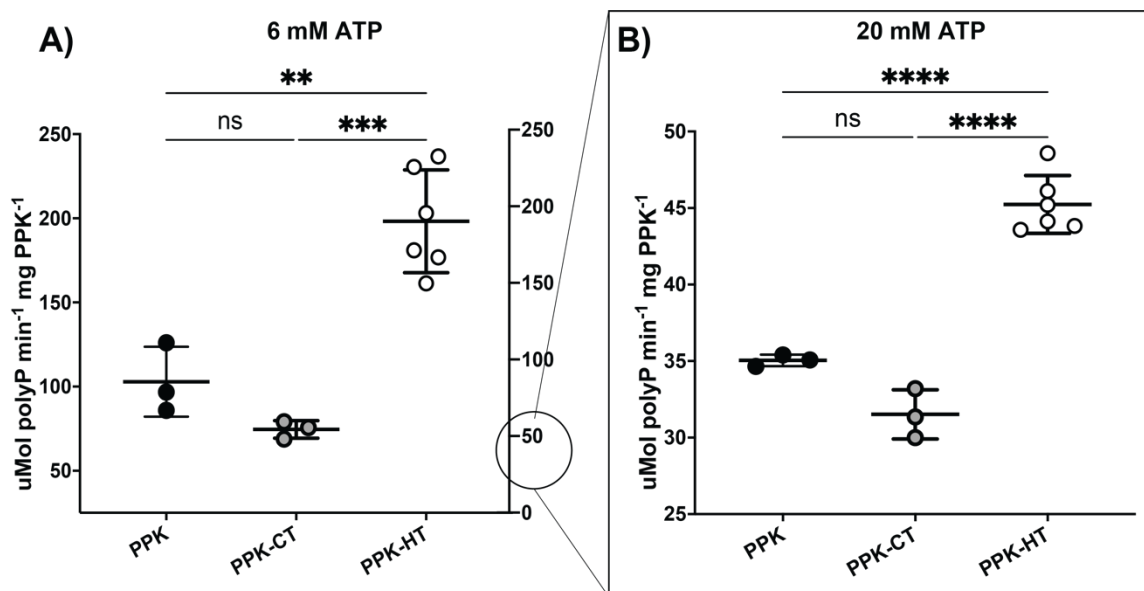


Figure 2 | A Poly-histidine Tag Increases the Specific Activity of PPK. Purified PPK enzyme was tested under reaction conditions with either **A)** optimal substrate concentration (6 mM) or **B)** inhibitory substrate concentration (20 mM). In both instances, the PPK-HT enzyme (open circles) exhibits a specific activity significantly higher than both PPK (black circles) and PPK-CT (gray circles). Results represent three or more independent replicates. Data analyzed via one-way ANOVA with Tukey's multiple comparisons and plotted with SD. ** $p < 0.01$, *** $p < 0.001$, **** $p < 0.0001$.

We next performed a more detailed kinetic comparison of PPK-CT and PPK-HT activity (**Figure 3**). A comparison of fits using an extra sums-of-squares F test confirmed that a substrate inhibition model (**Figure 3A, 3B**) was appropriate for analysis for both PPK-CT (**Figure 3A**) and PPK-HT (**Figure 3B**) ($p = 0.0015$ and 0.0027 , respectively). The resulting curves were well fitted (PPK-CT and PPK-HT $r^2 = 0.9234$ and 0.9754 , respectively). Unlike kinetic curves of enzymes that follow classic Michaelis-Menten kinetics where the enzyme reaches a plateau of activity that isn't affected by further

increases in substrate concentration, substrate inhibition curves peak and drop as substrate concentration increases. Substrate inhibition models, therefore, calculate a theoretical V_{\max} for the enzyme as if it were not inhibited by substrate. The specific activity measurements in **Figure 2** better reflect the maximum PPK activity achievable in actual experiments. The resulting calculated kinetic parameters showed distinct differences between PPK-CT and PPK-HT. PPK-CT had a 1.7-fold higher theoretical V_{\max} and a 1.9-fold higher K_m compared to PPK-HT. Interestingly, there was a 3.3-fold increase in K_i for the PPK-HT enzyme. Taken together, the PPK-HT enzyme has a perturbed kinetic profile that demonstrates a lower reaction rate, an increase in substrate affinity, and an increased resistance to substrate inhibition compared to PPK-CT.

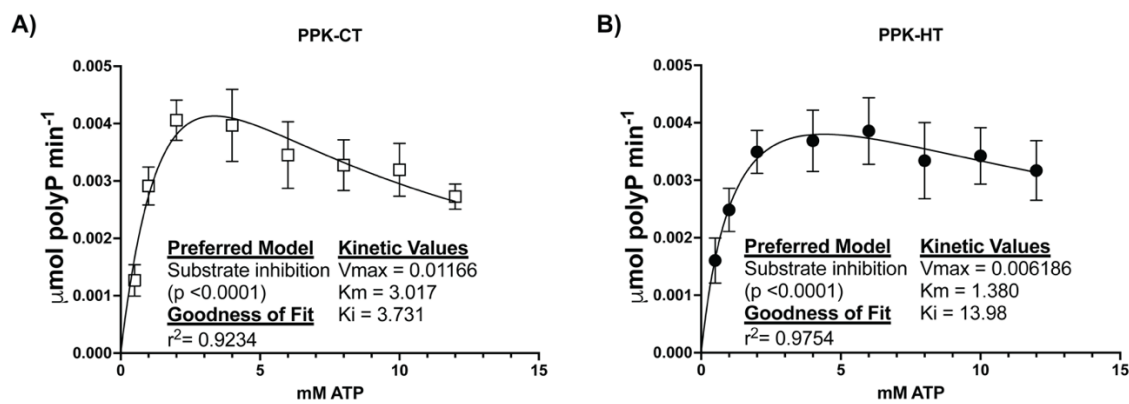


Figure 3 | Kinetics of Tagged PPK Enzymes. A) Kinetic curve for PPK-CT. B) Kinetic curve for PPK-HT. The fit preferred model and quality of fit to the model are displayed in the bottom left corner of each plot. The kinetic parameters for each enzyme are displayed in the bottom right corner. Data generated in at least three independent experiments. Statistical analysis of the model quality was determined via extra sum-of-squares analysis. Curve fit and kinetic parameters were calculated by the substrate inhibition model in GraphPad Prism 10.0.1(170).

The poly-histidine tag alters the oligomeric distribution of PPK

The oligomeric state of PPK plays a known role in its activity (3, 4, 22, 23, 38).

PolyP synthesis begins with the autophosphorylation of residue H435 of the PPK

monomer. At low substrate concentrations ($> 5 \mu\text{M}$ ATP), autophosphorylation is expected to occur in a tetrameric state that then dissociates to a dimer to synthesize polyP. At higher substrate concentrations (*e.g.* 1 mM ATP) it can autophosphorylate as a dimer (21, 23). The active form of the enzyme is generally thought to be the dimeric form. As PPK's oligomeric state affects its activity, we measured the oligomerization of PPK, PPK-CT, and PPK-HT under non-reactive buffer conditions (20 mM HEPES pH 7.5, 0.8 M NaCl, 1 mM EDTA and 15% glycerol) using mass photometry (39). Mass photometry provides a highly accurate visual measurement of the mass of individual molecules in a solution (**Supporting Video S1**), allowing the calculation of the distribution of size species in one pool at low concentration. The oligomeric profile of untagged PPK (**Figure 4A**), showed three primary peaks – two small peaks that correspond to the monomer (~ 75 kDa) and dimer (~ 140 kDa), and a major peak which corresponds to the tetramer (~ 310 kDa). It is important to note that, due to the method used to enrich and purify untagged PPK, there are some peptide fragments that affect the tightness of the peaks. This same distribution of oligomeric states was clear for PPK-CT as well (**Figure 4B**), which, having an affinity purification tag, allows for clean, tight peaks and a more clearly visible dimer peak. However, the oligomeric distribution of PPK-HT (**Figure 4C**) was overwhelmingly tetrameric with only a small population of monomer present.

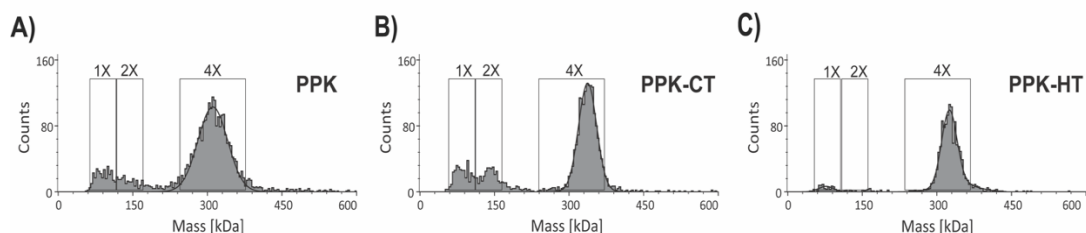


Figure 4 | Oligomeric Distributions of Purified PPK. **A)** PPK demonstrates three populations: a monomer at ~75-78 kDa, a dimer at ~135-150 kDa, and a tetramer at ~310-320 kDa. The predominant peak is the tetramer. **B)** PPK-CT has the same populations as PPK, with the tetrameric peak being the dominant peak. **C)** PPK-HT has a distinctly different distribution pattern, with almost all the enzyme being in a tetrameric form and little to no detectable monomer or dimer in the sample. Samples were run at ~50 nM.

Whether this shift in oligomeric state directly leads to a shift in enzymatic activity is difficult to ascertain. The earliest reports demonstrated the untagged enzyme acting as a tetramer (3, 4). Subsequent studies, including crystallography studies using both a poly-histidine tag and a non-hydrolyzable ATP analog to “trap” the enzyme in an active form, suggested that the dimeric form was responsible to synthesizing polyP (21, 23). Whether the tetrameric or dimeric form is the true active state for polyP synthesis is beyond the scope of this study. It is possible that PPK-HT exists almost exclusively as an active tetramer, which might allow it to produce polyP faster. Alternatively, the PPK-HT enzyme might more readily autophosphorylate and dissociate into the active dimer in the presence of ATP. We can, however, confidently conclude that a C-terminal poly-histidine tag alters the oligomeric distribution of the enzyme in a way different from PPK or PPK-CT. These results, combined with the effect the poly-histidine tag had on kinetics, lead us to conclude that the C-terminal poly-histidine tag alters PPK properties in multiple ways,

and that the properties of the PPK-HT enzyme are neither indicative of endogenous activity nor reliable for therapeutic and pharmaceutical development.

Characterizing PPK Enzymes Without Tag Interference*

We next returned to the question of the mechanism by which PPK* variants lead to increased *in vivo* polyP accumulation. Using our C-tag system, we purified PPK* enzymes which represented three distinct mutations – PPK*E56K, PPK*D230N, and PPK*E245K. We then tested the specific activity of each enzyme (**Figure 5A**) and found that only PPK*E56K had a significantly increased specific activity compared to the other enzymes (~ 1.3-fold increase compared to WT). However, as we previously observed, this increase in activity seems unlikely to explain the > 100-fold increase in *in vivo* polyP accumulation levels observed in *ppk** mutant cultures (26). To determine if the kinetic properties of PPK were altered by the *ppk** mutations, we measured enzymatic activity over a range of substrate concentrations and plotted substrate inhibition curves (**Figure 5B**). This allowed us to identify the theoretical V_{\max} (**Figure 5C**), K_m (**Figure 5D**), and K_i (**Figure 5E**) for each PPK enzyme. Fitting curves to a substrate inhibition model, we were able to determine that PPK*E56K had an increased theoretical V_{\max} and K_m compared to WT. This suggests that PPK*E56K does indeed have an increased capacity for polyP synthesis. PPK*E245K had a significantly lower K_m than WT, indicating a higher affinity for substrate, though the theoretical V_{\max} was comparable to WT. Interestingly, both PPK*D230N and PPK*E245K had higher K_i values, indicating that they were less sensitive to substrate inhibition compared to the WT enzyme. Taken together, the data so far suggests different mechanisms of effect for each PPK* mutant.

PPK*E56K has an increased capacity for polyP synthesis as seen by the increase in V_{max} and, concurrently K_m . PPK*D230N has no change in polyP synthesis efficacy but is more resistant to substrate inhibition than WT enzyme, meaning it can function at peak activity even in higher ATP concentrations. PPK*E245K has an increased affinity for substrate and a decrease in substrate inhibition sensitivity, indicating it has a higher range of optimal ATP concentrations for polyP production. Whether these kinetic changes can fully account for the dramatic *in vivo* effects of PPK* mutations on polyP accumulation, however, remains to be determined.

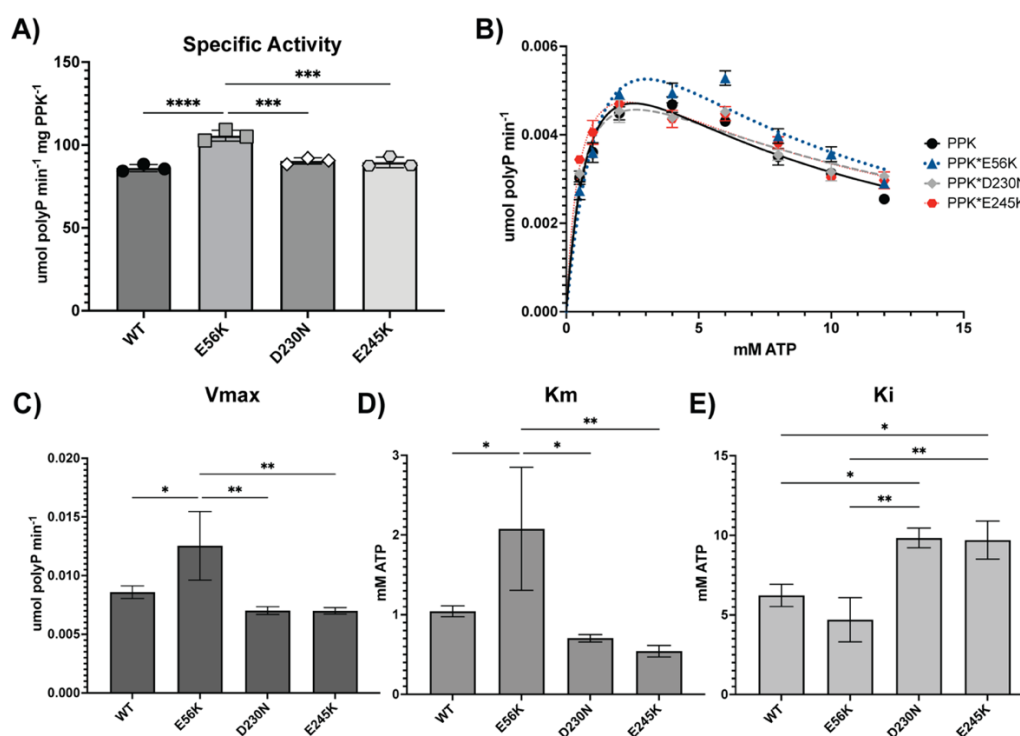


Figure 5 | Activity and Kinetics of PPK* Enzymes. A) Specific activities of the PPK* variants at optimal substrate concentration. B) Kinetic curves of PPK* enzymes fit to a substrate inhibition model in GraphPad Prism 10.0.1(170). C) V_{Max} values calculated from the curves in B. D) K_M of each enzyme calculated from the curves in B. E) K_I of ATP for enzymes. All experiments were performed in individual triplicates. Statistical analysis of the specific activities was done via ordinary one-way ANOVA with Tukey's multiple comparisons. Kinetic values reported in C-D were analyzed via one-way ANOVA with Tukey's multiple comparisons test. Statistically significant relationships are indicated. * $p < 0.05$, ** $p < 0.01$, *** $p < 0.001$, **** $p < 0.0001$.

PPK mutations alter the oligomeric state of PPK*

We next asked whether the PPK* mutations affected the oligomeric distribution of the enzyme. As shown in **Figure 4C**, the poly-histidine tag overwhelmingly drove the PPK oligomeric distribution into a tetrameric state. This suggested that any effects of the PPK* mutations on oligomeric distribution might be masked by a poly-histidine tag. This is important, because when mapped onto the crystal structure (PDB ID 1XDP) (23), most of the mutant sites are located in regions that could interfere with monomer-monomer or dimer-dimer interactions (**Supporting Video S2**). Indeed, when we measured the oligomeric distributions of C-tagged PPK* enzymes by mass photometry, we found distinct differences compared to the WT enzyme (**Figure 6**). As in **Figure 4A**, the oligomeric distribution of wild-type PPK (**Figure 6A**) was visible as three populations: a monomer, a small amount of dimer, and the majority tetramer. Conversely, PPK*E56K (**Figure 6B**) had a substantial dimeric population. PPK*D230N (**Figure 6C**), a mutation relatively distant from the monomer interfaces of PPK, had a similar oligomeric distribution to WT enzyme. Most interestingly, the PPK*E245K mutant (**Figure 6D**) had a decidedly different distribution, with the predominant peak being monomeric rather than tetrameric. Additionally, the dimeric and tetrameric peaks were similar in intensity, which did not occur in any of the other variants. Taken together with the kinetic data and specific activities of individual enzymes, our data suggests that the PPK* mutants probably have varied mechanisms of action that enhance *in vivo* polyP accumulation in multiple ways. We are currently working to understand which of these enzymatic properties contribute to *in vivo* polyP accumulation and how this may be related to the natural regulation of PPK activity in bacteria under stress.

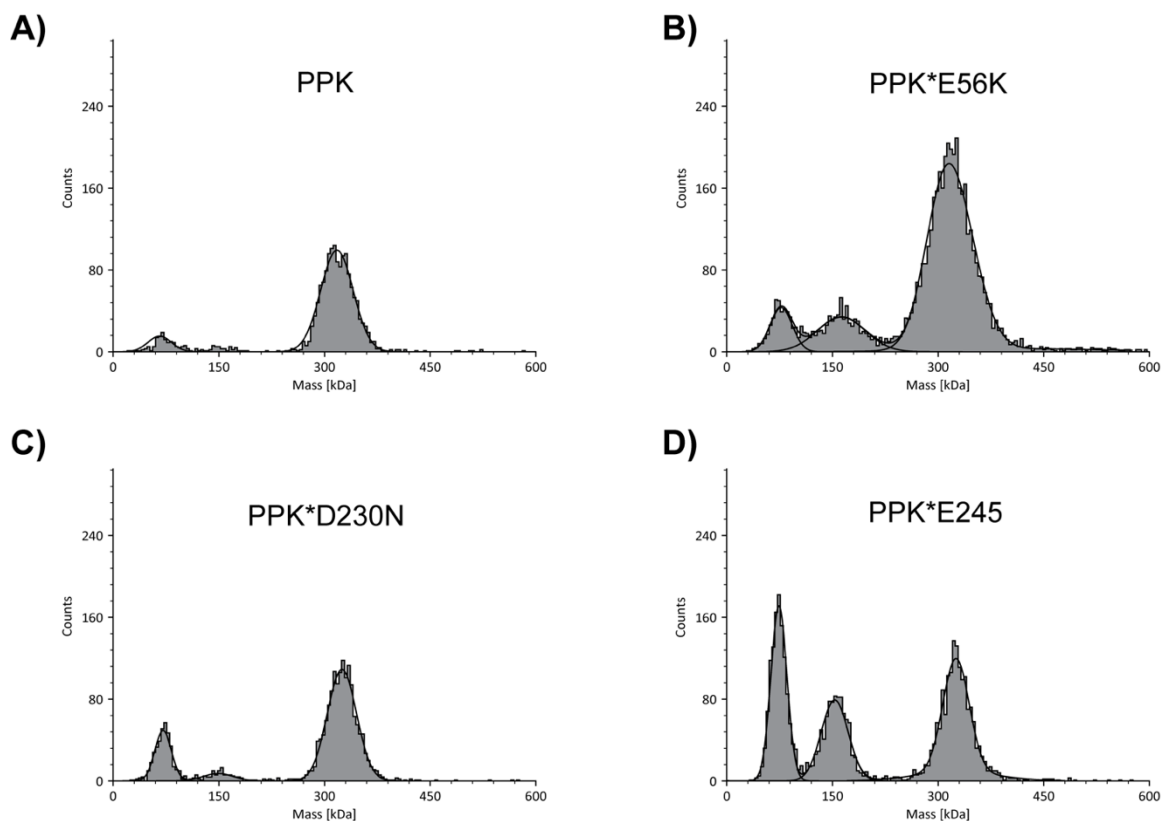


Figure 6 | Oligomeric Distribution of PPK* Variants. A) The oligomeric distribution of PPK enzyme as a reference with the monomer, small dimer, and tetramer peaks. **B-D)** Oligomeric distribution of PPK* variants as labeled. Each graph shown is from a final concentration of 125 nM enzyme. Graphs are representatives of multiple individual measurements.

Inhibition of PPK Activity

We next questioned whether the PPK* mutations might affect the sensitivity to an endogenous competitive inhibitor, ADP. ADP is a byproduct of polyP synthesis, and the accumulation of ADP results in a shift in the equilibrium reaction to break down polyP and produce ATP. If the PPK* mutants had an increased resistance to ADP inhibition, then they would be able to synthesize more polyP before being driven to reverse the

reaction. To test this, we measured the polyP production by each enzyme at 6 mM ATP and either 0.1, 0.2, 0.3, or 0.6 mM ADP.

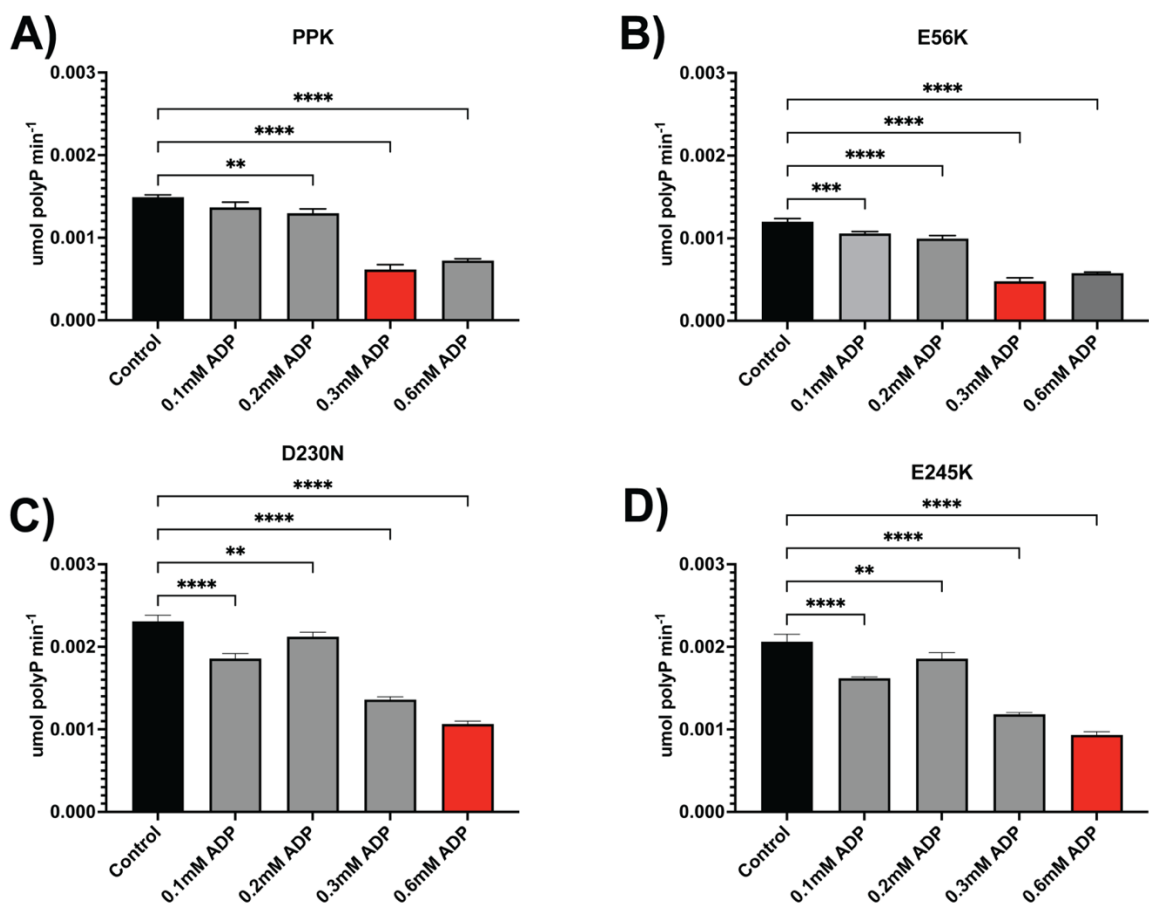


Figure 7 | Sensitivity to ADP Inhibition. Enzymatic reactions lacking the creatine kinase ATP reconstitution system and including 0 - 0.6 mM ADP were prepared and polyP synthesis rates were measured at 6 mM ATP with the goal of identifying a concentration that inhibited activity by 50% or greater (indicated by the red bar). Statistical significance was determined by standard one-way ANOVA. ** $p < 0.01$, *** $p < 0.001$, **** $p < 0.0001$.

As seen in **Figure 7A**, we found that the addition of 0.2 mM ADP was the minimum concentration necessary to produce a significant decrease in wild-type PPK activity. However, for >50% inhibition, the addition of 0.3 mM ADP was necessary.

Figure 7B shows that, while PPK*E56K was sensitive to just 0.1 mM ADP inhibition, 0.3 mM ADP was necessary for >50% inhibition. For both PPK*D230N (**Figure 7C**) and

PPK*E245K (**Figure 7D**), the addition of 0.1 mM ADP induced a significant, albeit small level of inhibition. However, for >50% inhibition, 0.6 mM ADP was required. This further supports our working model that each PPK* mutant has a different mechanism of action by which it alters the accumulation of polyP *in vivo*, with PPK*D230N and PPK*E245K being substantially less sensitive to inhibition by ADP than wild-type PPK.

The development of PPK inhibitors for medical use is not a novel concept (2, 40-43). The gold standard pharmaceutical treatment for ulcerative colitis is the use of 5-ASA, a known PPK inhibitor (10). 5-ASA rapidly decreases the polyP levels in several species of intestinal bacteria, sensitizing them to the less hospitable conditions of the gut. Concurrently, the bacterial burden and inflammation levels of the gut is reduced in patients treated with 5-ASA. 5-ASA was identified as a PPK inhibitor using PPK-HT, and the addition of a very high concentration of 5-ASA (1 mM) resulted in only modest inhibition *in vitro* (9). In contrast, the addition of only 100 μ M 5-ASA resulted in 50-60% reduction in bacterial polyP accumulation *in vivo*. The contrast between the relatively potent effect of 5-ASA on polyP levels *in vivo* and weak inhibition of PPK *in vitro*, along with our data showing the poly-histidine tag affects kinetic properties, suggested to us that the purification tag might be masking the true effects of 5-ASA on PPK.

We measured the rate of polyP synthesis for PPK and the three PPK* enzymes over a range of ATP concentrations in the presence of either DMSO or 1 mM 5-ASA. 1 mM 5-ASA had a substantial inhibitory effect on the activity of PPK-CT (**Figure 8A**).

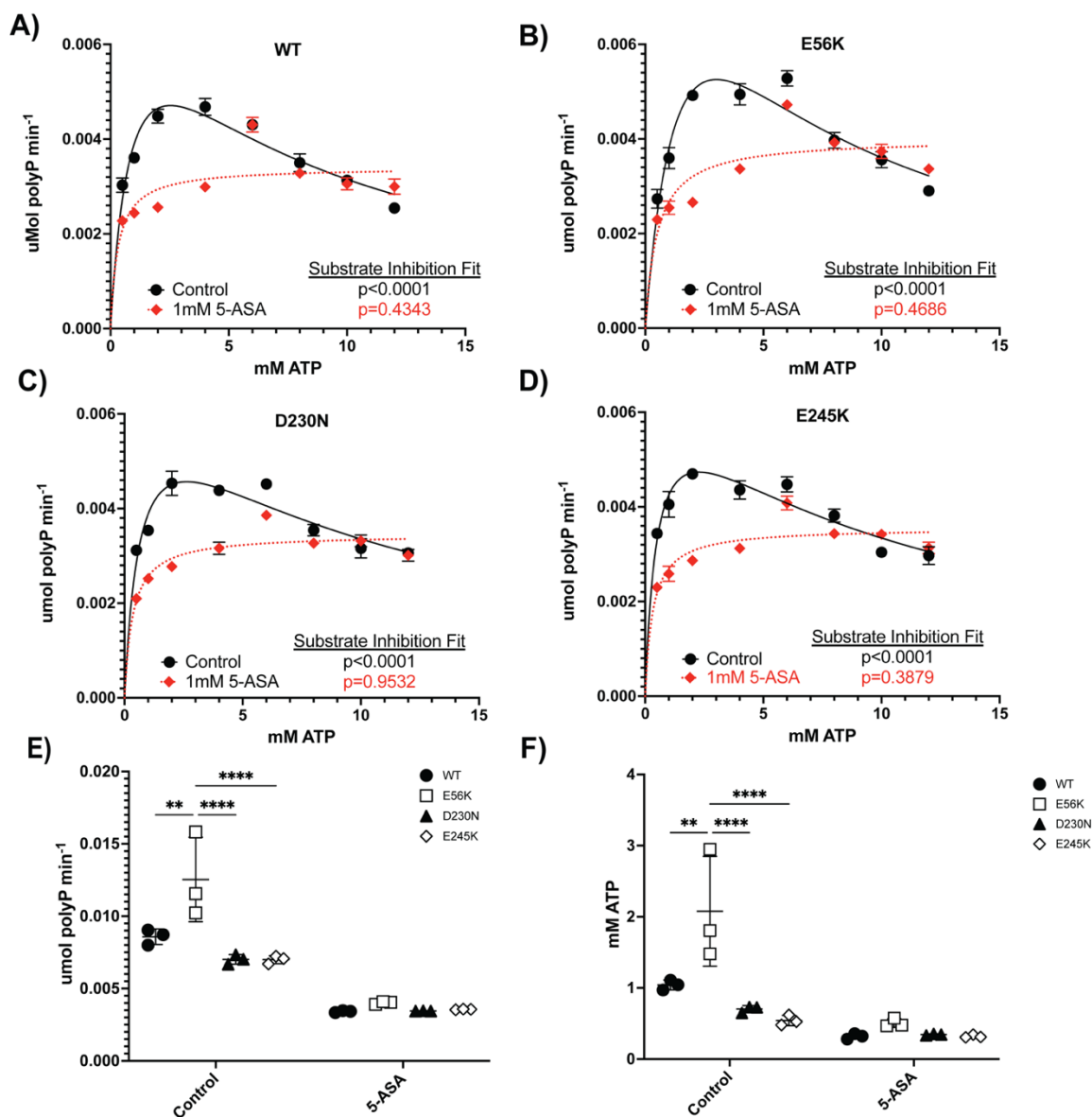


Figure 8 | 5-ASA Inhibition Sensitivity of PPK-CT and PPK*-CT Enzymes. Treatment with 1 mM 5-ASA results in significant inhibition for **A)** WT PPK, **B)** PPK*E56K, **C)** PPK*D230N, and **D)** PPK*E245K. Independent reactions in triplicate of each enzyme were run with 6 mM ATP and either DMSO control (black) or 1 mM 5-ASA (red). Curves were plotted using a substrate inhibition model and an extra sums-of-squares F test was used to determine if the substrate inhibition model was appropriate, with $p < 0.05$ indicating an appropriate fit. Model fit analysis results are indicated by the p values in the lower right corner of each graph. The appropriate models were used to calculate **E)** V_{max} and **F)** K_m . V_{max} and K_m were analyzed using a two-way ANOVA with multiple comparisons. Significant values are indicated. ** $p < 0.01$, **** $p < 0.0001$.

Using an extra sums-of-squares F test, we tested whether the data for each curve fit the Michaelis-Menten or substrate inhibition model. We set the confidence threshold to 95%, so that a p value of less than 0.05 would be indicative of the more complex substrate inhibition model being preferred. We saw that untreated enzyme for all samples tightly fit the substrate inhibition model ($p < 0.0001$). However, treatment with 5-ASA resulted in data that fits the simpler standard Michaelis-Menten model instead for each enzyme (WT $p = 0.4343$, E56K $p = 0.4686$, D230N $p = 0.9532$, E245K $p = 0.3879$). This indicates that 5-ASA completely overwhelmed the ATP inhibition normally seen in this enzyme while also substantially reducing polyP synthesis activity. This is contrary to the previous report using PPK-HT, which found a modest effect on activity and no loss of substrate inhibition (9). For each of the PPK* enzymes (**Figures 8B-D**), the same effect was observed, indicating the PPK* mutations do not greatly affect 5-ASA response. When looking at the relative effects of treatment on V_{\max} and K_m (**Figure 8E-F**), we found no difference in response between the PPK and PPK* enzymes. These data show that the poly-histidine tag used in previous studies significantly affects the activity and inhibitor sensitivity of PPK, and that 5-ASA is a more potent *in vitro* inhibitor of PPK than was previously reported. In addition, we found that the PPK* mutations do not confer resistance to the therapeutic inhibitor test.

DISCUSSION

In this study, we have shown that the C-terminal poly-histidine tag acts in a way that alters the specific activity, kinetic values, and oligomeric stability of recombinant *E. coli* PPK. As a purification method, the poly-histidine tag offers the convenience of

speed, efficiency, and high yield and purity. This is especially true given the highly complex method of untagged PPK purification which gives low, dilute yields and is time consuming. However, the effects the tag exerts on intrinsic properties of PPK makes it difficult to interpret *in vitro* activity results obtained from enzymes purified in this manner. We have identified a purification method that rivals the poly-histidine tag in ease and productivity for production of PPK: the C-terminal C-tag. We have shown that the C-tagged enzyme has comparable activity and oligomeric distribution to the untagged enzyme. Using this new purification method, we were able to purify and characterize several PPK* mutants in ways we were unable to previously. We found that the PPK* mutants all have different profiles compared to the wild-type enzyme, which is summarized in **Table 1**.

Table 1 | Summary of PPK* Differences. Each of the PPK* mutants has distinct profiles that are different from the wild-type enzyme. The oligomeric distribution differences, kinetic differences, and inhibition sensitivities are collected here to clarify the changes each PPK* mutation induces in the enzyme.

	Oligomeric Distribution Differences	Kinetic Differences	Inhibition Sensitivity
PPK*E56K	Increase in dimer population	Vmax, Km, SA increased	<u>ATP and ADP</u> : Comparable to WT <u>5ASA</u> : Comparable to WT
PPK*D230N	Comparable to WT	Vmax, Km, SA comparable to WT	<u>ATP and ADP</u> : Increased Resistance <u>5ASA</u> : Comparable to WT
PPK*E245K	Monomer population is dominant, dimer and tetramer populations are equal in size	Vmax, Km, SA comparable to WT	<u>ATP and ADP</u> : Increased resistance <u>5ASA</u> : Comparable to WT

We observed distinct and significant differences between PPK-HT and both PPK and PPK-CT. PPK-HT had a significantly higher specific activity (~2 fold increase) compared to both the PPK-CT and PPK enzymes. The oligomeric distribution of PPK-HT was also distinctly different. PPK and PPK-CT samples had three populations: a monomeric population, a dimeric population, and a large tetrameric population. Conversely, PPK-HT samples had only a small monomeric population and a large tetrameric population. Consistent with previous studies, we found that a substrate inhibition model was the best-fit model for analysis of PPK-HT and PPK-CT kinetics. However, PPK-HT had a lower V_{\max} than PPK-CT, but had a higher K_m and K_i for ATP, indicating a higher affinity for substrate and a higher capacity for polyP synthesis in high substrate levels.

The current model of PPK activity is that the tetrameric form of PPK autophosphorylates at low ATP concentrations, then dissociates into dimers to produce polyP (21). Our data suggests that the poly-histidine tag stabilizes the tetrameric form, impairing dimer formation. This oligomeric alteration is concurrent with an increased specific activity compared to both the untagged and PPK-CT enzymes, indicating the PPK-HT enzyme is enzymatically more productive. Comparing the kinetic values of PPK-CT and PPK-HT, we find that PPK-HT has a lower V_{\max} , but higher K_m and K_i . This indicates the poly-histidine tag alters the enzyme's affinity for its substrate. If the dimeric form is predominately responsible for polyP synthesis, a stabilized tetramer would explain both an increase in K_m and a decrease in V_{\max} ; the tetramer readily binds ATP to autophosphorylate even at lower ATP concentrations but does not as effectively

synthesize polyP. The increase in K_i indicates that the poly-histidine tag confers resistance to substrate inhibition, meaning that PPK-HT enzyme can synthesize polyP more effectively at higher ATP levels than PPK-CT enzyme. With a stabilized tetramer, more monomeric subunits have an opportunity to be activated via autophosphorylation, meaning more active enzyme complexes overall. Thus, we would see an increase in substrate affinity (lower K_m). Subsequently, the accumulation of polyP would increase in the reaction because of more active enzyme:substrate complexes. Regardless of the mechanism, our data show that the C-terminal poly-histidine tag alters the intrinsic properties of PPK enzyme, while the C-terminal C-tag does not.

Using PPK-CT, we were able to investigate the effects of PPK* mutations on PPK free of effects caused by the purification method. We found that different PPK* mutations have different effects on PPK activity. PPK*E56K had a higher specific activity than wild-type PPK. This coincided with an increase in the population of dimeric enzyme. The theoretical V_{max} of the enzyme was higher as well, though the K_m increased significantly, too. PPK*D230N had a comparable oligomeric distribution, specific activity, V_{max} , and K_m to wild-type PPK. However, it had a significantly higher K_i for ATP, meaning it is more resistant to substrate inhibition and can produce polyP effectively at higher ATP levels. PPK*E245K had a similar specific activity, V_{max} , K_m , and K_i to PPK*D230N, but a very different oligomeric profile. Interestingly, the monomeric population is the dominant species in the oligomeric profile, with the dimeric population being similar to the tetrameric population. When we tested the sensitivity of PPK and PPK* enzymes to the endogenous inhibitor ADP, we saw that the wild-type and

PPK*E56K enzymes both experienced a ~50% reduction in activity at 0.3 mM ADP. PPK*D230N and PPK*E245K both had increased resistance, requiring 0.6 mM ADP to see a ~50% reduction in activity. Taken with the kinetic and oligomeric data, this suggests that the D230N and E245K can function more effectively in an environment with high concentrations of both ADP and ATP, offering a glimpse at how they might improve polyP accumulation *in vivo*. PPK*E56K's increased V_{\max} and resistance to ADP inhibition indicate an improved activity in an otherwise inhibitory environment. These results show that each PPK* mutation has a different mechanism of affecting the enzyme. We are currently working to understand how the altered *in vitro* properties of PPK* enzymes contribute to very high accumulation of polyP *in vivo*.

Testing the PPK inhibitor 5-ASA on C-tagged enzymes showed that a 1 mM 5-ASA treatment resulted in a significant decrease in activity across all tested enzymes and completely suppressed substrate inhibition by ATP. This is in contrast to the previously reported relatively modest *in vitro* effects of 5-ASA on PPK-HT and may help explain the potent *in vivo* effect of 5-ASA on bacterial polyP accumulation (9). These results also indicate that caution needs to be taken when evaluating potential therapeutics against purified PPK, as the commonly used poly-histidine tag results in increased resistance to at least one PPK inhibitor. All the published PPK inhibitor screens we are aware of have used PPK-HT (9, 29, 44-46). We expect that PPK-CT would be a much more appropriate enzyme to use as a target in screens for medically useful PPK inhibitors (43).

MATERIALS AND METHODS

Plasmid and strain construction

The previously described pPPK2 plasmid (47) was repaired using the QuikChange™ site-directed mutagenesis method (Agilent Technologies), modified to use a single primer and 35 cycles of amplification, using primer 5'-GAA GGA GAT ATA CAT ATG GGT CAG GAA AAG-3' to remove a two-residue insertion at the N-terminus of the resultant protein, producing plasmid pPPK29, which encodes PPK-HT. The pPPK33 (PPK-CT) vector was designed by us to incorporate the *ppk* sequence with an additional 21 bps on the 3' end (5'-GGC GCG GAA CCG GAA GCG TAA-3') encoding the G-A linker, EPEA C-tag, and native stop codon into the *NdeI* and *HindIII* sites of pET-21b(+) and synthesized by Genscript. pPPK35, encoding untagged PPK, was generated via single-primer QuikChange™ mutagenesis with primer 5'-CGA ACA ACC TGA ATA AAA GCT TGC GGC C-3' to introduce the native stop codon immediately after the last PPK codon of plasmid pPPK29. Plasmids pPPK43 (encoding PPK*D230N C-tagged enzyme), pPPK44 (PPK*-E56K C-tagged enzyme), and pPPK45 (pPPK*E245K C-tagged enzyme) were generated via via single-primer QuikChange™ mutagenesis of pPPK33 with primers 5'-CAA TGA AGA TGA CCC GCA ATG CCG AAT ACG ATT TAG-3', 5'-GTC CGC TTC GCT AAA CTG AAG CGA CG-3', and 5'-GAA GCC AGC CTG ATG AAG TTG ATG TCT TCC-3' respectively. All plasmid sequences were verified by full plasmid sequencing through Plasmidsaurus. The Δppk *E. coli* strain MJG0598 (F-, *rph-1 ilvG- rfb-50* Δppk λ (DE3 [*lacI lacUV5-T7 gene 1 ind1 sam7 nin5*])) was generated by DE3 lysogenization of strain MJG0224 (F-, λ -, *rph-1*

ilvG- rfb-50 Δppk) (47) with the Novagen λDE3 Lysogenization Kit, according to the manufacturer's instructions. All strains and plasmids are available upon request.

Protein Overexpression and Purification

Overexpression of each enzyme was done as previously described with minor modifications. (47) An overnight culture in 50 ml of LB supplemented with 10 mM MgCl₂ and 0.1 mg ml⁻¹ ampicillin was grown at 37°C with shaking. The overnight culture was then subcultured into a 1-liter volume of Protein Expression Media (PEM; 12 g l⁻¹ tryptone, 24 g l⁻¹ yeast extract, 4% v/v glycerol, 23.14 g l⁻¹ KH₂PO₄, 125.4 g l⁻¹ K₂HPO₄) supplemented with 10 mM MgCl₂ and 0.1 mg ml⁻¹ ampicillin and grown at 37°C with shaking until an OD₆₀₀ of ~0.8. Cultures were then chilled to 20°C for one hour with shaking. After one hour, cultures were induced with 150 μM IPTG and allowed to overexpress for 18 hours at 20°C with shaking. Cultures were then pelleted at 6000 x g at 4°C in an Avanti J-26 XP rotor model JLA8.1000, the media was decanted, and the pellets frozen at -80°C.

Purification of PPK-HT was done as previously described (26). PPK-CT overexpression culture pellets were fully resuspended in C-tag wash buffer (20 mM Tris-HCl, pH 7.4) and incubated on ice for 45 minutes with 0.3 mg ml⁻¹ hen egg lysozyme (Fisher) then heat shocked at 42°C for 10 minutes with constant stirring. The lysozyme digestion was supplemented with 5 mM MgCl₂, 30 U ml⁻¹ Pierce universal nuclease (ThermoFisher), and Pierce EDTA-free protease inhibitor cocktail tablets (ThermoFisher), then sonicated on ice for 5 minutes in 5s pulses of 50% amplitude with a

Fisher Model 120 Sonic Dismembrator. The sonicated solution was fractionated into soluble and insoluble fractions via centrifugation at 20,000 x g for 1 hour at 4°C. PPK-CT was then extracted from the solid fraction using a previously described KCl extraction method with minor modifications (48). The KCl extraction was dialyzed against the C-tag wash buffer then loaded onto the C-tag resin column at a flow rate of 1 ml min⁻¹ in an ÄKTA Start FPLC (Cytiva). The column was washed with ten column volumes of C-tag wash buffer, then eluted over a gradient of 0-100% C-tag Elution Buffer (20 mM Tris-HCl, pH 7, 2 M MgCl₂) before dialysis of PPK-containing fractions into 20 mM HEPES-KOH pH 8.0, 150 mM NaCl, 1 mM EDTA, 15% glycerol.

Purification of recombinant untagged PPK (**Supporting Information Figure S1**) required several modifications to the original native purification protocol (3). The cell pellet was resuspended in Untagged Buffer A (50 mM Tris-HCl, pH 7.5, 10% w/v sucrose). 0.3 mg ml⁻¹ hen egg lysozyme (Fisher) was added, and the suspension was digested on ice for 45 minutes, then heat-shocked at 42°C for 10 minutes with stirring. The digestion was then pelleted at 20,000 x g for 1 hour at 4°C and the supernatant discarded. The pellet was then resuspended in Untagged Buffer A supplemented with 5 mM MgCl₂, 30 U ml⁻¹ Pierce universal nuclease, and Pierce EDTA-free protease inhibitor cocktail tablets, sonicated on ice for 5 minutes in 5s pulses of 50% amplitude, then centrifuged at 30,000 x g for 30 minutes at 4°C. The supernatant was discarded, and the insoluble fraction was resuspended in Untagged Buffer A by sonication for 5 minutes in 5s pulses on ice. To the resuspended pellet was added dry KCl for a 1 M final concentration and 1 M Na₂CO₃ equal to 10% of the resuspension volume. The solution

was stirred at 4°C for 30 minutes, then sonicated briefly for 2 minutes in 5s pulses of 50% amplitude. The sonicated solution was then pelleted at 10,000 x g for 1 hour at 4°C. The supernatant was filtered through a 0.22 µm syringe filter to remove any sizable particles that did not fully pellet down. The filtered supernatant was then dialyzed against Untagged Buffer B (0.2 M Potassium Phosphate Buffer, pH 7.0, 10% glycerol, 1 mM EDTA, 1 mM DTT) for two hours at a ratio of 1:50 minimum in a dialysis membrane with a 50,000 kDa molecular weight cut-off rating. The dialysis was repeated twice for a total of three times. The dialyzed solution was treated with an ammonium sulfate cut of 0.2 mg ml⁻¹ divided over 20 minutes, allowing the solution to stir at 4°C after each treatment. After the last treatment the solution was stirred at 4°C for 30 minutes, then pelleted at 37,900 x g for 30 minutes. To the supernatant we added an additional 0.108 g ml⁻¹ ammonium sulfate and stirred until fully dissolved. The solution was centrifuged again at 37,900 x g for 30 minutes, and the pellet was resuspended in Untagged Buffer C (20 mM HEPES-KOH pH 8.0, 0.2 M NaCl, 1 mM EDTA, 15% glycerol). The resuspended solution was dialyzed against Untagged Buffer C for at least three hours at a minimum ratio of 1:50. This dialysis was repeated three more times. The final dialyzed sample was filtered through a 0.22 µm syringe filter to remove any precipitate, then run over a HiTrap Q HP anion exchange column prepared with 10 column volumes of untagged buffer C to reduce negatively charged particles in the solution. The solution was then loaded slowly (1 ml min⁻¹) onto a HiTrap SP cation exchange column equilibrated with buffer C. The resuspension was allowed to incubate for 10 minutes, then the column was rinsed with 10 CVs of Untagged Buffer C. Finally, the cation exchange column was eluted over a gradient of 30-100% Untagged Buffer D (20 mM HEPES-KOH pH 8.0, 0.8

M NaCl, 1 mM EDTA, 15% glycerol) and fractionated. Fractions containing protein peaks were analyzed by SDS-PAGE to identify those containing PPK. PPK-containing fractions were tested for activity, and all fractions with detectable activity and clean bands on the gel were pooled and dialyzed against protein storage buffer (20 mM HEPES-KOH pH 8.0, 150 mM NaCl, 1 mM EDTA, 15% glycerol) at a 1:50 ratio for three hours. The dialysis was repeated twice more. The final product contained a dilute concentration of untagged PPK (~ 0.001 mg ml⁻¹). Concentration attempts using additional cation exchange passages resulted in the enzyme crashing out of solution (22).

All purified proteins were suspended in PPK storage buffer (20 mM HEPES-KOH pH 8.0, 150 mM NaCl, 1 mM EDTA, 15% glycerol), aliquoted and frozen at -80°C.

Recovery Curves

Cultures of MJG0598 (Δppk DE3) containing either pET-21b(+), pPPK29, pPPK33, or pPPK35 were grown overnight at 37°C with shaking in LB supplemented with 10 mM MgCl₂ and 100 μ g ml⁻¹ ampicillin to establish a stationary culture. Cultures were diluted to a starting OD₆₀₀ of 0.01 in PEM with 10 mM MgCl₂, 0.150 mM IPTG, and 100 μ g ml⁻¹ ampicillin. Individual replicates (200 μ l) were plated in a 96 well plate and grown at 37°C with shaking in an incubating plate reader (Tecan M1000) for 24 hours with OD₆₀₀ measurements every 30 minutes.

Enzyme Activity and Inhibition Assay

PPK activity assays were performed at the noted substrate concentrations according to previously reported methods (26). Kinetic curves were generated by varying the concentration of ATP over a range of 0.5 - 12 mM ATP. All kinetic assays were conducted in the presence of 1 mM TCEP as a reducing agent. The level of inhibition experienced by each enzyme in response to the ATP substrate was determined using the substrate inhibition model for enzyme kinetics. For 5-ASA inhibition, freshly prepared 1 mM 5-ASA in DMSO was added to each reaction over varying ATP concentrations to measure the inhibitory effect of the compound. Where indicated (*i.e.* in **Figure 7**), the creatine kinase ATP regeneration system was left out of the reaction mixture and ADP was added at the indicated concentrations.

Mass Photometry

For analysis of tagged enzyme samples by mass photometry (UNC UNC Protein Expression and Purification & Macromolecular Crystallography core), glass slides were prepared by cleansing with 100% isopropanol then ddH₂O followed by drying with a filtered air stream. Silicone gaskets were placed on the slides to create sample wells. Immediately prior to data acquisition, proteins were diluted in PPK storage buffer to achieve final concentrations of 15 - 75 nM. Samples were analyzed on a Refeyn One instrument using the manufacturer's proprietary software. Masses were calculated against a curve generated from protein standards of known mass (Thermo).

Statistics and Graphing

Statistics and graphs were generated in GraphPad Prism software, version 10.0.2 (171). Statistical tests are indicated in each figure when applicable. To determine the appropriate model for generating a kinetic curve, we used an extra sums-of-squares F test to determine if the simpler model (Michaelis-Menten kinetics) was suitable or if the complicated substrate inhibition model was more suitable. One-way ANOVA with multiple comparisons was selected for the specific activities analysis. In comparing the effect of 5-ASA inhibition, we used a two-way ANOVA with Tukey's multiple comparisons test to compare the theoretical kinetic values of each enzyme in the absence of 5-ASA. We used the same test to compare the Michaelis-Menten values of each enzyme in the presence of 5-ASA. Due to the nature of the different models we could not directly compare the two sets of values.

Data Availability

The raw data for all figures is available in the FigShare data repository (DOI: [10.6084/m9.figshare.c.6831231](https://doi.org/10.6084/m9.figshare.c.6831231)). All strains and plasmids generated in this work are available from the corresponding author upon request to mjgray@uab.edu.

NOTE: For review purposes, the raw data can be accessed at the pre-publication link: <https://figshare.com/s/8560fa5b3fd4f1e624cc>

ACKNOWLEDGEMENTS

The authors would like to acknowledge the mass photometry work performed by Nathan Nicely at the UNC Protein Expression and Purification & Macromolecular

Crystallography core lab supported by the National Cancer Institute of the National Institutes of Health under award number P30CA016086. The content is solely the responsibility of the authors and does not necessarily represent the official views of the National Institutes of Health.

FUNDING AND ADDITIONAL INFORMATION

The work of presented in this article was funded by NIH grant R35GM124590 and the University of Alabama at Birmingham Department of Microbiology Start Up fund. The content of this article is solely the responsibility of the authors and does not necessarily represent the official views of the National Institutes of Health.

CONFLICT OF INTEREST

The authors have no known or perceived conflicts of interest to declare.

REFERENCES

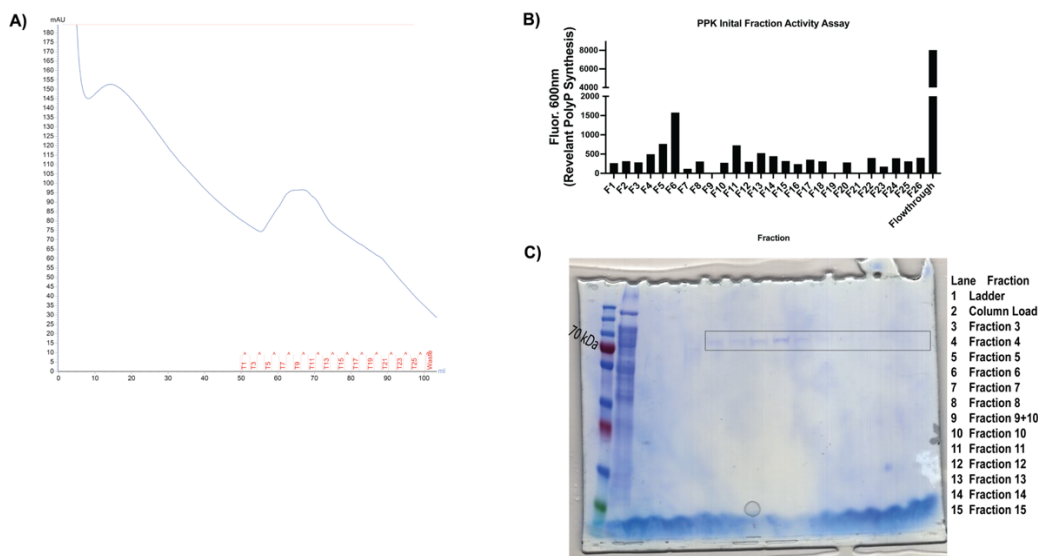
1. Kornberg, A., Rao, N. N., and Ault-Riche, D. (1999) Inorganic polyphosphate: a molecule of many functions *Annu Rev Biochem* **68**, 89-125 10.1146/annurev.biochem.68.1.89
2. Bowlin, M. Q., and Gray, M. J. (2021) Inorganic polyphosphate in host and microbe biology *Trends Microbiol* **29**, 1013-1023 10.1016/j.tim.2021.02.002
3. Ahn, K., and Kornberg, A. (1990) Polyphosphate kinase from *Escherichia coli*. Purification and demonstration of a phosphoenzyme intermediate *J Biol Chem* **265**, 11734-11739
4. Akiyama, M., Crooke, E., and Kornberg, A. (1992) The polyphosphate kinase gene of *Escherichia coli*. Isolation and sequence of the *ppk* gene and membrane location of the protein *J Biol Chem* **267**, 22556-22561
5. Achbergerová, L., and Nahálka, J. (2014) PPK1 and PPK2 — which polyphosphate kinase is older? *Biologia* **69**, 263-269 10.2478/s11756-013-0324-x
6. Zhang, H., Ishige, K., and Kornberg, A. (2002) A polyphosphate kinase (PPK2) widely conserved in bacteria *Proc Natl Acad Sci U S A* **99**, 16678-16683 10.1073/pnas.262655199
7. Achbergerova, L., and Nahalka, J. (2011) Polyphosphate--an ancient energy source and active metabolic regulator *Microb Cell Fact* **10**, 63 10.1186/1475-2859-10-63
8. Campos, F., Alvarez, J. A., Ortiz-Severin, J., Varas, M. A., Lagos, C. F., Cabrera, R. *et al.* (2019) Fluorescence enzymatic assay for bacterial polyphosphate kinase 1 (PPK1) as a platform for screening antivirulence molecules *Infect Drug Resist* **12**, 2237-2242 10.2147/IDR.S181906
9. Dahl, J. U., Gray, M. J., Bazopoulou, D., Beaufay, F., Lempart, J., Koenigs-knecht, M. J. *et al.* (2017) The anti-inflammatory drug mesalamine targets bacterial polyphosphate accumulation *Nat Microbiol* **2**, 16267 10.1038/nmicrobiol.2016.267
10. Dignass, A., Lindsay, J. O., Sturm, A., Windsor, A., Colombel, J. F., Allez, M. *et al.* (2012) Second European evidence-based consensus on the diagnosis and management of ulcerative colitis part 2: current management *J Crohns Colitis* **6**, 991-1030 10.1016/j.crohns.2012.09.002
11. Candon, H. L., Allan, B. J., Fraley, C. D., and Gaynor, E. C. (2007) Polyphosphate kinase 1 is a pathogenesis determinant in *Campylobacter jejuni* *J Bacteriol* **189**, 8099-8108 10.1128/JB.01037-07
12. Rao, N. N., and Kornberg, A. (1996) Inorganic polyphosphate supports resistance and survival of stationary-phase *Escherichia coli* *J Bacteriol* **178**, 1394-1400
13. Ogawa, N., Tzeng, C. M., Fraley, C. D., and Kornberg, A. (2000) Inorganic polyphosphate in *Vibrio cholerae*: genetic, biochemical, and physiologic features *J Bacteriol* **182**, 6687-6693

14. Rashid, M. H., Rao, N. N., and Kornberg, A. (2000) Inorganic polyphosphate is required for motility of bacterial pathogens *J Bacteriol* **182**, 225-227
15. Kim, K. S., Rao, N. N., Fraley, C. D., and Kornberg, A. (2002) Inorganic polyphosphate is essential for long-term survival and virulence factors in *Shigella* and *Salmonella* spp *Proc Natl Acad Sci U S A* **99**, 7675-7680 10.1073/pnas.112210499
16. Rao, N. N., Gomez-Garcia, M. R., and Kornberg, A. (2009) Inorganic polyphosphate: essential for growth and survival *Annu Rev Biochem* **78**, 605-647 10.1146/annurev.biochem.77.083007.093039
17. Tunpiboonsak, S., Mongkolrob, R., Kitudomsab, K., Thanwatanaying, P., Kiettipirodom, W., Tungboontina, Y. *et al.* (2010) Role of a *Burkholderia pseudomallei* polyphosphate kinase in an oxidative stress response, motilities, and biofilm formation *J Microbiol* **48**, 63-70 10.1007/s12275-010-9138-5
18. Cha, S. B., Rayamajhi, N., Lee, W. J., Shin, M. K., Jung, M. H., Shin, S. W. *et al.* (2012) Generation and envelope protein analysis of internalization defective *Brucella abortus* mutants in professional phagocytes, RAW 264.7 *FEMS Immunol Med Microbiol* **64**, 244-254 10.1111/j.1574-695X.2011.00896.x
19. Peng, L., Luo, W. Y., Zhao, T., Wan, C. S., Jiang, Y., Chi, F. *et al.* (2012) Polyphosphate kinase 1 is required for the pathogenesis process of meningitic *Escherichia coli* K1 (RS218) *Future Microbiol* **7**, 411-423 10.2217/fmb.12.3
20. Ortiz-Severin, J., Varas, M., Bravo-Toncio, C., Guiliani, N., and Chavez, F. P. (2015) Multiple antibiotic susceptibility of polyphosphate kinase mutants (ppk1 and ppk2) from *Pseudomonas aeruginosa* PAO1 as revealed by global phenotypic analysis *Biol Res* **48**, 22 10.1186/s40659-015-0012-0
21. Tzeng, C. M., and Kornberg, A. (2000) The multiple activities of polyphosphate kinase of *Escherichia coli* and their subunit structure determined by radiation target analysis *J Biol Chem* **275**, 3977-3983
22. Zhu, Y., Lee, S. S., and Xu, W. (2003) Crystallization and characterization of polyphosphate kinase from *Escherichia coli* *Biochem Biophys Res Commun* **305**, 997-1001
23. Zhu, Y., Huang, W., Lee, S. S., and Xu, W. (2005) Crystal structure of a polyphosphate kinase and its implications for polyphosphate synthesis *EMBO Rep* **6**, 681-687 10.1038/sj.embor.7400448
24. Bowlin, M. Q., Long, A. R., Huffines, J. T., and Gray, M. J. (2022) The role of nitrogen-responsive regulators in controlling inorganic polyphosphate synthesis in *Escherichia coli* *Microbiology (Reading)* **168**, 10.1099/mic.0.001185
25. Gray, M. J. (2019) Inorganic Polyphosphate Accumulation in *Escherichia coli* Is Regulated by DksA but Not by (p)ppGpp *J Bacteriol* **201**, 10.1128/JB.00664-18

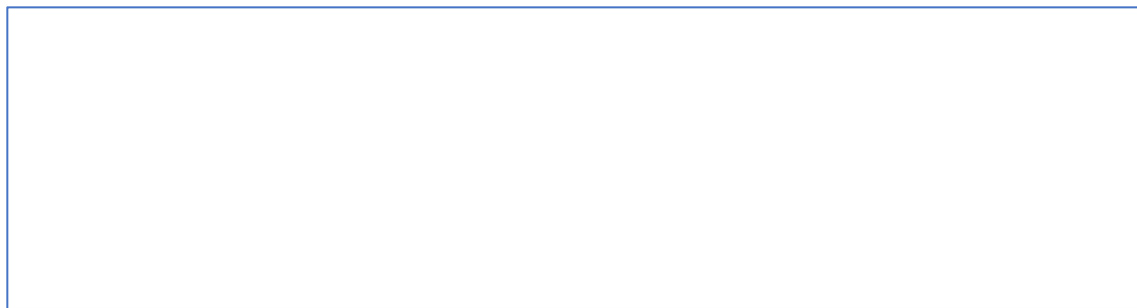
26. Rudat, A. K., Pokhrel, A., Green, T. J., and Gray, M. J. (2018) Mutations in *Escherichia coli* polyphosphate kinase that lead to dramatically increased in vivo polyphosphate levels *J Bacteriol* 10.1128/JB.00697-17
27. Zago, A., Chugani, S., and Chakrabarty, A. M. (1999) Cloning and characterization of polyphosphate kinase and exopolyphosphatase genes from *Pseudomonas aeruginosa* 8830 *Appl Environ Microbiol* **65**, 2065-2071 10.1128/AEM.65.5.2065-2071.1999
28. Iwamoto, S., Motomura, K., Shinoda, Y., Urata, M., Kato, J., Takiguchi, N. *et al.* (2007) Use of an *Escherichia coli* recombinant producing thermostable polyphosphate kinase as an ATP regenerator to produce fructose 1,6-diphosphate *Appl Environ Microbiol* **73**, 5676-5678 10.1128/AEM.00278-07
29. Neville, N., Roberge, N., Ji, X., Stephen, P., Lu, J. L., and Jia, Z. (2021) A Dual-Specificity Inhibitor Targets Polyphosphate Kinase 1 and 2 Enzymes To Attenuate Virulence of *Pseudomonas aeruginosa* *mBio* **12**, e0059221 10.1128/mBio.00592-21
30. Roberge, N., Neville, N., Douchant, K., Noordhof, C., Boev, N., Sjaarda, C. *et al.* (2021) Broad-Spectrum Inhibitor of Bacterial Polyphosphate Homeostasis Attenuates Virulence Factors and Helps Reveal Novel Physiology of *Klebsiella pneumoniae* and *Acinetobacter baumannii* *Front Microbiol* **12**, 764733 10.3389/fmicb.2021.764733
31. Majorek, K. A., Kuhn, M. L., Chruszcz, M., Anderson, W. F., and Minor, W. (2014) Double trouble-Buffer selection and His-tag presence may be responsible for nonreproducibility of biomedical experiments *Protein Sci* **23**, 1359-1368 10.1002/pro.2520
32. Zhao, D., and Huang, Z. (2016) Effect of His-Tag on Expression, Purification, and Structure of Zinc Finger Protein, ZNF191(243-368) *Bioinorg Chem Appl* **2016**, 8206854 10.1155/2016/8206854
33. Booth, W. T., Schlachter, C. R., Pote, S., Ussin, N., Mank, N. J., Klapper, V. *et al.* (2018) Impact of an N-terminal Polyhistidine Tag on Protein Thermal Stability *ACS Omega* **3**, 760-768 10.1021/acsomega.7b01598
34. Zeng, R., Ma, Y., Qiao, X., Zhang, J., Luo, Y., Li, S. *et al.* (2018) The effect of His-tag and point mutation on the activity of irisin on MC3T3-E1 cells *Biosci Trends* **12**, 580-586 10.5582/bst.2018.01207
35. Kutyshenko, V. P., Mikoulinskaia, G. V., Chernyshov, S. V., Yegorov, A. Y., Prokhorov, D. A., and Uversky, V. N. (2019) Effect of C-terminal His-tag and purification routine on the activity and structure of the metalloenzyme, l-alanyl-d-glutamate peptidase of the bacteriophage T5 *Int J Biol Macromol* **124**, 810-818 10.1016/j.ijbiomac.2018.11.219
36. Neville, N., Lehotsky, K., Yang, Z., Klupt, K. A., Denoncourt, A., Downey, M. *et al.* (2023) Ionic polyphosphorylation of histidine repeat proteins by inorganic polyphosphate *bioRxiv* 2023.2004.2010.536149 10.1101/2023.04.10.536149
37. Jin, J., Hjerrild, K. A., Silk, S. E., Brown, R. E., Labbe, G. M., Marshall, J. M. *et al.* (2017) Accelerating the clinical development of protein-based vaccines for malaria by

- efficient purification using a four amino acid C-terminal 'C-tag' *Int J Parasitol* **47**, 435-446 10.1016/j.ijpara.2016.12.001
38. Kuroda, A., and Kornberg, A. (1997) Polyphosphate kinase as a nucleoside diphosphate kinase in *Escherichia coli* and *Pseudomonas aeruginosa* *Proc Natl Acad Sci U S A* **94**, 439-442
 39. Young, G., Hundt, N., Cole, D., Fineberg, A., Andrecka, J., Tyler, A. *et al.* (2018) Quantitative mass imaging of single biological macromolecules *Science* **360**, 423-427 10.1126/science.aar5839
 40. Kornberg, A. inventors; KORNBERG ARTHUR assignee. Novel Antimicrobial Therapies A1 2001/06/28
 41. Shum, K. T., Lui, E. L., Wong, S. C., Yeung, P., Sam, L., Wang, Y. *et al.* (2011) Aptamer-mediated inhibition of *Mycobacterium tuberculosis* polyphosphate kinase 2 *Biochemistry* **50**, 3261-3271 10.1021/bi2001455
 42. Singh, M., Tiwari, P., Arora, G., Agarwal, S., Kidwai, S., and Singh, R. (2016) Establishing Virulence Associated Polyphosphate Kinase 2 as a drug target for *Mycobacterium tuberculosis* *Sci Rep* **6**, 26900 10.1038/srep26900
 43. Gautam, L. K., Sharma, P., and Capalash, N. (2019) Bacterial Polyphosphate Kinases Revisited: Role in Pathogenesis and Therapeutic Potential *Curr Drug Targets* **20**, 292-301 10.2174/1389450119666180801120231
 44. Burda-Grabowska, M., Macegoniuk, K., Flick, R., Nocek, B. P., Joachimiak, A., Yakunin, A. F. *et al.* (2019) Bisphosphonic acids and related compounds as inhibitors of nucleotide- and polyphosphate-processing enzymes: A PPK1 and PPK2 case study *Chem Biol Drug Des* **93**, 1197-1206 10.1111/cbdd.13439
 45. Bravo-Toncio, C., Alvarez, J. A., Campos, F., Ortiz-Severin, J., Varas, M., Cabrera, R. *et al.* (2016) *Dictyostelium discoideum* as a surrogate host-microbe model for antivirulence screening in *Pseudomonas aeruginosa* PAO1 *Int J Antimicrob Agents* **47**, 403-409 10.1016/j.ijantimicag.2016.02.005
 46. Peng, L., Zeng, L., Jin, H., Yang, L., Xiao, Y., Lan, Z. *et al.* (2020) Discovery and antibacterial study of potential PPK1 inhibitors against uropathogenic *E. coli* *J Enzyme Inhib Med Chem* **35**, 1224-1232 10.1080/14756366.2020.1766453
 47. Gray, M. J., Wholey, W. Y., Wagner, N. O., Cremers, C. M., Mueller-Schickert, A., Hock, N. T. *et al.* (2014) Polyphosphate is a primordial chaperone *Mol Cell* **53**, 689-699 10.1016/j.molcel.2014.01.012
 48. Kumble, K. D., Ahn, K., and Kornberg, A. (1996) Phosphohistidyl active sites in polyphosphate kinase of *Escherichia coli* *Proc Natl Acad Sci U S A* **93**, 14391-14395 10.1073/pnas.93.25.14391

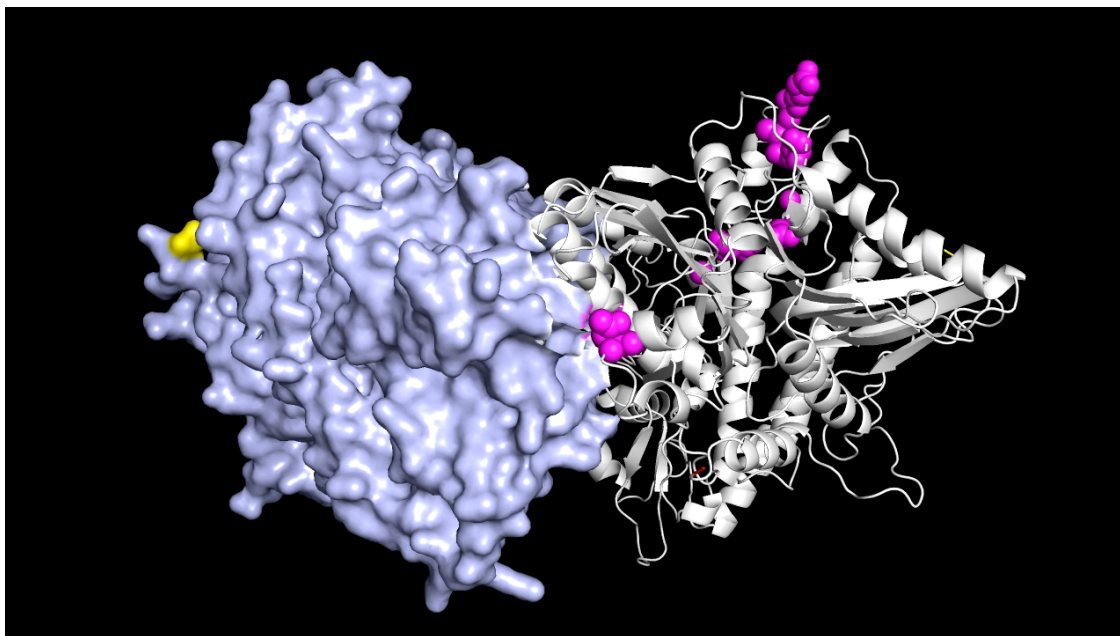
SUPPORTING INFORMATION

**Supplemental Figure 1 | Purification of Untagged PPK from Overexpression Culture.**

A) The initial overexpression and extraction protocol produced a small elution peak as indicated by the blue UV trace. B) Fractions from the elution peak were tested for polyP synthesis activity, showing activity was not particularly prevalent in any one fraction, although F6 had the most relative activity in one fraction. Fractions 3-15 were analyzed via SDS-PAGE to determine the pool used to purify untagged PPK resulted in multiple fractions containing polyP synthesizing activity. Fractions containing a band of PPK size with little other bands were selected, pooled, dialyzed, and used in subsequent experiments to characterize the untagged enzyme.



Supporting Video 1 | Mass Photometry of PPK-HT Enzyme. This is a live read of the mass photometry technique. Sample is diluted directly onto the read slide at a 1:1 dilution. Individual molecules impact the slide and are recorded. The light scattering (ring around the solid molecule) is measured and compared to the scattering of a known-size protein ladder, and the molecular mass of the molecule is calculated from the standard. As seen in the video, molecules of various sizes can be detected and catalogued, allowing for a highly accurate count of each species of size in the sample.



Supporting Video 2 | Location of PPK* Mutation Sites in Dimeric Structure. Visualization of each PPK* mutation site in the dimeric structure. Each mutation (in magenta) represents either a full charge shift or a loss of charge. Two mutations – E173K and N331D – are located at the monomer-monomer interface region of the dimer structure. Four more – D230N, E240G, E245K, and M247I – are located in a loop structure where the second dimer set would bind in the tetrameric formation. Only mutation E56K is internal of the structure, and it has some slight proximity to the active site. The N and C-termini of each monomer are indicated in yellow. Video generated from PDB ID 1XDP. One monomer is represented as a ribbon for clean visuals.

OBSERVATIONS ON PPK PURIFICATION, ACTIVITY, AND DETECTION

Profinity Purification Is Unsuitable for PPK Studies

PPK purification requires a great deal of consideration. The issues with the polyhistidine (poly-H) tag (see previous chapter) necessitated the development of a new purification method. However, the native purification and overexpression purification techniques both required extensive resources and large amounts of time. This led us to consider alternative purification methods. The first method we tried was the Profinity eXact purification system.

This system utilizes an N-terminal purification tag (residue sequence EEDKLFKAL) which is fused to the N-terminus of the target protein (98). This construct is then passed over a chromatography column with an immobilized, highly mutated subtilisin subunit that recognizes the tag and binds the construct. Cleavage occurs on the column in response to the addition of 100 mM of potassium fluoride, eluting the protein of interest with, at most, a two residue scar on the N-terminus (this can be reduced or entirely removed, but the efficiency drops) (98).

The main benefit to this system was the simple method of purification that allowed for a “tagless” enzyme. We amplified the *ppk* sequence from *E. coli* MG1655 genomic DNA using one of two forward primers (708 included a spacer sequence between the last tag codon and first *ppk* codon, 708 had no spacer) and the reverse primer listed in the table below. The forward primers were designed to include a protease

cleavage site for the LguI protease, while the reverse primer contains an XhoI site. Many cloning attempts using primer 708 failed to produce a successful insert. A single instance of successful insertion was obtained for primer 709, which was subsequently sequenced and found to contain the whole PPK insert in correct orientation. Verified plasmid pPPK27 was mutated using the quick-change mutagenesis method with primer 517 previously described to introduce the *ppk**^{G733A} mutation to produce an expression vector for PPK*E245K enzyme.

Table 1 PPK27 and PPK28 Vector Construction Primers. Primers 708, 709, and 739 were designed by MQB. Primer 517 was designed by MJG.

Primer ID	Name	Sequence (5'->3')
708	Ec_PPK LguI_Spacer_F	5'-CTGCTCTTCAAAGCTTTG ACTTCTATGGGTCAGGAAAA GCTATACATCG-3'
709	Ec_PPK LguI_F	5'-CTGCTCTTCAAAGCTTTGATGGGTC AGGAAAAGCTATACATCG-3'
739	Ec_PPK XhoI_pPAL7 R	5'-CGCTCGAGTTATTCAG GTTGTTTCGAGTGATTTG-3'
517	Ec_ppk_G733A	5'-GAAGCCAGCCTGATGA AGTTGATGTCTTCC-3'

The overexpression protocol recommended in the Profinity manual was unsuitable for PPK expression, which requires low temperature expression for hours to ensure proper folding. Overexpression from the newly constructed pPPK27 vector using our overexpression protocol was successful, as seen in Total Rows of Figure 1. However, after lysis and fractionation according to the Profinity protocol, PPK presence in either the soluble or insoluble fraction was minimal. Subsequent attempts from this overexpression were unsuccessful.

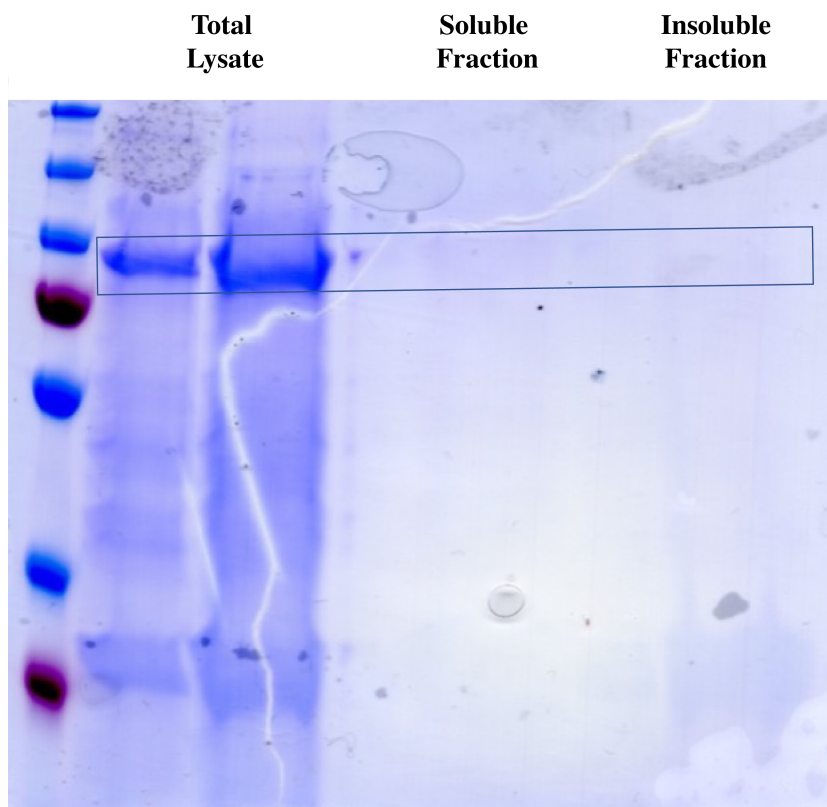


Figure 1 | Expression and Isolation of Profinity-tagged PPK. Overexpression of the enzyme from the plasmid was successful. Total lanes represent a 1:2 and 1:1 dilution of lysate in loading buffer. Both lanes contain a sizable band of PPK as indicated by the box. However, upon lysis and fractionation, the amount of PPK detectable in the two fractions was severely reduced.

A new attempt at purification from pPPK27 was done with a hybrid protocol between the PPK purification protocol used in the lab and the Profinity eXact manual. Some key differences include the buffer type used throughout the protocol: Profinity protocol calls for sodium phosphate buffers, while the lab method utilizes Tris-HCl buffers. One major modification was required to utilize the lab protocol, in that the inclusion of chloride ions was not possible as the protease cleavage is triggered by halide ions, among others. Changes to this process are detailed in Appendix A. This purification attempt produced measurable quantities of PPK enzyme at 0.143 mg ml^{-1} in about 1.8 mL total volume, for a total of 0.257 mg isolated. This was lower than the polyhistidine tag

yield which normally produced upwards of 5 mg of purified protein. Purification of the PPK*E245K enzyme produced 1 mL of 0.607 mg ml⁻¹, which, while a better yield, is still less than the polyhistidine tag system. An SDS-PAGE analysis of the products revealed a potential degradation or cleavage event occurred in the Profinity-tagged PPK enzymes (Figure 3). For both the PPK-HT and E245K-HT enzymes, there was a single, uniform band with a size around 73-75 kDa, which is consistent with previous reports (15, 78, 80, 81). However, for both the detagged PPK and PPK*E245K enzymes (labeled as PPK-DT and E245K-DT in Figure 3A) there were multiple bands. What appeared to be a cleavage or degradation event resulted in the reduction of the PPK-sized band in both samples.

For the PPK-DT sample there was virtually no detectable PPK-sized band. Instead, we found the predominate band to be less than 70 kDa. Likewise, the E245K-DT sample also had a sharp reduction in the PPK-sized band. However, there was a faint band in the appropriate range, situated just above the major band in the lane which appears to be slightly more than 70 kDa in size. The PPK sequence does not contain a Profinity recognition sequence, and the full length of the gene was confirmed to be present in the pPPK27 and pPPK28 plasmids. Therefore, we conclude that a cleavage event occurred that decreased the size of the purified enzymes. Given the lack of smearing in the lane and the consistent appearance of certain bands, this cleavage seems likely to be specific to a certain region of the enzyme.

The cleavage or degradation of the enzyme coincided with a drop or loss of polyP synthesis activity (Figure 3B). There was no detectable polyP synthesized by the PPK-DT enzyme under reaction conditions. PolyP synthesis of the E245K-DT enzyme was

significantly reduced, to roughly half the activity of the E245K-HT enzyme. The predominant band in the E245K-DT lane is slightly smaller than PPK size. Importantly both the PPK-sized band and the smaller sized band is severely reduced or even absent in the PPK-DT lane.

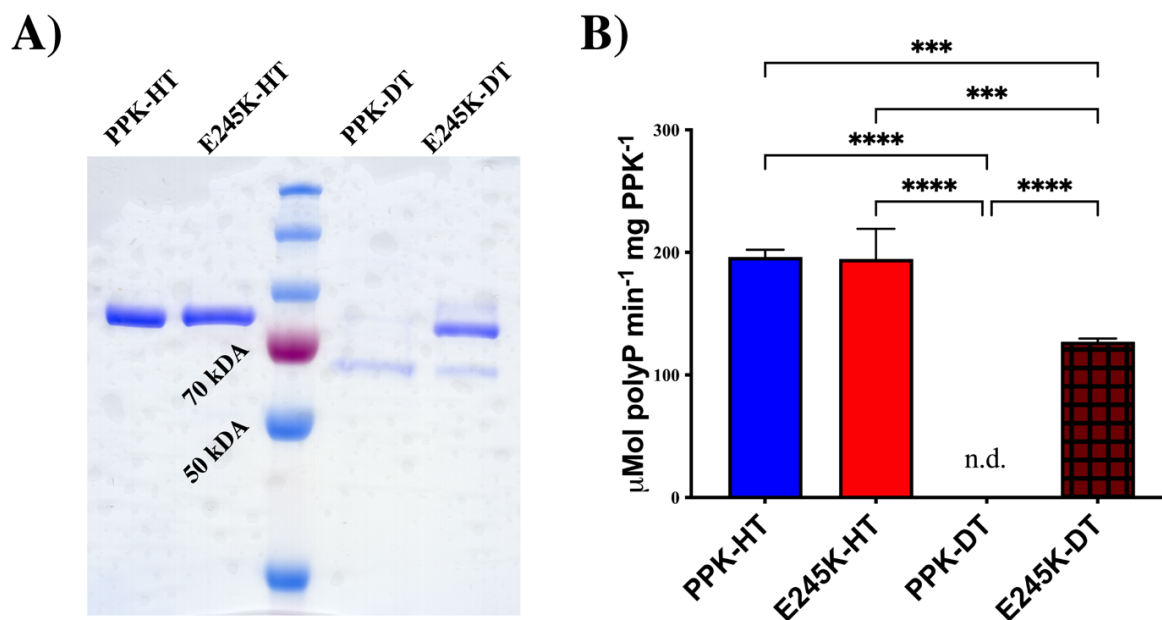


Figure 2 | PPK Purification Using the Profinity System Results in Protein Degradation and Loss In Activity. A) Samples of purified PPK enzyme from each culture were run on an SDS-PAGE gel under denaturing conditions to determine the size of each product. B) Specific activities of purified PPK enzymes were tested under normal reaction conditions with equimolar concentrations of enzyme in each reaction. Statistical analysis was conducted using an ordinary ANOVA with Tukey's multiple comparisons test. *** p < 0.001 **** p < 0.0001.

This leads us to conclude that the Profinity system produces an enzyme that is unstable and degraded in a way specific to the system. Because the E245K-DT sample has this intermediate band that may conserve some polyP synthesis activity, it is possible that the E245K mutation confers some resistance to the degradation.

A possible explanation as to why the Profinity system produces this truncated enzyme could be that the addition of the tag when being expressed triggers a conformational change which exposes a specific protease target site in the molecule. That site could be targeted and cleaved to release the roughly 10 kDa missing from the band present in both Profinity purification samples from the enzyme *in vivo*. The subsequent purification method would cleave off the tag leaving the shortened enzyme to elute from the column. Any cleavage would have to be from the C-terminus to maintain the ability to purify the enzyme with the Profinity column. The addition of the E245K mutation might alter the conformation enough to impair the cleavage event. While further testing might be useful to clarify these results, the important observation is that an N-terminal purification method, even one which would result in a “tagless” enzyme, seems to affect the enzyme’s stability and activity. Therefore, the C-terminus of the enzyme is the only terminus we should consider suitable for purification tags. It is interesting to note that this is not the first time an N-terminal modification has been shown to impair PPK activity, as the crystallography study first showed an N-terminal polyhistidine tag significantly reduced polyP production (81).

Alternatively, a recent study has shown that fluoride, which is the main triggering anion for cleavage from the Profinity column, reduces polyP accumulation in *Rothia dentocariosa* by up to 90.7% compared to untreated cultures (99). They hypothesize that this is due in part to fluoride inhibiting glycolysis and indirectly inhibiting polyP formation, but it is possible that fluoride is directly interfering with PPK activity or even triggering degradation. Measuring the activity of PPK in the presence of fluoride is a

promising experiment, as it may offer insight into PPK stability or even a novel PPK inhibitor.

Increased PolyP Levels In Vivo Are Due to the ppk Mutations*

The major unanswered question from the PPK* study was how the *ppk** mutations increased the amount of polyP *in vitro* (8). Two basic questions to be addressed were the copy number of the plasmids and the physiological significance. The sequence of *ppk* and the various *ppk** mutations was verified in the work. However, the full sequence of the plasmids, including the vector backbone, were not sequenced. One explanation for the increase in polyP could be that the PPK* vectors had a mutation that resulted in an increase in plasmid copy numbers. The vectors used to test *in vivo* polyP accumulation were built in the low-copy number pWSK129 backbone (100). A mutation in the backbone could affect plasmid copy number. More copies of the gene could lead to more copies of the enzyme and more polyP accumulation.

Full plasmid sequencing confirmed no major mutations in the vector backbone of our plasmids. Because the strains used to test the polyP accumulation *in vivo* were built in a *Δppk* background, the chromosomal copy of *ppx* remained intact. Using RT-PCR, we could easily compare the ratio of chromosome to plasmid. To do this, we extracted total DNA from cultures of bacteria carrying either pPPK10 (wild-type PPK low copy number plasmid) or pPPK10b (PPK*E245K low copy number plasmid). We probed these samples with primers targeting *ppk*, which should only be on the plasmid, and *ppx*, which should only be on the chromosome. We set up reactions ranging from 20 ng of genomic DNA to 2.5 ng of genomic DNA to have a clear range of concentrations to measure.

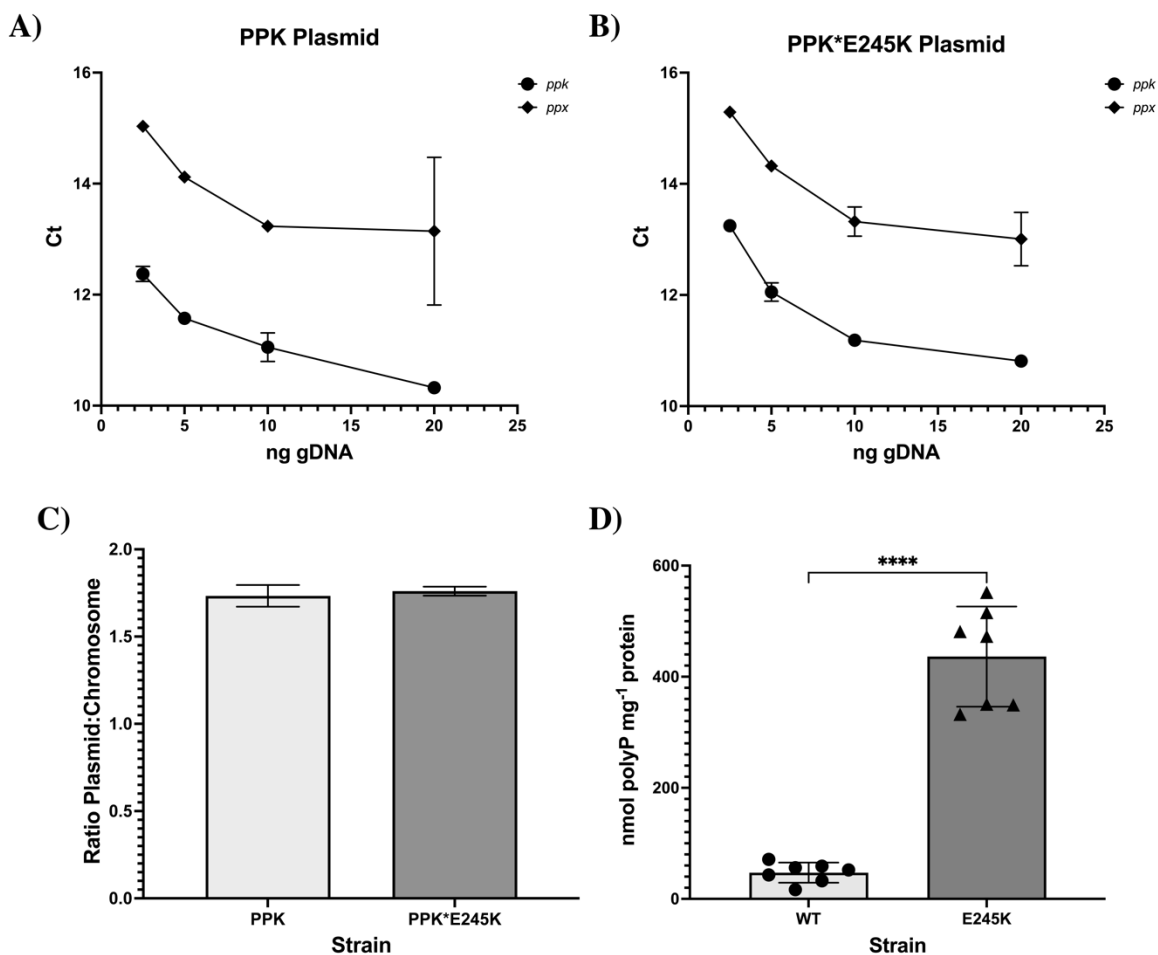


Figure 3 | Quantification of Low Copy Number PPK Plasmids *In Vivo*. Total DNA extractions from *Appk* + A) pPPK10 or B) pPPK10b cultures were prepared using genomic DNA extraction kits. RT-PCR reactions were prepared using 20, 10, 5, or 2.5 ng of total DNA. The cycle thresholds were measured for *ppk* and *ppx*. C) The average ratio was found to be roughly 2 copies of plasmid per 1 copy of genome. D) The chromosomal PPK*E245K mutant accumulates significantly more polyP following stress than the PPK WT strain. Statistical analysis conducted using an unpaired two-tailed t test. **** p < 0.0001

The results are shown in Figure 4, with the ratio of plasmid (*ppk* line) to chromosome (*ppx* line) graphed in terms of detection cycle threshold. As seen in Figure 3A and 3B, both the wild-type PPK plasmid and the PPK*E245K plasmid were present at higher levels than the chromosomal gene. This is to be expected, as the reported copy number for this vector backbone is between 2 and 5 (100). Taking the average of ratios

across the varying concentrations of genomic DNA present, we find that the ratios of plasmid to genomic DNA were 1.73 and 1.76 for wild-type PPK and PPK*E245K, respectively (Figure 4C). This leads us to conclude that both plasmids are present in their respective cell lines at a copy number of 2 per cell and that copy number alone did not explain the difference in polyP accumulation between the two strains.

To further confirm that the *ppk** mutations are responsible for the observed increase in polyP accumulation, we tested the effect of the mutation when introduced to the chromosomal *ppk* gene. To do this, the *ppk**^{G733A} sequence was introduced into the chromosome using the no-SCAR CRISPR-Cas9 gene editing system (101). Briefly, MG1655 *E. coli* was transformed with the pCas9-CR4 plasmid encoding the Cas9 nuclease and chloramphenicol resistance to generate the editing strain. The *ppk**^{G733A} mutation encoding PPK*E245K was cloned into the guide RNA plasmid pKDsgRNA-p15 using the round-the-horn method of molecular cloning (102) with protospacer primer 5'-PO4-gtgctcagtatctctatcactga 3'(101) and *ppk* primer sequence 5'-TGAGATGGAAGCCAGCCTGAGTTTTAGAGCTAGAAATAGCAAG-3'. The resultant pKDsgRNA-E245K plasmid encoding streptomycin resistance was transformed into the editing strain. Colonies that were streptomycin and chloramphenicol double resistant were selected and sequenced to confirm mutation in the *ppk* gene. The plasmids were cured from the strains as described in the protocol (101) to produce a clean *ppk**^{G733A}. Strain construction was conducted by Amanda Rudat. Subsequent full genomic sequencing confirmed no off-target effects of the editing process.

Using the *ppk** strain, we measured the amount of polyP accumulation before and after stress. Unlike with the plasmid strains, there was no detectable polyP prior to stress (data not shown). Following stress, we found that, while the level of polyP accumulation *in vivo* was lower than that of the plasmid-bearing strains, it was still significantly higher than the *ppk* wild-type strain (Figure 3D). This leads us to conclude that the PPK* mutants have a perturbed polyP accumulation phenotype that is directly and intrinsically linked to the *ppk** mutation rather than any plasmid effects.

Development Of Anti-PPK Antibodies

The regulation of PPK activity is an outstanding question that requires novel tools to address. While transcriptional levels of *ppk* do not change in response to stress, there is no data regarding the levels of enzyme (103). Previous work detecting PPK enzyme from *in vivo* samples utilized an anti-PPK serum technique (78). The development of a modern, high-specificity method is necessary for the *in vivo* detection and measurement of PPK.

One benefit of the C-tag system described in the previous chapters is that it allows for the detection of target protein on a blot using a commercially available anti-C-tag antibody (104). However, this system has several potential issues. Firstly, the EPEA epitope recognized by the anti-C-tag antibody could be found in multiple peptide sequences generated during the lysis and denaturing process. Secondly, it is not specific to PPK, which is required for many downstream techniques such as pulldowns to identify potential PPK-interacting partners. Finally, the expense of the anti-C-tag antibody represents a hurdle for many research groups interested in studying PPK.

We contracted Genscript to produce a monoclonal anti-PPK antibody and hybridoma cell line using the purified PPK-CT enzyme as the antigen. During the process of developing this product, we tested a wide variety of sera samples. While Genscript ultimately provided hybridomas of all selected clones rather than the two initially expected, two clones (8C9 and 7A5) were selected. The detection of the antibody is distinct and specific, as shown in sera blot of Figure 4. Lane 2 contains PPK KO lysate. Lanes 3-6 are two samples of purified PPK enzyme – PPK-HT in lane 3, E245K-HT in lane 4, PPK-CT in lane 5, and untagged PPK in lane 6. Lane 7 contained 6 μ g total protein from a PPK WT strain, but the sera was unable to detect PPK at that concentration.

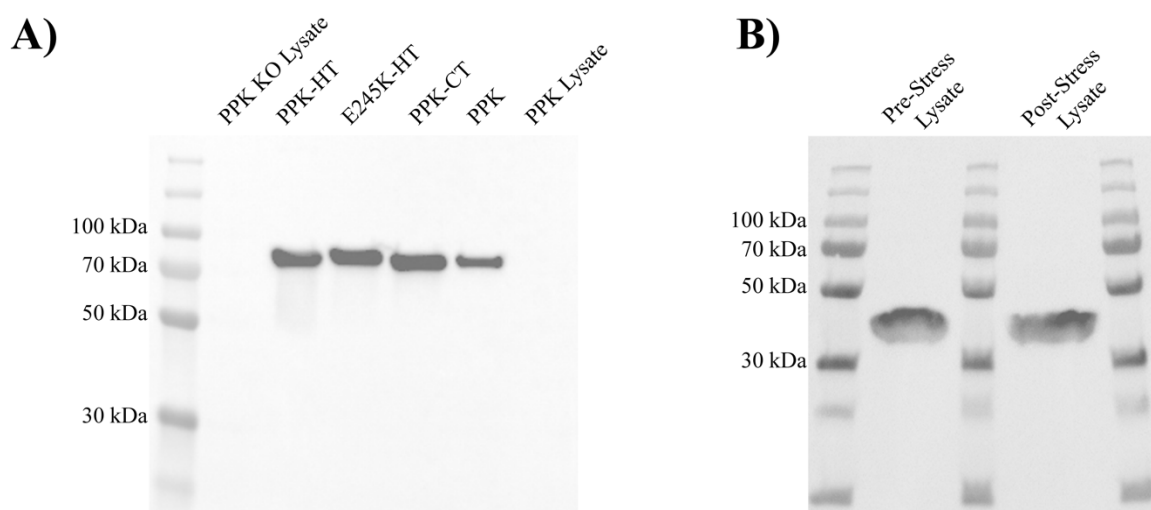


Figure 4 | Development of PPK Western Blotting Techniques. A) Antibody clone 7A5 probing against indicated samples. B) Protein levels of RecA before and after nutrient limitation stress. RecA levels do not change in response to stress, making it a suitable target to normalize PPK expression to. Panel B was previously published as supplemental for Bowlin et al 2022 (54).

If the antibody cannot detect chromosomal levels of PPK, we will have to use plasmids. Thus, we require a stable marker to compare *in vivo* PPK levels. We selected RecA. While RecA expression is increased in response to low temperatures or DNA

damage, it does not appear to have differential expression in response to nutrient starvation (105, 106). To confirm this, we measured RecA levels before and after nutrient starvation stress (Figure 5B). We found that the levels of RecA did not significantly change in response to stress, making the use of RecA levels as a normalization target suitable for measuring PPK levels in nutrient starvation responses. These results leave us poised to answer questions regarding PPK expression and stability in response to stress.

DISCUSSION AND CONCLUSIONS

In bacteria, survival is contingent on enduring and adapting to environmental stresses as they are encountered. Many aspects of bacterial stress survival have been studied, yet one of the most primordial and fundamental responses is poorly understood: the use of polyP. The focus of this work is on understanding how the production of polyP is regulated, as this elementary aspect of the system is almost entirely unknown. In many bacterial species, the production of polyP is carried out by a PPK enzyme. Some bacteria, like *E. coli*, only have a single copy of *ppk* encoding the PPK1 enzyme. Other bacteria, like *F. tularensis*, carry multiple versions of the *ppk1* and *ppk2* genes (59, 69, 107). Still, other bacteria like *B. subtilis*, have neither *ppk1* nor *ppk2*, yet still possess specialized systems to utilize polyP (94). The function of the *ppk1* family of enzymes has been tied to a multitude of pathogenic aspects – including expression of virulence factors and antibiotic resistance (31, 107, 108). Therefore, understanding the regulation of this family of enzymes is essential in developing strong, reliable, persistent approaches to dealing with bacterial infections.

There are serious questions unresolved about PPK regulation. After stress, what leads to PPK activation? Does PPK autoregulate based on ATP consumption and polyP production, or are there other agents controlling its activity? When enough polyP has been produced, how is PPK inactivated? The bulk of this work has been dedicated to developing methods to answer these questions.

For example, based on the PPK* data from 2018, we know that PPK activity must be tightly regulated, as under non-stress conditions there is no detectable polyP accumulation. When expressing a PPK* enzyme, however, there is considerable detectable polyP in the pre-stress cultures. Additionally, expression of a highly active PPK* mutant results in toxic levels of polyP accumulation, requiring the addition of magnesium to keep the cells alive and growing (8). This indicates that the cell needs to keep polyP production under lock and key. We also know that the transcript of *ppk* does not change in response to stress (54, 103).

The pathway that is triggered by stress and induces PPK activity is not well understood. Previous work identified *DksA* as an upstream regulator of polyP synthesis (53, 103). In this work building off that, the role of several signaling elements have been investigated. The bEBPs *GlnG* and *GlrR* were both identified as regulators of polyP production. *GlnG*, a DNA-binding transcription regulation factor that regulates, among other things, the synthesis of glutamine synthetase *GlnA*, positively regulates polyP synthesis in response to stress. Further exploration into this observation revealed a complex story where the presence of nitrogen compounds in the pre-stress media affected the subsequent polyP production of the stress response. Interestingly, this implication of the cellular nitrogen conditions showed that by supplementing rich media with glutamine, the decrease in polyP production associated with both *ΔrpoN* and *ΔglnG* mutants could be eliminated. For the *ΔrpoN* mutant, varying levels of glutamine, glutamic acid, and ammonium all eliminated the polyP production defect associated with the mutation. Interestingly, the *ΔdksA* mutant was not rescued with the addition of nitrogen metabolites in the pre-stress media, indicating a different mechanism involved in the polyP regulation

through DksA. The differences between these mechanisms is a promising area for future studies.

GlrR, which is only known to regulate the expression of RpoE and the sRNA *glmY* (109, 110), impairs the expression of polyP in response to stress. Since GlrR is indicated as a negative polyP regulator, its activity positively regulating the expression of a positive regulator (RpoE) was unlikely to be the cause of the observed polyP synthesis defect. So, we focused on the other GlrR-regulated sequence, *glmY*. We found that the elements of the system which *glmY* belongs to – RapZ, *glmZ*, and GlmS, which ultimately regulate the production of the peptidoglycan-precursor glucosamine-6phosphate – had a modest, and at best, indirect effect on polyP production. This means that the regulatory effect of GlrR is more complicated and represents an additional avenue of exploration on polyP synthesis.

We identified PtsN, a major component of the nitrogen phosphotransferase system, as a positive regulator of polyP synthesis as well, and showed that its effect was independent of glutamine levels in the pre-stress media. We also found that PtsN acts downstream of RpoN, but upstream of DksA, giving us a better understanding of one possible polyP regulatory pathway. The relationship between PtsN's activity in the nitrogen phosphotransferase system and its role in regulating polyP synthesis is an open question, especially given the observations we've made on other nitrogen-regulating agents like GlnG and GlnR.

The model in the Figure 6, “Current Model For PolyP Regulation In *E. coli*” from the third chapter of this work shows our new understanding of polyP regulation

incorporating elements of what we've discovered about the nitrogen response. We have identified a new collection of genes and metabolites with limited or no roles in polyP synthesis regulation, including nitrogen metabolites and elements of the nitrogen phosphotransferase system. Ultimately, understanding the pathway that regulates polyP synthesis requires more nuanced approaches. Our work so far has identified key players – RpoN, PtsN, DksA – which form the backbone of at least one regulatory cascade to be fleshed out. The roles for other factors like RpoE and GlnG remain to be characterized. Whether they form part of the same regulatory cascade or are separate elements is an important question that we are poised to investigate further down the road.

One of the most crippling aspects of PPK research is the apparently incongruity between *in vivo* and *in vitro* data. For example, in the report identifying mesalamine as a PPK inhibitor, the *in vivo* effects of mesalamine treatment were significantly different from the *in vitro* effects of the drug on the enzyme. When patient-derived bacterial cultures were grown with 250 µg of mesalamine, there was a fifty-percent reduction in polyP accumulation. However, when testing the enzyme's activity when treated with mesalamine, the use of 1 mM of mesalamine was required to produce a significant reduction in polyP (75). In the PPK* study, we found that the polyP accumulation *in vivo* of PPK* mutants was significantly higher than that of wild-type cells. However, *in vitro* activity of PPK* enzymes were not significantly different (8). In trying to understand the stark difference between *in vivo* and *in vitro* PPK data, we discovered that the widely used purification method of a C-terminal polyhistidine tag seemed to significantly alter many attributes of the enzyme, including kinetic parameters and oligomeric distributions. Testing enzymes with a different tag produced results that were more informative and

more in line with *in vivo* observations. We found that PPK sensitivity to mesalamine was significantly different compared to the previous published polyhistidine-tagged data, with mesalamine completely altering the kinetic curve at 1 mM concentrations so that the substrate inhibition model no longer fits the reaction. We also found altered sensitivity to the endogenous inhibitor ADP, which was not found in the polyhistidine tagged enzyme. The results of these experiments allowed us to test the difference of the PPK* mutants in a condition where the tag was not affecting enzyme activity. We found that the PPK* enzymes still did not display drastically different polyP production levels. However, between differences in kinetic parameters and oligomeric distribution, each of the PPK* enzymes appeared to have a different mechanism that could be altering *in vivo* polyP production. This leads us to a point where we are poised to answer several questions on PPK regulation from the molecular level rather than the genetic level.

A promising avenue of study is the expression and stability of PPK. PolyP synthesis begins to occur within 5 minutes of stress, so the activity of the enzyme suggests the expression is not a regulatory element of the activity. However, whether more PPK enzyme is produced in the course of the response is unknown. Likewise the stability of the enzyme over the course of the reaction is another interesting question. It is possible that PPK is proteolytically regulated. There are several reasons why the cell might opt to produce this enzyme during permissive periods and destroy it during stress. Production of polyP consumes ATP, which is essential for cell growth, among other things. The consumption of ATP at the beginning of the stress response could assist the cell in arresting cell cycle progression. The polyP molecule also serves as an effective chaperone to prevent aggregate protein from crashing out of solution and killing the cell.

Certain genes are regulated by polyP activity as well. All of this paints a picture of a helpful product at the beginning of the response.

However, later on, after the cell has entered a stage where all energy is being devoted to withstanding the hostile environment, the rapid consumption of ATP could become an undesirable burden. Add to that the chelating effects of polyP on several metal ions like magnesium – essential cofactors in many enzymatic reactions – and suddenly the production of polyP becomes a burden rather than a tool of survival. So, it is possible that bacteria have adopted a double-edge sword that must be carefully wielded and sheathed once it has served its purpose. The most effective and irreversible way to do that is to degrade the enzyme once it has served its purpose, as it prevents the risk of polyP production beyond its useful timeframe.

In these possibilities, PPK could be synthesized in response to stress and degraded as the stress response progresses. As these are both simple measurements of enzyme level, they represent easily tested regulatory mechanisms. However, both of these options require the ability to visualize and measure the enzyme. In this work, we describe the development of a monoclonal PPK antibody that should facilitate the measurement of PPK from *in vivo* samples before and after stress. The development of this antibody and subsequent technique will be essential for questioning the expression levels of PPK enzyme in the cell. With this antibody prepared and hybridoma lines for multiple clones in storage, the characterization of this aspect of the enzyme is only a matter of time. It is the opinion of the author that this particular avenue of pursuit should be the first thing investigated for a variety of reasons.

Primarily, RpoN is another stress response-induced protein that is degraded when no longer needed, and which also plays a role in the regulation of elements identified as being upstream of PPK activation (53, 54, 111). Secondly, considering the PPK* mutants, each mutation is located within 4 residues of a predicted protease target site, including two that are target residues themselves as shown in Figure 1 below. Additionally, three of the PPK* mutations occur in an accessible loop region rich in predicted protease sites. If these enzymes were resistant to degradation, that would explain why we see no changes in polyP production *in vitro* where the responsible protease is absent, but significant increases *in vivo* where undegraded enzymes would be free to continue synthesizing polyP beyond the normal regulatory threshold.



Figure 1 | Localization of *ppk Mutations and Predicted Protease Target Sites.** A) Location of each *ppk** mutation in PPK. B) Location of each PPK* mutation in the first 404 residues of PPK. Each triangle represents a predicted cleavage spot: yellow for metalloproteases, blue for serine proteases, and green cysteine proteases. The red triangle is multiple families. In both panels, the red box represents a loop region in the crystal structure that is enriched for both mutation sites and predicted protease target sites. Mutation E245K is indicated in red in panel B. Panel A is adapted from Rudat et al 2018 (8). The protease prediction analysis was conducted using PROSPER/iProt-Sub (112).

There are several questions regarding PPK inhibitor sensitivity that should be addressed in the near future. As listed in the table “Structures and Activities of PPK1 Inhibitors”, there are a wide variety of known PPK1 inhibitors. However, each of these

inhibitors has been characterized against a polyhistidine-tagged PPK enzyme, which we have shown to be significantly different from the enzyme developed to behave like untagged enzyme (see: figure “5-ASA Inhibition Sensitivity of PPK-CT and PPK*-CT enzymes” and (75)). It is important that a more accurate understanding of PPK inhibitor sensitivity be developed, as several PPK inhibitors are potential therapeutics.

Another question of interest regards the PPK* mutant enzymes. Our work in chapter four of this body indicated that the oligomeric distribution of each of the PPK* enzymes was different in some way. This raises several questions. First, are the specific mutations responsible for these differences? Is the E245K mutation required to see the drastic drop in tetramer we observe, or would an E245A mutation do the same? Most of the PPK* mutations are full charge shifts, so it is possible that the changes we observe *in vivo* could be the result of increased stability in the dimer form, which is thought to be the polyP synthesizing form (80, 81). Would charge-neutral changes induce the same effects on oligomeric distribution and activity? The oligomerization is a major focus of PPK activity. We know that the tetrameric form allows the enzyme to autophosphorylate (15). The current model predicts that the enzyme produces polyP as a dimer (80, 81). If the current model is correct, and the dimeric form is the form that synthesizes polyP, then the tetramer could represent an arrested state where the enzyme is ready to produce polyP but not actively doing so. In that situation, the PPK* mutations that appear to destabilize the tetramer *in vitro* could be increasing polyP accumulation *in vivo* by increasing the amount of dimer active in response to stress. Understanding if the PPK* amino acid changes are disrupting oligomerization through charge interference would clarify this.

The oligomeric distribution of PPK represents the most promising bioanalytical pathway. We have identified multiple mutations that alter oligomeric distribution and have an *in vivo* effect on bacterial polyP production. The stability of each oligomer is an important question that needs to be answered, as it is possible that the oligomeric form determines sensitivity to proteases active in the stress response. It is a feasible model that, in the early stress response, the tetrameric form dissociates into a dimeric form, which begins to produce polyP. As the stress response progresses a protease or proteases becomes active that targets PPK but can only recognize dimeric enzyme. This protease inactivates the polyP-producing enzyme, reducing the production. Meanwhile, the tetrameric form of the enzyme remains as a pool ready to continue polyP synthesis if needed. Combining the oligomeric analysis through mass photometry and the molecular stability using monoclonal PPK antibodies, we can potentially identify the first solid regulatory mechanism of PPK and begin to understand the downstream results of the polyP stress response.

In summary the work presented here represents the culmination of multiple attempts to understand how an evolutionarily ancient molecule is regulated and used in *E. coli*. Through genetic, biophysical, and biochemical techniques, we have identified several previously unknown regulatory traits that have begun to build a clearer understanding of polyP biosynthesis regulation. When techniques have been insufficient or prone to error, adaptations, improvements, and innovations have been developed. Through the advances made throughout this work, we are poised to uncover how polyP synthesis is initiated, regulated, and arrested in response to stress in the environment.

While many questions remain about how polyP biosynthesis is regulated, this work lays the foundation for the answers to come.

GENERAL METHODS

Polyp Detection, PPK Activity Measurement, and Growth Curves

Methods for these techniques are described in previous publications and preceding chapters (54, 113, 114).

Plasmid Copy Quantification

Δppk strains carrying either pPPK10 encoding a single copy of the wild-type *ppk* gene or pPPK10b encoding a single copy of the *ppk*^{G733A} were cultured overnight at 37 °C. Total DNA was extracted from each culture using the PureLink Genomic DNA kit (Thermo cat # K182001) and quantified via nanodrop measurement. Individual RT-PCR reactions were prepared using the SsoAdvanced Universal SYBR Green Supermix (Bio-Rad cat #1725271) with primers 5'- ACTCTCATTCCCGCCATTTAC-3' and 5'- CGTAATGTGCTGACGCAGATA-3' for *ppk* or 5'- CAGCTTTGCCAGCTTTATTT-3' and 5'- CGCCCATTTCCATTAACACTTC-3' for *ppx*. Reactions were run with either 20, 10, 5, or 2.5 ng of total DNA. Run conditions were with the initial melting step was at 98 °C for 2.5 m, then dropped to 95 °C for 30 s. Amplification was done in three steps – 95 for 5s to melt, 60 °C for 30 s to anneal and extend, repeated 39 more times (40 total cycles). A melt curve was included at the end, 65 °C to 95 °C in 5 s increments. The detection threshold was measured for each reaction and the ratio of *ppk* to *ppx* was determined using the 2^{-ΔΔCt} method (115)

Sample Preparation and Western Blotting

Purified PPK-CT, E245K-HT, and PPK-HT enzyme were diluted 1:4 with SDS-PAGE loading dye and heated at 95 °C for 10 minutes. Log phase lysate samples were prepared by culturing appropriate *E. coli* strains in 6 mL LB until they reached an OD₆₀₀ of 0.3-0.5, pelleting the entire culture, and lysing the pellet by resuspension in RIPA lysis buffer (150 mM sodium chloride, 1.0% NP-40 or Triton X-100, 0.5% sodium deoxycholate, 0.1% sodium dodecyl sulfate, 50 mM Tris, pH 8.0) and heating at 95 °C for 10 minutes.

Samples were loaded in onto a 15 well Any kD stain-free gel (Bio-Rad #4568123) at 10 µg total protein (for purified protein) and 6 µg total protein for lysates. The gel ran at 120 V until the dye front reached the bottom of the gel. Gels were blotted in the previous described manner (54). When probing with anti-PPK hybridoma supernatant, 2 mL of supernatant was applied to the blot after blocking and blots incubated room temperature for 1 hour before being washed 3x with TBS + 0.2% Tween-20 and probed with secondary antibody (Goat Anti-Mouse IgG (H+L) HRP conjugate, Abcam # ab205719) For RecA, each blot with probed 1:10,000 of primary (Rabbit anti-*E. coli* RecA polyclonal, Abcam #ab63797) at room temperature for 1 hour, washed 3X in TBS +0.2% Tween-20, and incubated 1 hour at room temperature in 1:20,000 secondary (goat anti-rabbit IgG (H+L) HRP conjugate, Abcam. #ab6721). Blots were imaged as described previously (54).

Statistical Analysis, Graphing, and Graphics

Statistical analysis was carried out using Prism GraphPad software version Version 10.0.2 (171). Figure legends specify statistical tests used for analysis. All graphs were developed in GraphPad as well.

When indicated, figure graphics were generated using Biorender and used with permission.

Acknowledgements

The development and construction of the chromosomal *ppk** strain was undertaken by Michael Gray and Amanda Rudat.

GENERAL REFERENCES

1. Kornberg, A., Kornberg, S. R., and Simms, E. S. (1956) Metaphosphate synthesis by an enzyme from *Escherichia coli* *Biochim Biophys Acta* **20**, 215-227
10.1016/0006-3002(56)90280-3
2. Kornberg, S. R. (1957) Adenosine triphosphate synthesis from polyphosphate by an enzyme from *Escherichia coli* *Biochim Biophys Acta* **26**, 294-300
10.1016/0006-3002(57)90008-2
3. Ghosh, S., Shukla, D., Suman, K., Lakshmi, B. J., Manorama, R., Kumar, S. *et al.* (2013) Inositol hexakisphosphate kinase 1 maintains hemostasis in mice by regulating platelet polyphosphate levels *Blood* **122**, 1478-1486 10.1182/blood-2013-01-481549
4. Hou, Q., Liu, F., Chakraborty, A., Jia, Y., Prasad, A., Yu, H. *et al.* (2018) Inhibition of IP6K1 suppresses neutrophil-mediated pulmonary damage in bacterial pneumonia *Sci Transl Med* **10**, 10.1126/scitranslmed.aal4045
5. Maffucci, T., and Falasca, M. (2020) Signalling Properties of Inositol Polyphosphates *Molecules* **25**, 10.3390/molecules25225281
6. Michell, R. H. (2008) Inositol derivatives: evolution and functions *Nat Rev Mol Cell Biol* **9**, 151-161 10.1038/nrm2334
7. Beaufay, F., Quarles, E., Franz, A., Katamanin, O., Wholey, W. Y., and Jakob, U. (2020) Polyphosphate Functions In Vivo as an Iron Chelator and Fenton Reaction Inhibitor *mBio* **11**, 10.1128/mBio.01017-20
8. Rudat, A. K., Pokhrel, A., Green, T. J., and Gray, M. J. (2018) Mutations in *Escherichia coli* polyphosphate kinase that lead to dramatically increased in vivo polyphosphate levels *J Bacteriol* 10.1128/JB.00697-17

9. Gray, M. J., Wholey, W. Y., Wagner, N. O., Cremers, C. M., Mueller-Schickert, A., Hock, N. T. *et al.* (2014) Polyphosphate is a primordial chaperone *Mol Cell* **53**, 689-699 10.1016/j.molcel.2014.01.012
10. Bolesch, D. G., and Keasling, J. D. (2000) Polyphosphate binding and chain length recognition of *Escherichia coli* exopolyphosphatase *J Biol Chem* **275**, 33814-33819 10.1074/jbc.M002039200
11. Christ, J. J., Willbold, S., and Blank, L. M. (2019) Polyphosphate Chain Length Determination in the Range of Two to Several Hundred P-Subunits with a New Enzyme Assay and ³¹P NMR *Anal Chem* **91**, 7654-7661 10.1021/acs.analchem.9b00567
12. Rao, N. N., Roberts, M. F., and Torriani, A. (1985) Amount and chain length of polyphosphates in *Escherichia coli* depend on cell growth conditions *J Bacteriol* **162**, 242-247 10.1128/jb.162.1.242-247.1985
13. Yoo, N. G., Dogra, S., Meinen, B. A., Tse, E., Haefliger, J., Southworth, D. R. *et al.* (2018) Polyphosphate Stabilizes Protein Unfolding Intermediates as Soluble Amyloid-like Oligomers *J Mol Biol* **430**, 4195-4208 10.1016/j.jmb.2018.08.016
14. Ogawa, N., DeRisi, J., and Brown, P. O. (2000) New components of a system for phosphate accumulation and polyphosphate metabolism in *Saccharomyces cerevisiae* revealed by genomic expression analysis *Mol Biol Cell* **11**, 4309-4321 10.1091/mbc.11.12.4309
15. Kumble, K. D., Ahn, K., and Kornberg, A. (1996) Phosphohistidyl active sites in polyphosphate kinase of *Escherichia coli* *Proc Natl Acad Sci U S A* **93**, 14391-14395 10.1073/pnas.93.25.14391
16. Kornberg, A., Rao, N. N., and Ault-Riche, D. (1999) Inorganic polyphosphate: a molecule of many functions *Annu Rev Biochem* **68**, 89-125 10.1146/annurev.biochem.68.1.89
17. Muller, W. E. G., Schroder, H. C., and Wang, X. (2019) Inorganic Polyphosphates As Storage for and Generator of Metabolic Energy in the Extracellular Matrix *Chem Rev* **119**, 12337-12374 10.1021/acs.chemrev.9b00460
18. Schulz-Vogt, H. N., Pollehne, F., Jurgens, K., Arz, H. W., Beier, S., Bahlo, R. *et al.* (2019) Effect of large magnetotactic bacteria with polyphosphate inclusions on

the phosphate profile of the suboxic zone in the Black Sea ISME J **13**, 1198-1208
10.1038/s41396-018-0315-6

19. Gunther, S., Trutnau, M., Kleinstaub, S., Hause, G., Bley, T., Roske, I. *et al.* (2009) Dynamics of polyphosphate-accumulating bacteria in wastewater treatment plant microbial communities detected via DAPI (4',6'-diamidino-2-phenylindole) and tetracycline labeling Appl Environ Microbiol **75**, 2111-2121
10.1128/AEM.01540-08
20. Zheng, Y., Wan, Y., Zhang, Y., Huang, J., Yang, Y., Tsang, D. C. W. *et al.* (2022) Recovery of phosphorus from wastewater: A review based on current phosphorous removal technologies Crit Rev Environ Sci Technol **53**, 1148-1172
10.1080/10643389.2022.2128194
21. Lai, Y. C., Liang, C. M., Hsu, S. C., Hsieh, P. H., and Hung, C. H. (2017) Polyphosphate metabolism by purple non-sulfur bacteria and its possible application on photo-microbial fuel cell J Biosci Bioeng **123**, 722-730
10.1016/j.jbiosc.2017.01.012
22. Srisanga, K., Suthapot, P., Permsirivisarn, P., Govitrapong, P., Tungpradabkul, S., and Wongtrakoongate, P. (2019) Polyphosphate kinase 1 of Burkholderia pseudomallei controls quorum sensing, RpoS and host cell invasion J Proteomics **194**, 14-24
10.1016/j.jprot.2018.12.024
23. Shi, X., Rao, N. N., and Kornberg, A. (2004) Inorganic polyphosphate in Bacillus cereus: motility, biofilm formation, and sporulation Proc Natl Acad Sci U S A **101**, 17061-17065
10.1073/pnas.0407787101
24. Tocheva, E. I., Dekas, A. E., McGlynn, S. E., Morris, D., Orphan, V. J., and Jensen, G. J. (2013) Polyphosphate storage during sporulation in the gram-negative bacterium Acetonema longum J Bacteriol **195**, 3940-3946
10.1128/JB.00712-13
25. Candon, H. L., Allan, B. J., Fraley, C. D., and Gaynor, E. C. (2007) Polyphosphate kinase 1 is a pathogenesis determinant in Campylobacter jejuni J Bacteriol **189**, 8099-8108
10.1128/JB.01037-07
26. Kumar, A., Gangaiah, D., Torrelles, J. B., and Rajashekara, G. (2016) Polyphosphate and associated enzymes as global regulators of stress response and virulence in Campylobacter jejuni World J Gastroenterol **22**, 7402-7414
10.3748/wjg.v22.i33.7402

27. Rashid, M. H., Rao, N. N., and Kornberg, A. (2000) Inorganic polyphosphate is required for motility of bacterial pathogens J Bacteriol **182**, 225-227, <https://www.ncbi.nlm.nih.gov/pubmed/10613886>
<https://www.ncbi.nlm.nih.gov/pmc/articles/PMC94263/pdf/jb000225.pdf>
28. Tan, S., Fraley, C. D., Zhang, M., Dailidienne, D., Kornberg, A., and Berg, D. E. (2005) Diverse phenotypes resulting from polyphosphate kinase gene (ppk1) inactivation in different strains of *Helicobacter pylori* J Bacteriol **187**, 7687-7695
10.1128/JB.187.22.7687-7695.2005
29. Tiwari, P., Gosain, T. P., Singh, M., Sankhe, G. D., Arora, G., Kidwai, S. *et al.* (2019) Inorganic polyphosphate accumulation suppresses the dormancy response and virulence in *Mycobacterium tuberculosis* J Biol Chem **294**, 10819-10832
10.1074/jbc.RA119.008370
30. Chen, J., Su, L., Wang, X., Zhang, T., Liu, F., Chen, H. *et al.* (2016) Polyphosphate Kinase Mediates Antibiotic Tolerance in Extraintestinal Pathogenic *Escherichia coli* PCN033 Front Microbiol **7**, 724
10.3389/fmicb.2016.00724
31. Chuang, Y. M., Dutta, N. K., Hung, C. F., Wu, T. C., Rubin, H., and Karakousis, P. C. (2016) Stringent Response Factors PPX1 and PPK2 Play an Important Role in *Mycobacterium tuberculosis* Metabolism, Biofilm Formation, and Sensitivity to Isoniazid In Vivo Antimicrob Agents Chemother **60**, 6460-6470
10.1128/AAC.01139-16
32. Gangaiah, D., Kassem, II, Liu, Z., and Rajashekara, G. (2009) Importance of polyphosphate kinase 1 for *Campylobacter jejuni* viable-but-nonculturable cell formation, natural transformation, and antimicrobial resistance Appl Environ Microbiol **75**, 7838-7849
10.1128/AEM.01603-09
33. Ortiz-Severin, J., Varas, M., Bravo-Toncio, C., Guiliani, N., and Chavez, F. P. (2015) Multiple antibiotic susceptibility of polyphosphate kinase mutants (ppk1 and ppk2) from *Pseudomonas aeruginosa* PAO1 as revealed by global phenotypic analysis Biol Res **48**, 22
10.1186/s40659-015-0012-0
34. Ogawa, N., Tzeng, C. M., Fraley, C. D., and Kornberg, A. (2000) Inorganic polyphosphate in *Vibrio cholerae*: genetic, biochemical, and physiologic features J Bacteriol **182**, 6687-6693, <https://www.ncbi.nlm.nih.gov/pubmed/11073913>
<https://www.ncbi.nlm.nih.gov/pmc/articles/PMC111411/pdf/jb006687.pdf>

35. Achbergerova, L., and Nahalka, J. (2011) Polyphosphate--an ancient energy source and active metabolic regulator *Microb Cell Fact* **10**, 63 10.1186/1475-2859-10-63
36. Cha, S. B., Rayamajhi, N., Lee, W. J., Shin, M. K., Jung, M. H., Shin, S. W. *et al.* (2012) Generation and envelope protein analysis of internalization defective *Brucella abortus* mutants in professional phagocytes, RAW 264.7 *FEMS Immunol Med Microbiol* **64**, 244-254 10.1111/j.1574-695X.2011.00896.x
37. Kim, K. S., Rao, N. N., Fraley, C. D., and Kornberg, A. (2002) Inorganic polyphosphate is essential for long-term survival and virulence factors in *Shigella* and *Salmonella* spp *Proc Natl Acad Sci U S A* **99**, 7675-7680 10.1073/pnas.112210499
38. Peng, L., Luo, W. Y., Zhao, T., Wan, C. S., Jiang, Y., Chi, F. *et al.* (2012) Polyphosphate kinase 1 is required for the pathogenesis process of meningitic *Escherichia coli* K1 (RS218) *Future Microbiol* **7**, 411-423 10.2217/fmb.12.3
39. Rao, N. N., Gomez-Garcia, M. R., and Kornberg, A. (2009) Inorganic polyphosphate: essential for growth and survival *Annu Rev Biochem* **78**, 605-647 10.1146/annurev.biochem.77.083007.093039
40. Rao, N. N., and Kornberg, A. (1996) Inorganic polyphosphate supports resistance and survival of stationary-phase *Escherichia coli* *J Bacteriol* **178**, 1394-1400, <https://www.ncbi.nlm.nih.gov/pubmed/8631717>
<http://jb.asm.org/content/178/5/1394.full.pdf>
41. Tunpiboonsak, S., Mongkolrob, R., Kitudomsab, K., Thanwatanaying, P., Kiettipirodom, W., Tungboontina, Y. *et al.* (2010) Role of a *Burkholderia pseudomallei* polyphosphate kinase in an oxidative stress response, motilities, and biofilm formation *J Microbiol* **48**, 63-70 10.1007/s12275-010-9138-5
42. Jenal, U., and Hengge-Aronis, R. (2003) Regulation by proteolysis in bacterial cells *Curr Opin Microbiol* **6**, 163-172 10.1016/s1369-5274(03)00029-8
43. Zygmunt, M. S., Hagijs, S. D., Walker, J. V., and Elzer, P. H. (2006) Identification of *Brucella melitensis* 16M genes required for bacterial survival in the caprine host *Microbes Infect* **8**, 2849-2854 10.1016/j.micinf.2006.09.002

44. Battesti, A., Majdalani, N., and Gottesman, S. (2011) The RpoS-mediated general stress response in *Escherichia coli* *Annu Rev Microbiol* **65**, 189-213
10.1146/annurev-micro-090110-102946
45. Battesti, A., Majdalani, N., and Gottesman, S. (2015) Stress sigma factor RpoS degradation and translation are sensitive to the state of central metabolism *Proc Natl Acad Sci U S A* **112**, 5159-5164 10.1073/pnas.1504639112
46. Weber, H., Polen, T., Heuveling, J., Wendisch, V. F., and Hengge, R. (2005) Genome-wide analysis of the general stress response network in *Escherichia coli*: sigmaS-dependent genes, promoters, and sigma factor selectivity *J Bacteriol* **187**, 1591-1603 10.1128/JB.187.5.1591-1603.2005
47. Ault-Riche, D., Fraley, C. D., Tzeng, C. M., and Kornberg, A. (1998) Novel assay reveals multiple pathways regulating stress-induced accumulations of inorganic polyphosphate in *Escherichia coli* *J Bacteriol* **180**, 1841-1847,
http://www.ncbi.nlm.nih.gov/entrez/query.fcgi?cmd=Retrieve&db=PubMed&dopt=Citation&list_uids=9537383
48. Brown, M. R., and Kornberg, A. (2008) The long and short of it - polyphosphate, PPK and bacterial survival *Trends Biochem Sci* **33**, 284-290
10.1016/j.tibs.2008.04.005
49. Kuroda, A., Murphy, H., Cashel, M., and Kornberg, A. (1997) Guanosine tetra- and pentaphosphate promote accumulation of inorganic polyphosphate in *Escherichia coli* *J Biol Chem* **272**, 21240-21243,
http://www.ncbi.nlm.nih.gov/entrez/query.fcgi?cmd=Retrieve&db=PubMed&dopt=Citation&list_uids=9261133
50. Kuroda, A., Nomura, K., Ohtomo, R., Kato, J., Ikeda, T., Takiguchi, N. *et al.* (2001) Role of inorganic polyphosphate in promoting ribosomal protein degradation by the Lon protease in *E. coli* *Science* **293**, 705-708
10.1126/science.1061315
51. Rao, N. N., and Kornberg, A. (1999) Inorganic polyphosphate regulates responses of *Escherichia coli* to nutritional stringencies, environmental stresses and survival in the stationary phase *Prog Mol Subcell Biol* **23**, 183-195,
<https://www.ncbi.nlm.nih.gov/pubmed/10448677>

52. Rao, N. N., Liu, S., and Kornberg, A. (1998) Inorganic polyphosphate in *Escherichia coli*: the phosphate regulon and the stringent response *J Bacteriol* **180**, 2186-2193 10.1128/JB.180.8.2186-2193.1998
53. Gray, M. J. (2020) Interactions between DksA and Stress-Responsive Alternative Sigma Factors Control Inorganic Polyphosphate Accumulation in *Escherichia coli* *J Bacteriol* **202**, 10.1128/JB.00133-20
54. Bowlin, M. Q., Long, A. R., Huffines, J. T., and Gray, M. J. (2022) The role of nitrogen-responsive regulators in controlling inorganic polyphosphate synthesis in *Escherichia coli* *Microbiology (Reading)* **168**, 10.1099/mic.0.001185
55. Zhang, H., Gomez-Garcia, M. R., Shi, X., Rao, N. N., and Kornberg, A. (2007) Polyphosphate kinase 1, a conserved bacterial enzyme, in a eukaryote, *Dictyostelium discoideum*, with a role in cytokinesis *Proc Natl Acad Sci U S A* **104**, 16486-16491 10.1073/pnas.0706847104
56. Gomez-Garcia, M. R., and Kornberg, A. (2004) Formation of an actin-like filament concurrent with the enzymatic synthesis of inorganic polyphosphate *Proc Natl Acad Sci U S A* **101**, 15876-15880 10.1073/pnas.0406923101
57. Baev, A. Y., Angelova, P. R., and Abramov, A. Y. (2020) Inorganic polyphosphate is produced and hydrolyzed in F₀F₁-ATP synthase of mammalian mitochondria *Biochem J* **477**, 1515-1524 10.1042/BCJ20200042
58. Archambaud, C., Nahori, M. A., Pizarro-Cerda, J., Cossart, P., and Dussurget, O. (2006) Control of *Listeria* superoxide dismutase by phosphorylation *J Biol Chem* **281**, 31812-31822 10.1074/jbc.M606249200
59. Batten, L. E., Parnell, A. E., Wells, N. J., Murch, A. L., Oyston, P. C., and Roach, P. L. (2015) Biochemical and structural characterization of polyphosphate kinase 2 from the intracellular pathogen *Francisella tularensis* *Biosci Rep* **36**, e00294 10.1042/BSR20150203
60. Chen, Y., Ross, W. H., Gray, M. J., Wiedmann, M., Whiting, R. C., and Scott, V. N. (2006) Attributing risk to *Listeria monocytogenes* subgroups: dose response in relation to genetic lineages *J Food Prot* **69**, 335-344 10.4315/0362-028x-69.2.335
61. Gray, M. J., Zadoks, R. N., Fortes, E. D., Dogan, B., Cai, S., Chen, Y. *et al.* (2004) *Listeria monocytogenes* isolates from foods and humans form distinct but

overlapping populations Appl Environ Microbiol **70**, 5833-5841
10.1128/AEM.70.10.5833-5841.2004

62. Michael, C. A., Dominey-Howes, D., and Labbate, M. (2014) The antimicrobial resistance crisis: causes, consequences, and management Front Public Health **2**, 145 10.3389/fpubh.2014.00145
63. Neville, N., Roberge, N., Ji, X., Stephen, P., Lu, J. L., and Jia, Z. (2021) A Dual-Specificity Inhibitor Targets Polyphosphate Kinase 1 and 2 Enzymes To Attenuate Virulence of *Pseudomonas aeruginosa* mBio **12**, e0059221 10.1128/mBio.00592-21
64. Pizarro-Cerda, J., and Cossart, P. (2006) Bacterial adhesion and entry into host cells Cell **124**, 715-727 10.1016/j.cell.2006.02.012
65. Pizarro-Cerda, J., and Cossart, P. (2006) Subversion of cellular functions by *Listeria monocytogenes* J Pathol **208**, 215-223 10.1002/path.1888
66. Rashid, M. H., and Kornberg, A. (2000) Inorganic polyphosphate is needed for swimming, swarming, and twitching motilities of *Pseudomonas aeruginosa* Proc Natl Acad Sci U S A **97**, 4885-4890 10.1073/pnas.060030097
67. Rashid, M. H., Rumbaugh, K., Passador, L., Davies, D. G., Hamood, A. N., Iglewski, B. H. *et al.* (2000) Polyphosphate kinase is essential for biofilm development, quorum sensing, and virulence of *Pseudomonas aeruginosa* Proc Natl Acad Sci U S A **97**, 9636-9641 10.1073/pnas.170283397
68. Roberge, N., Neville, N., Douchant, K., Noordhof, C., Boev, N., Sjaarda, C. *et al.* (2021) Broad-Spectrum Inhibitor of Bacterial Polyphosphate Homeostasis Attenuates Virulence Factors and Helps Reveal Novel Physiology of *Klebsiella pneumoniae* and *Acinetobacter baumannii* Front Microbiol **12**, 764733 10.3389/fmicb.2021.764733
69. Rohlfing, A. E., Ramsey, K. M., and Dove, S. L. (2018) Polyphosphate Kinase Antagonizes Virulence Gene Expression in *Francisella tularensis* J Bacteriol **200**, 10.1128/JB.00460-17
70. Sarabhai, S., Harjai, K., Sharma, P., and Capalash, N. (2015) Ellagic acid derivatives from *Terminalia chebula* Retz. increase the susceptibility of

Pseudomonas aeruginosa to stress by inhibiting polyphosphate kinase J Appl Microbiol **118**, 817-825 10.1111/jam.12733

71. Sillo, A., Matthias, J., Konertz, R., Bozzaro, S., and Eichinger, L. (2011) *Salmonella typhimurium* is pathogenic for *Dictyostelium* cells and subverts the starvation response Cell Microbiol **13**, 1793-1811 10.1111/j.1462-5822.2011.01662.x
72. Singh, M., Tiwari, P., Arora, G., Agarwal, S., Kidwai, S., and Singh, R. (2016) Establishing Virulence Associated Polyphosphate Kinase 2 as a drug target for *Mycobacterium tuberculosis* Sci Rep **6**, 26900 10.1038/srep26900
73. Singh, R., Singh, M., Arora, G., Kumar, S., Tiwari, P., and Kidwai, S. (2013) Polyphosphate deficiency in *Mycobacterium tuberculosis* is associated with enhanced drug susceptibility and impaired growth in guinea pigs J Bacteriol **195**, 2839-2851 10.1128/JB.00038-13
74. Tang-Fichaux, M., Chagneau, C. V., Bossuet-Greif, N., Nougayrede, J. P., Oswald, E., and Branchu, P. (2020) The Polyphosphate Kinase of *Escherichia coli* Is Required for Full Production of the Genotoxin Colibactin mSphere **5**, 10.1128/mSphere.01195-20
75. Dahl, J. U., Gray, M. J., Bazopoulou, D., Beaufay, F., Lempart, J., Koenigskecht, M. J. *et al.* (2017) The anti-inflammatory drug mesalamine targets bacterial polyphosphate accumulation Nat Microbiol **2**, 16267 10.1038/nmicrobiol.2016.267
76. Lang, A., Salomon, N., Wu, J. C., Kopylov, U., Lahat, A., Har-Noy, O. *et al.* (2015) Curcumin in Combination With Mesalamine Induces Remission in Patients With Mild-to-Moderate Ulcerative Colitis in a Randomized Controlled Trial Clin Gastroenterol Hepatol **13**, 1444-1449 e1441 10.1016/j.cgh.2015.02.019
77. Dignass, A., Lindsay, J. O., Sturm, A., Windsor, A., Colombel, J. F., Allez, M. *et al.* (2012) Second European evidence-based consensus on the diagnosis and management of ulcerative colitis part 2: current management J Crohns Colitis **6**, 991-1030 10.1016/j.crohns.2012.09.002
78. Ahn, K., and Kornberg, A. (1990) Polyphosphate kinase from *Escherichia coli*. Purification and demonstration of a phosphoenzyme intermediate J Biol Chem **265**, 11734-11739, <https://www.ncbi.nlm.nih.gov/pubmed/2164013>
<http://www.jbc.org/content/265/20/11734.full.pdf>

79. Akiyama, M., Crooke, E., and Kornberg, A. (1992) The polyphosphate kinase gene of *Escherichia coli*. Isolation and sequence of the *ppk* gene and membrane location of the protein *J Biol Chem* **267**, 22556-22561, <https://www.ncbi.nlm.nih.gov/pubmed/1331061>
<http://www.jbc.org/content/267/31/22556.full.pdf>
80. Zhu, Y., Huang, W., Lee, S. S., and Xu, W. (2005) Crystal structure of a polyphosphate kinase and its implications for polyphosphate synthesis *EMBO Rep* **6**, 681-687 10.1038/sj.embor.7400448
81. Zhu, Y., Lee, S. S., and Xu, W. (2003) Crystallization and characterization of polyphosphate kinase from *Escherichia coli* *Biochem Biophys Res Commun* **305**, 997-1001, <https://www.ncbi.nlm.nih.gov/pubmed/12767929>
<https://www.sciencedirect.com/science/article/pii/S0006291X03008866?via%3Dihub>
82. Ishige, K., Zhang, H., and Kornberg, A. (2002) Polyphosphate kinase (PPK2), a potent, polyphosphate-driven generator of GTP *Proc Natl Acad Sci U S A* **99**, 16684-16688 10.1073/pnas.26265299
83. Motomura, K., Hirota, R., Okada, M., Ikeda, T., Ishida, T., and Kuroda, A. (2014) A new subfamily of polyphosphate kinase 2 (class III PPK2) catalyzes both nucleoside monophosphate phosphorylation and nucleoside diphosphate phosphorylation *Appl Environ Microbiol* **80**, 2602-2608 10.1128/AEM.03971-13
84. Neville, N., Roberge, N., and Jia, Z. (2022) Polyphosphate Kinase 2 (PPK2) Enzymes: Structure, Function, and Roles in Bacterial Physiology and Virulence *Int J Mol Sci* **23**, 10.3390/ijms23020670
85. Nocek, B., Kochinyan, S., Proudfoot, M., Brown, G., Evdokimova, E., Osipiuk, J. *et al.* (2008) Polyphosphate-dependent synthesis of ATP and ADP by the family-2 polyphosphate kinases in bacteria *Proc Natl Acad Sci U S A* **105**, 17730-17735 10.1073/pnas.0807563105
86. Lavie, A., Ostermann, N., Brundiers, R., Goody, R. S., Reinstein, J., Konrad, M. *et al.* (1998) Structural basis for efficient phosphorylation of 3'-azidothymidine monophosphate by *Escherichia coli* thymidylate kinase *Proc Natl Acad Sci U S A* **95**, 14045-14050 10.1073/pnas.95.24.14045

87. Leipe, D. D., Koonin, E. V., and Aravind, L. (2003) Evolution and classification of P-loop kinases and related proteins *J Mol Biol* **333**, 781-815
10.1016/j.jmb.2003.08.040
88. Nahalka, J., and Patoprsty, V. (2009) Enzymatic synthesis of sialylation substrates powered by a novel polyphosphate kinase (PPK3) *Org Biomol Chem* **7**, 1778-1780 10.1039/b822549b
89. Akiyama, M., Crooke, E., and Kornberg, A. (1993) An exopolyphosphatase of *Escherichia coli*. The enzyme and its ppx gene in a polyphosphate operon *J Biol Chem* **268**, 633-639, <https://www.ncbi.nlm.nih.gov/pubmed/8380170>
<http://www.jbc.org/content/268/1/633.full.pdf>
90. Alvarado, J., Ghosh, A., Janovitz, T., Jauregui, A., Hasson, M. S., and Sanders, D. A. (2006) Origin of exopolyphosphatase processivity: Fusion of an ASKHA phosphotransferase and a cyclic nucleotide phosphodiesterase homolog *Structure* **14**, 1263-1272 10.1016/j.str.2006.06.009
91. Brown, M. R., and Kornberg, A. (2004) Inorganic polyphosphate in the origin and survival of species *Proc Natl Acad Sci U S A* **101**, 16085-16087
10.1073/pnas.0406909101
92. Achbergerová, L., and Nahálka, J. (2014) PPK1 and PPK2 — which polyphosphate kinase is older? *Biologia* **69**, 263-269 10.2478/s11756-013-0324-x
93. Zhang, H., Ishige, K., and Kornberg, A. (2002) A polyphosphate kinase (PPK2) widely conserved in bacteria *Proc Natl Acad Sci U S A* **99**, 16678-16683
10.1073/pnas.262655199
94. Garavaglia, S., Galizzi, A., and Rizzi, M. (2003) Allosteric regulation of *Bacillus subtilis* NAD kinase by quinolinic acid *J Bacteriol* **185**, 4844-4850
10.1128/JB.185.16.4844-4850.2003
95. Bessman, M. J., Lehman, I. R., Simms, E. S., and Kornberg, A. (1958) Enzymatic synthesis of deoxyribonucleic acid. II. General properties of the reaction *J Biol Chem* **233**, 171-177, <https://www.ncbi.nlm.nih.gov/pubmed/13563463>
96. Lehman, I. R., Bessman, M. J., Simms, E. S., and Kornberg, A. (1958) Enzymatic synthesis of deoxyribonucleic acid. I. Preparation of substrates and partial

- purification of an enzyme from *Escherichia coli* *J Biol Chem* **233**, 163-170,
<https://www.ncbi.nlm.nih.gov/pubmed/13563462>
97. Tzeng, C. M., and Kornberg, A. (2000) The multiple activities of polyphosphate kinase of *Escherichia coli* and their subunit structure determined by radiation target analysis *J Biol Chem* **275**, 3977-3983,
<https://www.ncbi.nlm.nih.gov/pubmed/10660553>
<http://www.jbc.org/content/275/6/3977.full.pdf>
 98. Ruan, B., Fisher, K. E., Alexander, P. A., Doroshko, V., and Bryan, P. N. (2004) Engineering subtilisin into a fluoride-triggered processing protease useful for one-step protein purification *Biochemistry* **43**, 14539-14546 10.1021/bi048177j
 99. Kumar, D., Mandal, S., Bailey, J. V., Flood, B. E., and Jones, R. S. (2023) Fluoride and gallein inhibit polyphosphate accumulation by oral pathogen *Rothia dentocariosa* *Lett Appl Microbiol* **76**, 10.1093/lambio/ovad017
 100. Wang, R. F., and Kushner, S. R. (1991) Construction of versatile low-copy-number vectors for cloning, sequencing and gene expression in *Escherichia coli* *Gene* **100**, 195-199, <https://www.ncbi.nlm.nih.gov/pubmed/2055470>
https://ac.els-cdn.com/037811199190366J/1-s2.0-037811199190366J-main.pdf?_tid=5866bf05-6492-4ff3-9af4-cd34c6c47eba&acdnat=1536929230_8cbeef033e3e716ba503553bed4a304b
 101. Reisch, C. R., and Prather, K. L. J. (2017) Scarless Cas9 Assisted Recombineering (no-SCAR) in *Escherichia coli*, an Easy-to-Use System for Genome Editing *Curr Protoc Mol Biol* **117**, 31 38 31-31 38 20 10.1002/cpmb.29
 102. Ochman, H., Gerber, A. S., and Hartl, D. L. (1988) Genetic applications of an inverse polymerase chain reaction *Genetics* **120**, 621-623
10.1093/genetics/120.3.621
 103. Gray, M. J. (2019) Inorganic Polyphosphate Accumulation in *Escherichia coli* Is Regulated by DksA but Not by (p)ppGpp *J Bacteriol* **201**, 10.1128/JB.00664-18
 104. Jin, J., Hjerrild, K. A., Silk, S. E., Brown, R. E., Labbe, G. M., Marshall, J. M. *et al.* (2017) Accelerating the clinical development of protein-based vaccines for malaria by efficient purification using a four amino acid C-terminal 'C-tag' *Int J Parasitol* **47**, 435-446 10.1016/j.ijpara.2016.12.001

105. Jones, P. G., and Inouye, M. (1996) RbfA, a 30S ribosomal binding factor, is a cold-shock protein whose absence triggers the cold-shock response *Mol Microbiol* **21**, 1207-1218 10.1111/j.1365-2958.1996.tb02582.x
106. Fernandez De Henestrosa, A. R., Ogi, T., Aoyagi, S., Chafin, D., Hayes, J. J., Ohmori, H. *et al.* (2000) Identification of additional genes belonging to the LexA regulon in *Escherichia coli* *Mol Microbiol* **35**, 1560-1572 10.1046/j.1365-2958.2000.01826.x
107. Richards, M. I., Michell, S. L., and Oyston, P. C. F. (2008) An intracellularly inducible gene involved in virulence and polyphosphate production in *Francisella* *J Med Microbiol* **57**, 1183-1192 10.1099/jmm.0.2008/001826-0
108. Sanyal, S., Banerjee, S. K., Banerjee, R., Mukhopadhyay, J., and Kundu, M. (2013) Polyphosphate kinase 1, a central node in the stress response network of *Mycobacterium tuberculosis*, connects the two-component systems MprAB and SenX3-RegX3 and the extracytoplasmic function sigma factor, sigma E *Microbiology (Reading)* **159**, 2074-2086 10.1099/mic.0.068452-0
109. Klein, G., Stupak, A., Biernacka, D., Wojtkiewicz, P., Lindner, B., and Raina, S. (2016) Multiple Transcriptional Factors Regulate Transcription of the *rpoE* Gene in *Escherichia coli* under Different Growth Conditions and When the Lipopolysaccharide Biosynthesis Is Defective *J Biol Chem* **291**, 22999-23019 10.1074/jbc.M116.748954
110. Reichenbach, B., Gopel, Y., and Gorke, B. (2009) Dual control by perfectly overlapping sigma 54- and sigma 70- promoters adjusts small RNA GlmY expression to different environmental signals *Mol Microbiol* **74**, 1054-1070 10.1111/j.1365-2958.2009.06918.x
111. Danson, A. E., Jovanovic, M., Buck, M., and Zhang, X. (2019) Mechanisms of sigma(54)-Dependent Transcription Initiation and Regulation *J Mol Biol* **431**, 3960-3974 10.1016/j.jmb.2019.04.022
112. Song, J., Wang, Y., Li, F., Akutsu, T., Rawlings, N. D., Webb, G. I. *et al.* (2019) iProt-Sub: a comprehensive package for accurately mapping and predicting protease-specific substrates and cleavage sites *Brief Bioinform* **20**, 638-658 10.1093/bib/bby028
113. Pokhrel, A., Lingo, J. C., Wolschendorf, F., and Gray, M. J. (2019) Assaying for Inorganic Polyphosphate in Bacteria *J Vis Exp* 10.3791/58818

114. Rudat, A. K., Pokhrel, A., Green, T. J., and Gray, M. J. (2018) Mutations in *Escherichia coli* Polyphosphate Kinase That Lead to Dramatically Increased In Vivo Polyphosphate Levels *J Bacteriol* **200**, 10.1128/JB.00697-17
115. Livak, K. J., and Schmittgen, T. D. (2001) Analysis of relative gene expression data using real-time quantitative PCR and the 2^{(-Delta Delta C(T))} Method *Methods* **25**, 402-408 10.1006/meth.2001.1262
116. Liu, T., Ryan, M., Dahlquist, F. W., and Griffith, O. H. (1997) Determination of pKa values of the histidine side chains of phosphatidylinositol-specific phospholipase C from *Bacillus cereus* by NMR spectroscopy and site-directed mutagenesis *Protein Sci* **6**, 1937-1944 10.1002/pro.5560060914
117. Neville, N., Lehotsky, K., Yang, Z., Klupt, K. A., Denoncourt, A., Downey, M. *et al.* (2023) Modification of histidine repeat proteins by inorganic polyphosphate *Cell Rep* **42**, 113082 10.1016/j.celrep.2023.113082

APPENDIX A

DEVELOPED PROTEIN PURIFICATION PROTOCOLS

Profinity Purification of PPK and PPK enzymes***A) Buffers.**

Buffer	Composition	Notes
Suspension/ Wash Buffer	100-300 mM Sodium Phosphate pH 7.2	
Lysis Buffer	100 mM Sodium Phosphate pH 7.2 5mM MgSO ₄ 6uL Nuclease 1 Inhibitor Tablet	
Ammonium Sulfate Extraction Buffer	50 mM Tris-Acetate pH 7.2 <i>Or</i> 50 mM HEPES-KOH pH 7.2 <i>And</i> 10% W/V sucrose	If using Tris, sodium acetate is an excellent additive as it will reduce non-specific binding to the column
Elution Buffer	100-300 mM Sodium Phosphate pH 7.2-7.4 100 mM Sodium Fluoride	
Cleaning Buffer	0.1 M Phosphoric Acid	Can use 0.1 M NaOH instead
Column Storage Buffer	100 mM Sodium Phosphate pH 7.2 0.02% w/v Sodium Azide	
Enzyme Storage Buffer	20 mM HEPES-KOH pH 8.0 150 mM NaCl 15% glycerol 1 mM EDTA	

Notes:

1. F⁻, Cl⁻, N₃, CO₂, and NO₂ cannot be included in any of the reaction buffers.
2. Increased concentrations of sodium phosphate can improve PPK extraction from the membrane fragments; however, it can also precipitate at 4C.

B) Part 1 – Lysosyme Treatment and Cell Lysis

1. Thaw 1 L pellet in up to 50 mL of a 100-300 mM Sodium Phosphate Buffer, pH 7.2 (Profinity Wash Buffer).
2. Add 30 mg of lysozyme and incubate on ice for 45 minutes, mixing occasionally.
3. Shift to 42 °C in a water bath for 10 minutes, mixing occasionally.
4. Pellet at 20,000 x g at 4 °C for 1 hour and discard supernatant.
5. Resuspend pellet in up to 50 mL of Profinity Wash Buffer. Supplement resuspended pellet with 5 mM MgSO₄, 1 50 mL protease inhibitor tablet, and 6 µL of nuclease.
6. Sonicate the resuspension at 4 °C for 5 minutes in 5 second bursts, 50% amplitude.
7. Pellet at 20,000 x g for 1 hour at 4 °C and reserve the supernatant and pellet.
 - i. Test the two fractions to determine the localization of PPK.
 - ii. If PPK is in the soluble fraction (which it might be due to the large size of the Profinity tag and the use of 300 mM Sodium Phosphate buffer), proceed to Part 3.
 - iii. If PPK is in the insoluble fraction, proceed to part 2.

C) Part 2: Extraction from the Pellet w/ Ammonium Sulfate

1. Resuspend pellet in 25 mL of 50 mM HEPES-KOH buffer or Tris-Acetate buffer, pH 7.2-7.4 + 10% sucrose.

2. Dissolve 5 g of Ammonium sulfate in 1 g increments over a 20-minute period (adding 1 g at T0, T5, T10, T15, and T20).
3. After the addition of the final 1 g increment, allow solution to stir at 4 °C for 30 minutes.
4. After stirring, pellet solution at 33,700 x g for 30 minutes to remove solids.
5. To the supernatant, add 2.7 g (0.108 g mL⁻¹) of ammonium sulfate and stir until dissolved (~10-20 min).
6. Pellet the solution by centrifuging at 33700 x g for 30 minutes at 4 °C
7. Decant the supernatant and resuspend the pellet in 20 mL of Profinity Wash Buffer.
8. Filter the solution through a syringe filter and proceed to Part 3.

D) Part 3: Column Loading and Elution

1. Prepare Profinity column by washing with 10 column volumes (CVs) at a rate of 3 mL per minute using Wash Buffer.
2. Take the PPK-containing solution and load slowly over the Profinity column (~1 mL per minute).
3. Wash the column with at least 10 CVs of Wash Buffer.
4. Elute PPK from the column by running 2-4 CVs of Elution Buffer, or enough to where the FPLC detect the conductivity shift.
5. Stop flow of buffer once conductivity shift is detected and allow the column to incubate in the elution buffer for 30 minutes, or overnight at 4 °C.
6. Resume flow and elute into collection tube.

7. Visualize collection on an SDS-PAGE gel to check purity and size.
8. Dialyze into protein storage buffer and freeze at -80 °C.

E) Part 4: Column Cleaning and Storage

1. Rinse column with 5-10 CVs of wash buffer.
2. Run 10 CVs of Cleaning Buffer over the column at a rate of 1 ml per minute.
3. Wash the column with 10 CVs of Wash Buffer, then store column in Column Storage buffer.

Untagged Purification of PPK From An Overexpression Culture

A) Buffers

Buffer	Composition	Notes
Buffer A	50 mM Tris-HCl pH 7.5 10% w/v Sucrose	
Buffer B	0.2 M Potassium Phosphate Buffer, pH 7.0 10% glycerol 1 mM EDTA	prepare a 1 L stock of 1 M Potassium Phosphate buffer pH 7.0 and add 200 mL to Buffer B
Buffer C – Cation Exchange Start Buffer	20 mM HEPES-KOH pH 8.0 0.2 M NaCl 1 mM EDTA 15% glycerol	
Buffer D – Cation Exchange Elution Buffer	20 mM HEPES-KOH pH 8.0 0.8 M NaCl 1 mM EDTA 15% glycerol	
Cleaning Buffer	1 M NaCl	1 M NaOH also works but must be washed quickly
Column Storage Buffer	20% Ethanol w/ 0.2 M Sodium Acetate	
Enzyme Storage Buffer	20 mM HEPES-KOH pH8.0 150 mM NaCl 15% glycerol 1 mM EDTA	

B) Part I: Generating the Lysozyme Extract Pellet

1. Thaw and/or resuspend an overexpression pellet in 10-100 mL Buffer A (50 mM Tris-HCl pH 7.5, 10% w/v sucrose (5 g in 50 mL)). Transfer to a 50 mL conical tube or appropriate container. Wash the bottle and transfer the wash to the resuspension.
2. Digest pellet with lysozyme (300 ug mL⁻¹, 7.5 mg in 25 mL) in Buffer A with gentle incubation on ice for 45 minutes, followed by a 10 minute heat shock at 42 °C and an ice bath chill.
3. Centrifuge the lysozyme digestion (20,000 x g, 1 hour at 4 °C). Slower speeds will be insufficient to pellet solution as it will be viscous.

C) Part II: Extracting the PPK from the Lysozyme Extract Pellet

4. Resuspend digested pellet in **25 mL** of **Buffer A** with 5 mM MgCl₂, one protease tablet, and 6 uL of nuclease.
5. Sonicate the solution for 5 minutes in 5 s pulses, amplitude set to 50%.
6. Pellet at 30,000 x g for 30 min at 4 °C and discard supernatant.
7. Resuspend pellet from step 4 in 25 mL of **Buffer A** (50 mM Tris-HCl pH 7.5, 10% w/v sucrose) via sonication for 5 minutes in 5 s pulses, 50% amplitude.
8. Add KCl to resuspended pellet at 1 M concentrations (1.86 g in 25 mL), then add 1/10 volume of 1 M Na₂CO₃ (~3 mL).
9. Incubate at 4 °C with stirring for 30 minutes.
10. Sonicate solution for 2 minutes in 5 s pulses, 50% amplitude.
11. Pellet solution at 10,000 x g for 1 hour at 4 °C.

12. Decant supernatant and filter through a syringe filter to remove any particulates that did not fully pellet.
13. Dialyze against **Buffer B** 3 times for 2 hours each at a ratio of 1:50 minimum (Preferably 1:100). Use the dialysis tubing with a 50 kDa MWCO rating.
14. To the dialyzed suspension, add **5 g** (or, 0.2 g mL^{-1} for various volumes) of Ammonium Sulfate solid over a 20 minute period (**1 g or 1/5 of total per 5 minutes at T0, T5, T10, T15, and T20**) with stirring between additions. After adding the last portion, stir at $4 \text{ }^{\circ}\text{C}$ for 30 minutes.
15. After stirring for 30 minutes, pellet the solution at $37,900 \times g$ for 30 minutes to remove the solids.
 - a. *Supernatant will be clear and yellowish in tint. Make sure there are no insoluble particles in the sup. From a 2 L pellet the insoluble pellet was pretty sizable.*
16. To the **supernatant** from the initial cut, add 2.7 g (0.108 g mL^{-1}) of Ammonium sulfate and stir until dissolved (~10-20 min).
 - a. *Shortly after the salt is added the supernatant should become milky and opaque. This is good – the milkier the better.*
17. Pellet the supernatant by centrifuging at $37900 \times g$ for 30 min at $4 \text{ }^{\circ}\text{C}$.
18. Decant supernatant and resuspend the **pellet** in 20 mL of **Buffer C**. Dialyze resuspension against 1-2 L of Buffer C (20 mM HEPES-KOH pH 8.0, 0.2 M NaCl, 1 mM EDTA, 15% glycerol) at $4 \text{ }^{\circ}\text{C}$ overnight or 3 hours. Repeat this for a total of three or four dialyses.

- a. *Optimal dialysis would be four 1 L dialysis runs for a total of 12 hours in four separate dialysis sets.*

D) Part III: Ion Exchange Chromatography Enrichment and Isolation

19. Filter dilute through a fine syringe filter. Prepare an anion exchange column by rinsing with 10 CVs of Buffer C at a pH of 8. Run the dialyzed solution over the column to extract all the negatively charged proteins from solution.
20. Prepare a cation exchange column by rinsing with 10 CVs of Buffer C. Equilibrate cation exchange column by incubating in Buffer C for at least 10 minutes.
21. Load anion-depleted filtered extract onto a cation exchange column slowly (~ 1 mL min^{-1} for 1 mL column, or no more than 3 mL min^{-1} for a 5 mL column).
22. Allow the column to incubate for 5 minutes, then rinse with 10 CVs of Buffer C.
23. Elute the bound protein using an isocratic gradient of 0-100% buffer D (20 mM HEPES-KOH pH 8.0, 0.8 M NaCl, 1 mM EDTA, 15% glycerol). PPK tends to come off in the earlier fractions, from 6-10, though the exact fraction will vary with gradient concentration and protein concentration.
24. Analyze the fractions on an SDS-PAGE gel to determine which fractions have PPK and which, if any, have PPK with other proteins. Pool the pure PPK fractions and dialyze against 1 L of Protein Storage Buffer (20 mM HEPES-KOH pH 8.0, 150 mM NaCl, 1 mM EDTA, 15% glycerol) at 4 °C for 3 hours or overnight.
25. Change buffer out once and dialyze for 3 hours or overnight.

26. Collect the dialyzed protein solution, measure the concentration via Bradford assay or nanodrop, aliquot into usable volumes, and freeze at -80 °C.

E) Column Storage

27. Strip the column using 10 CVs 1 M NaCl.
28. Rinse the column with 10 CVs of wash buffer.
29. Store column in storage buffer at 4 °C.

C-Tag Purification Of PPK From An Overexpression Culture

A) Buffers

Buffer	Composition	Notes
Wash/ Suspension Buffer	20 mM Tris-HCl pH 7.5 15% glycerol	
Elution Buffer	20 mM Tris-HCl pH 7 15% glycerol 2 M MgCl ₂	
Buffer A – Same as Untagged Protocol	50 mM Tris-HCl pH 7.5 10% w/v Sucrose	
Cleaning Buffer	Run 100% elution buffer for 10 CVs	
Column Storage Buffer	20% Ethanol w/ 0.2M Sodium Acetate	
Enzyme Storage Buffer	20 mM HEPES-KOH pH8.0 150 mM NaCl 15% glycerol 1 mM EDTA	

B) Part I – Lysing the Cells and Harvesting Soluble PPK

- Resuspend each pellet in a total volume of 100 mL of Wash/Suspension Buffer.
Add 30 mg of hen egg lysozyme and incubate on ice for 45 minutes.

2. Heat shock 10 minutes in a water bath heated at 42 C, stirring occasionally.
Return the lysate to ice.
3. Add 1 M MgCl₂ to 5 mM (500 uL of stock in 100 mL), 30 U mL⁻¹ Universal Nuclease (12 uL in 100 mL), and 2 (50 mL) protease inhibitor tablets to the resuspension.
4. Sonicate on ice for 5 minutes in 5 s pulses (5 on, 5 off).
5. Pellet lysate by centrifuging at 20,000 x g for 1 hour.
6. Poured off supernatant into container for filtering. Reserve the pellet for further use if necessary, keeping it on ice.
7. Filter through a 0.45 or 0.8 µm syringe filter to remove particulates, filtering into a clean 100 mL glass bottle for loading onto the column.
8. Load the column at a rate of 1 CV min⁻¹, keeping the pressure in acceptable range for the column settings.
9. Rinse column with 10 CVs of wash/suspension buffer.
10. Elute with elution buffer over a gradient of 0-100% (with Wash buffer being the other buffer used), 5 CVs, in 0.5-1 mL fractions.
 - a. *For a 1 L pellet it is best to use multiple C-tag resin columns in tandem. I've used up to 4 1 mL columns at once and gotten high purity, high concentrations of PPK with minimal jerry-rigging (flexible tubing between end of column connection and feed into UV detector).*

C) Optional – Harvesting PPK From Membrane Fraction

Note: This section of the protocol is appropriate for when PPK isn't isolated from the soluble fraction or is isolated in unusually low amounts. PPK is often associated with the membrane fraction, and so extraction from that fraction is sometimes necessary.

1. Resuspend pellet from step 6 in 25-100 mL (dependent on size of pellet) of Buffer A (50 mM Tris-HCl pH 7.5, 10% w/v sucrose) via sonication for 5 minutes in 5 s pulses, 50% amplitude.
2. Add KCl to resuspended pellet at 1 M concentrations (1.86 g in 25 mL), then add 1/10 volume of 1 M Na₂CO₃ (~3 mL).
3. Incubate at 4 °C with stirring for 30 minutes.
4. Sonicate solution for 2 minutes in 5 s pulses, 50% amplitude.
5. Pellet solution at 17,000 x g for 1 hour at 4 °C.
6. Decant supernatant and immediately mix 1:1 with chilled mqH₂O to dilute ionic concentration.
7. Filter the solution into a clean container via syringe filtration with pore size of 0.2-0.45 µm.
8. Load diluted solution onto C-tag affinity column and resume the above protocol at step 8.

D) Dialysis of Purified PPK

1. Based on the chromatograph of the elution process, select fractions that cover the entire peak of protein elution (generally 10-12 fractions).
2. Take 20 µL from each of these fractions and add 1 µL of SDS Loading Dye to them in a 1.5 mL microfuge tube.

3. Heat at 95 °C for 10 minutes.
4. Load 15 µL of each sample onto an SDS PAGE gel and run at 200 V for 20 minutes.
5. Stain the gel using Fairbanks solution A by placing the gel in the solution and microwaving for 2 minutes, breaking to prevent boiling over.
6. Destain the gel by transferring it into Fairbanks B and heating for 1 minute, then letting is shake at room temperature (RT) for 1 minute.
7. Transfer the gel to Fairbanks C and heat for 1 minute in the microwave, then shake for 1 minute at RT.
8. For final destaining, prepare the Fairbanks D solution and sandwich the gel between two masses of chemwipes. Heat the solution for 2 minutes or until hot in the microwave, then let destain. Repeat this process as needed so that the bands can be detected, replacing the chemwipes every time. For optimal clarity, the gel can be left overnight at RT.
9. Image the gel and note the fractions with PPK bands (~76-80 kDa) and no other detectable bands. Collect these fractions and pool them together.
10. Prepare a dialysis cassette by soaking the membrane for a few minutes in dH₂O.
11. Using a syringe and needle, transfer the pooled fractions into a dialysis cassette with a molecular weight cut-off of at least 3000 Da (3 kDa). A 10,000 Da cut-off is preferable. Be careful not to damage the dialysis membrane. Draw out all the air in the cassette to ensure maximum contact with the membrane.

12. Place a floatie on the top of the cassette (whichever side you pierced with a needle to inject the sample) and gently place in the 4 L bucket of PPK Storage Buffer.

Dialyze at 4 °C for at least 4 hours, preferably overnight.

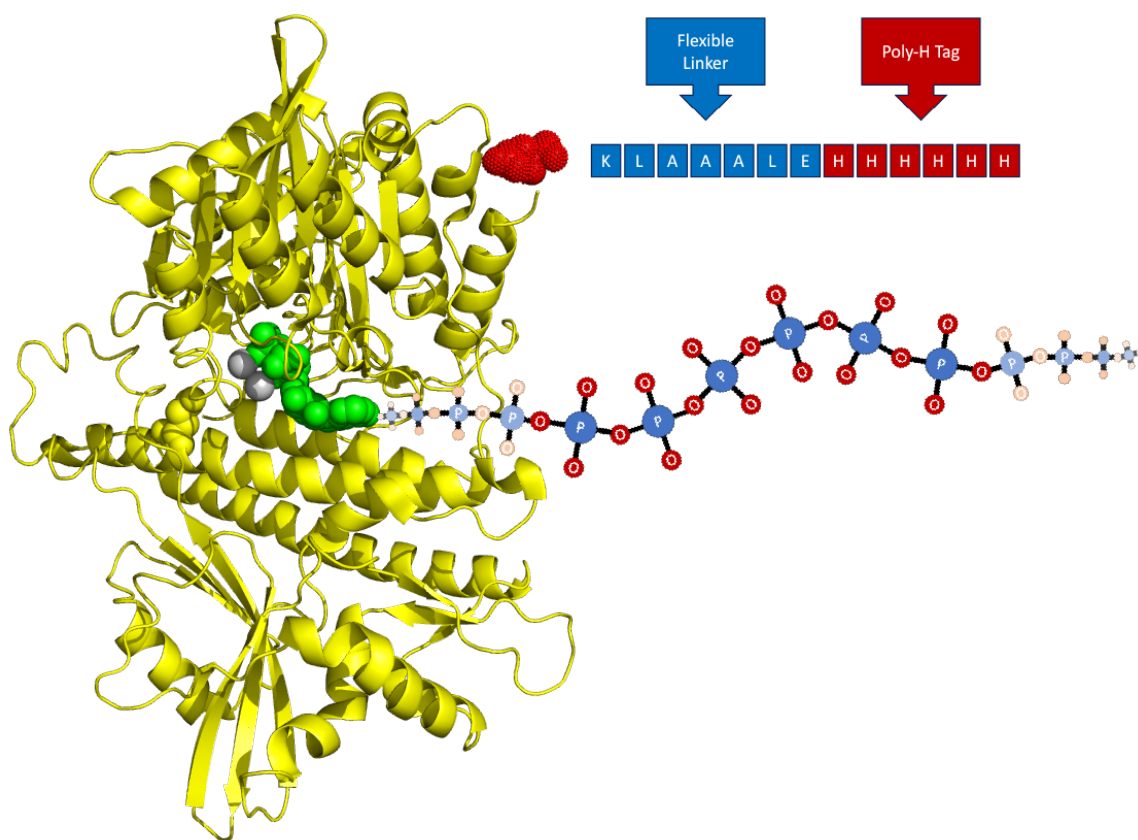
13. Replace the dialysis buffer with fresh buffer and dialyze another 4 hours.

Extract the dialyzed protein solution from the cassette and aliquot into appropriate portions – 100 µL is general a good option. Store at -80 °C.

APPENDIX B

A PSEUDO-UNCOMPETITIVE INHIBITON MODEL OF POLY-HISTIDINE
TAGGED PPK

Through this work, we have shown that the PPK-HT enzyme functionally differs from the untagged equivalent. However, the mechanism by which the PPK-HT enzyme acts so differently from PPK and PPK-CT enzymes is unknown. There are some oligomeric state changes of the enzyme in solution (see Figure 4 of Chapter 4). The tetramer form of PPK, as previously discussed, is the form in which PPK initiates polyP synthesis (15). As such, the PPK-HT enzyme being in that form almost exclusively means that it is more prepared to activate than PPK or PPK-CT, both of which have notable monomeric and dimeric populations.



Appendix B Figure 1 | The C-terminal Tag and the PolyP Chain. The PPK monomer active site (modeled with ATP in green) extrudes polyP chains in a processive manner. The poly-H tag is attached to the C-terminus (red spheres) by a flexible linker (blue squares). This allows it to move and potentially bind with polyP.

One issue of concern is the charge of the poly-H tag at reaction conditions. The pKa of histidine is roughly 6.04 (116). At reaction conditions of pH 7.5, the poly-H tag

represents a six-residue patch of positive charge at the C-terminus of the monomer. The C-terminus, however, is proximal to the channel through which the growing polyP chain is extruded (Appendix Figure 1). Recently, poly-H sequences have been shown to form a tight ionic bond with polyP chains in a highly specific manner (117). The flexible linker sequence used for the poly-H tag, and the flexible polyP chain allow for mobility. This suggests that the poly-H tag could be binding to the polyP chain as it is being produced.

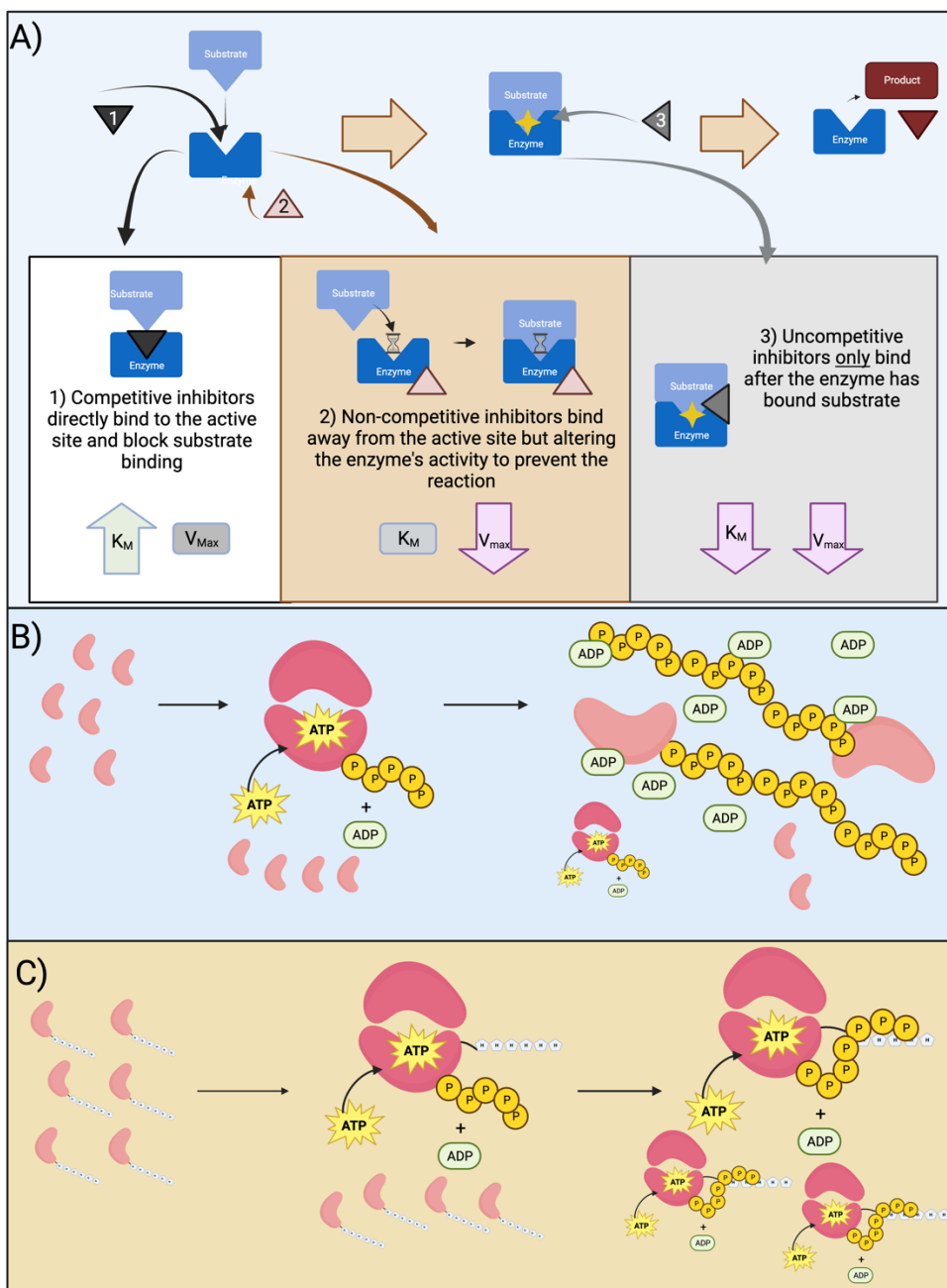
The binding of the polyP chain to the poly-H tag could have two major effects. The first possibility would be that the poly-H tag acts as a chaperone to pull the polyP chain out of the enzyme active site, increasing the rate at which the chain can be expanded. This would result in an increase in V_{max} and a decrease in K_m . However, as shown in Figure 3 of Chapter 4 (“Kinetics of Tagged PPK Enzymes”), we see a decrease in the V_{max} with a decrease in the K_m , indicating that while the enzyme binds the substrate more readily, it seems to have an issue producing the product. The second possibility is that the poly-H tag binding to polyP would result in a “clogged” enzyme, with the polyP chain being stuck in the channel after a sufficient length was produced to allow for poly-H:polyP interaction.

If the poly-H:polyP interaction occurs and results in the polyP chain clogging the enzyme, we would expect to see several signals of this event. Consider the enzymatic reaction of $E + S \Rightarrow ES \Rightarrow E + P$, where E is an enzymatic molecule, S is the substrate, and P is the product. At the initiation of the reaction, some amount of E binds to some amount of S to form the ES complex. Because the enzyme will have first bound substrate (ATP) and produced a polyP chain of some n length, our polyP detection assay will detect polyP production. In the enzymatic reaction process of $E + S \Rightarrow ES \Rightarrow E + P$, if

the ES population decreases due to the enzyme clogging and being unable to release product, more of ES will form from the E + S pool to maintain equilibrium. So, we would expect to see an increase in the binding affinity of the enzyme for the substrate, or a lower K_m , as more enzyme is binding more substrate that would normally happen. However, because the amount of polyP produced is limited by how much an ES complex can produce before it clogs and becomes inactive, the overall V_{max} would decrease as the concentration of free enzyme decreased over the course of the reaction.

The expected observations of a poly-H:polyP clogging event would kinetically mimic the rare uncompetitive inhibitor effect (Appendix Figure 2A), where the inhibitor only binds to the ES substrate. Because the inhibitor only binds to ES complexes to prevent the release of product, the V_{max} decreases because less product is being produced. The inactivated ES complex imbalances the equilibrium of the reaction, driving the formation of more ES complex. This formation of ES complex decreases the perceived K_m because more substrate is being bound at a higher rate than what would happen in an uninhibited reaction.

As shown in Appendix Figure 2B, the normal course of an active PPK reaction would result in some amount of polyP chains of a length of n . At the end of the reaction cycle, there will be some amount of polyP present as long chains. When we measure the amount of the polyP present with the DAPI detection assay, we will measure a signal indicative of how much polyP is present – but not how long the chain is. We then calculate the amount of polyP produced over the amount of time the reaction ran with the assumption that the amount of enzyme producing polyP remains constant.



Appendix B Figure 2 | Pseudo-uncompetitive Inhibition Model of PPK Activity. A) Three types of inhibitors and the effects they have on V_{max} and K_M . B) The model of PPK activity, where PPK is activated to complex with ATP, produce polyP, and eventually stop. C) A pseudo-uncompetitive inhibition model of PPK-HT activity, where the poly-H tag complexes with polyP being produced by the enzyme, resulting in a phenotype that mimics the behavior of an uncompetitive inhibitor which can only bind when the substrate and enzyme have complexed.

In Appendix Figure 2C, however, we see how a pseudo-uncompetitive inhibitory effect could affect the PPK-HT enzyme. As with the normal reaction the PPK-ATP

complex will form to produce some amount of polyP of an n length. However, because of the poly-H:polyP interaction the polyP chain will become trapped, preventing the movement of the chain and incorporation of the next phosphate. This stalled enzyme complex would then be inactivated and removed from the activity of the reaction while still having produced some amount of polyP we would detect with our detection method. The elimination of an active ES complex will drive the formation of more PPK-ATP complexes, which will produce some amount of polyP before suffering the same fate. The result would be that we detect an amount of polyP produced by the enzymes which would be used to calculate the kinetic values, but the assumptions of the kinetic model would be invalid – namely, constant enzyme concentration and constant rate of substrate binding. As time progresses, the concentration of free enzyme in the reaction will decrease while the number of PPK molecules with some polyP attached will increase. Calculations with the assumption that the amount of enzyme able to react remained the same will give us a higher level of product than expected, because we assumed that the reaction is a true catalytic reaction: one E binds to one S, reacts, and releases one E and one P. Instead, we would see one E binding to one S, forming an ES complex that works for a few cycles before it becomes incapable of producing product. This disrupts the equilibrium of the reaction, which causes another E to bind S to restore equilibrium. As each ES complex becomes clogged, the cycle would repeat.

We have observed several indicators that this hypothetical pseudo-uncompetitive inhibition event is occurring. For starters, our specific activity assays (Figure 2 of Chapter 4) show us that the PPK-HT enzyme seems to maintain a roughly two-fold increase in activity compared to untagged enzyme. If we consider that every PPK-ATP

complex that becomes clogged pulls another PPK and ATP into the reaction to maintain equilibrium as shown in the model of Appendix Figure 2C, this would explain the roughly two-fold difference in the perceived reaction rate between the WT and PPK-HT enzymes. Additionally, if we look at the kinetic curves of the enzymes (Figure 3 of Chapter 4), the PPK-HT enzyme maintains a curve that is consistent with what would be expected from an uncompetitive inhibitor: both the V_{max} and K_m decrease compared to the PPK-CT enzyme.

Unfortunately, we cannot use existing mathematical models to define a curve to validate this hypothesis due to the unique properties of PPK. Firstly, PPK experiences substrate inhibition which prevents us from using normal Michaelis-Menten kinetic models. Like all kinetic equations, substrate inhibition models require steady levels of substrate to be present to successfully model the effect of substrate inhibition. This requires the addition of an ATP regeneration system in each reaction. Secondly, a product of the reaction, ADP, is the substrate for polyP hydrolysis by PPK. For that reason, the same ATP regeneration system is required for PPK reactions to ensure the stability of polyP produced by the enzyme. The rate of product production from these reactions is influenced by ATP inhibition, ADP inhibition and the rate of the reverse reaction (ADP-driven polyP hydrolysis), enzyme availability which cannot be measured during the course of the reaction, and equilibrium pressure.

One possible solution that would not require novel mathematical models is if we were able to replace the ATP regeneration system with an ADP depletion system. In this situation, by removing ADP from the reaction while not changing the amount of ATP present, we could measure the disappearance of substrate rather than the appearance of

product. The lack of ADP would prevent any reverse-reaction pressure on the system, allowing us to measure how rapidly ATP is consumed. We could then measure the chain-length of the polyP molecules produced and compare it to the amount of ATP consumed. The standard in this experiment would be PPK-CT enzyme which behaves identically to untagged enzyme. If the PPK-HT enzyme consumes more ATP but produces shorter chains of polyP than the PPK-CT enzyme, it would indicate that more of the PPK-HT enzyme was active in the reaction, rather than the enzyme was more active per unit of enzyme. This would confirm the pseudo-uncompetitive inhibition model.

Unfortunately, at the time of writing, the construction of an ADP-removal system that neither produces nor consumes ATP is beyond the scope of the lab. However, this pseudo-uncompetitive inhibition model remains a solid explanation for the observed differences of the PPK-HT enzyme compared to PPK-CT activity. It explains the unusual decrease in maximum enzyme activity that occurs with the increase in substrate affinity. It explains why under normal reaction conditions PPK-HT enzyme maintains a two-fold increase in activity over the PPK and PPK-CT enzymes. The fundamental mechanism of this model that explains the inhibitory effect – namely, the interaction of polyP chains and poly-H sequences – has recently been confirmed (117). While the conclusions of the previous chapters have shown the PPK-HT enzyme is an undesirable construct for the use of therapeutics development or enzyme characterization experiments, this model does not have the “smoking gun” data available yet to be the best explanation as to why that is the case. Still, the circumstantial data so far supports this model and justifies its consideration for future studies of the PPK-HT abnormalities.